

Aus dem Institut für Schlaganfall- und Demenzforschung (ISD)
Klinik der Universität München

Direktor: Prof. Dr. med. Martin Dichgans



***Hit (the Nail) on the Head:
A Characterization of Chronic Sequelae in
Experimental Traumatic Brain Injury.***

Dissertation

zum Erwerb des Doktorgrades der Medizin
an der Medizinischen Fakultät der
Ludwig-Maximilians-Universität zu München

vorgelegt von

Antonia Clarissa Wehn

aus

Bukarest

Jahr

2023

Mit Genehmigung der Medizinischen Fakultät
der Universität München

Berichterstatter: Prof. Dr. Nikolaus Plesnila

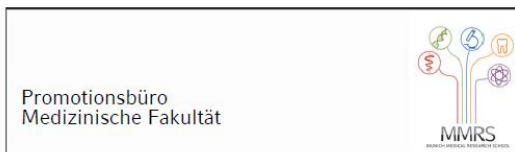
Mitberichterstatter: Prof. Dr. Jovica Ninkovic
PD Dr. Florence Bareyre
Prof. Dr. Inga Katharina Koerte

Mitbetreuung durch den
promovierten Mitarbeiter: PD Dr. Nicole Angela Terpolilli

Dekan: Prof. Dr. med. Thomas Gudermann

Tag der mündlichen Prüfung: 27.04.2023

Affidavit



Eidesstattliche Versicherung

Wehn, Antonia Clarissa

Name, Vorname

Ich erkläre hiermit an Eides statt, dass ich die vorliegende Dissertation mit dem Titel:

Hit (the Nail) on the Head: A Characterization of Chronic Sequelae in Experimental Traumatic Brain Injury.

selbständig verfasst, mich außer der angegebenen keiner weiteren Hilfsmittel bedient und alle Erkenntnisse, die aus dem Schrifttum ganz oder annähernd übernommen sind, als solche kenntlich gemacht und nach ihrer Herkunft unter Bezeichnung der Fundstelle einzeln nachgewiesen habe.

Ich erkläre des Weiteren, dass die hier vorgelegte Dissertation nicht in gleicher oder in ähnlicher Form bei einer anderen Stelle zur Erlangung eines akademischen Grades eingereicht wurde.

München, 19.06.2023

Antonia Wehn

Table of Contents

Affidavit	2
Table of Contents	3
List of Abbreviations.....	4
List of Publication	5
1. Contributions of the author	6
1.1 Contribution to Paper I	6
1.2 Contribution to Paper II	6
1.3 Contribution to Paper III	7
2. Introduction	8
2.1 Epidemiology.....	8
2.2 Classification and Clinical Outcome	9
2.3 Clinical Management	10
2.3.1 Emergency and ICU Treatment	10
2.3.2 Imaging	11
2.4 Pathophysiology.....	12
2.4.1 Primary Brain Damage.....	12
2.4.2 Secondary Brain Damage.....	13
2.5 Animal Models	15
2.5.1 TBI models.....	15
2.5.2 Structural analysis.....	17
2.5.3 Behavioral assessment.....	17
2.6 Aims of the Present Thesis	18
3. Summary.....	20
4. Zusammenfassung	22
5. Paper I	24
6. Paper II	45
7. Paper III	70
8. References.....	91
Acknowledgements.....	98
Curriculum vitae	Error! Bookmark not defined.

List of Abbreviations

AMPA	α -Amino-3-hydroxy-5-methyl-4-isoxazol-Propionic Acid
ASIC	Acid sensing ionic channel
CT	Computed tomography
CYLD	Cylindromatosis gene
DC	Decompressive craniectomy
DNA	Deoxyribonucleic acid
FOUR	Full Outline of Unresponsiveness
GCS	Glasgow Coma Scale
GPX	Glutathione peroxidase
ICAM	Intracellular adhesion molecules
ICP	Intracranial pressure
ICU	Intensive Care Unit
IL	Interleukin
iNOS	Inducible nitric oxide synthase
MLKL	Mixed lineage kinase domain like pseudokinase
MRI	Magnetic resonance imaging
NMDA	N-Methyl-D-Aspartate
NO	Nitric oxide
RCT	Randomized Controlled Trial
RIP	Receptor interacting protein
RNA	Ribonucleic acid
ROS	Reactive oxygen species
SDI	Sociodemographic index
TBI	Traumatic brain injury
TNF	Tumor necrosis factor
VCAM	Vascular adhesion molecules
VDAC	Voltage-dependent anion channels
Xc-	Cystine-glutamate antiporter

List of Publication

Publications in the Present Work

RIPK1 or RIPK3 deletion prevents progressive neuronal cell death and improves memory function after traumatic brain injury.

Wehn A, Khalin I, Düring M, Vandernabeele P, Hellal F, Culmsee C, Vandenabeele P, Plesnila N & Terpolilli NA
Acta Neuropathologica Communications, 2021, Aug 17. doi: 10.1186/s40478-021-01236-0.

Progressive Histopathological Damage Occurring Up to One Year after Experimental Traumatic Brain Injury Is Associated with Cognitive Decline and Depression-Like Behavior.

Mao X, Terpolilli NA, **Wehn A**, Cheng S, Hellal F, Liu B, Seker B, Plesnila N
J Neurotrauma. 2020, Feb 5. doi: 10.1089/neu.2019.6510.

Acid-ion sensing channel 1a deletion reduces chronic brain damage and neurological deficits after experimental traumatic brain injury.

Cheng S, Mao X, Lin X, **Wehn A**, Khalin I, Wostrak M, Ringel F, Plesnila N, Terpolilli NA
J Neurotrauma, 2021, Jun 1. doi: 10.1089/neu.2020.7568.

Additional Publications

T1-MPRAGE and T2-FLAIR segmentation of cortical and subcortical brain regions—an MRI evaluation study.

Beller E, Keeser D, **Wehn A**, Malchow B, Karali T, Schmitt A, Papazova I, Papazov B, Schoeppe F, Figueiredo G, Ertl-Wagner B, Stoecklein S
Neuroradiology, 2018 Nov 6. doi: 10.1007/s00234-018-2121-2.

Dynamic tracing using ultra-bright labeling and multi-photon microscopy identifies endothelial uptake of poloxamer 188 coated poly(lactic-co-glycolic acid) nano-carriers in vivo.

Khalin I, Severi C, Heimburger D, **Wehn A**, Hellal F, Reisch A, Klymchenko A, Plesnila N
Nanomedicine, 2021, Dec 1. doi: 10.1016/j.nano.2021.102511.

Size-Selective Transfer of Lipid Nanoparticle-Based Drug Carriers Across the Blood Brain Barrier Via Vascular Occlusions Following Traumatic Brain Injury.

Khalin I, Adarsh N, Schifferer M, **Wehn A**, Groschup B, Misgeld T, Klymchenko A, Plesnila N

1. Contributions of the author

1.1 Contribution to Paper I

Title: Progressive Histopathological Damage Occurring Up to One Year after Experimental Traumatic Brain Injury Is Associated with Cognitive Decline and Depression-Like Behavior.

Authors: Xiang Mao (XM), Nicole Angela Terpolilli (NT), **Antonia Clarissa Wehn (AW)**, Shiqi Cheng (SC), Farida Hellal (FH), Baiyun Liu (BL), Burcu Fatma Seker (BS), Nikolaus Plesnila (NP)

Planning of experiments: XM, NT, NP

Data acquisition: XM, **AW**, SC

Data analysis: XM, BS, **AW**, SC

Writing of the manuscript: XM, NT, NP, **AW**, FH, BL, BS

1.2 Contribution to Paper II

Title: RIPK1 or RIPK3 deletion prevents progressive neuronal cell death and improves memory function after traumatic brain injury.

Authors: **Antonia Clarissa Wehn (AW)**, Igor Khalin (IK), Marco Düring (MD), Farida Hellal (FH), Carsten Culmsee (CC), Peter Vandernabeele (PV), Nikolaus Plesnila (NP), Nicole Angela Terpolilli (NT)

Planning of experiments: **AW**, NT, IK, NP

Data acquisition: **AW**

Data analysis: **AW**, IK, NT

Writing of the manuscript: **AW**, NT, NP, IK, FH, CC, PV

1.3 Contribution to Paper III

Acid-ion sensing channel 1a deletion reduces chronic brain damage and neurological deficits after experimental traumatic brain injury.

Authors: Shiqi Cheng (SC), Xiang Mao (XM), Xiangjiang Lin (XL), **Antonia Clarissa Wehn (AW)**, Igor Khalin (IK), Maria Wostrak (MW), Florian Ringel (FR), Nikolaus Plesnila (NP), Nicole Angela Terpolilli (NT)

Planning of experiments: SC, NT, NP

Data acquisition: SC, XM, XL, **AW**

Data analysis: SC, XM, XL, **AW**, FR

Writing of the manuscript: SC, NT, NP, **AW**, IK, MW, FR

Herewith, I confirm the contributions to the article/manuscripts

München, 15.06.2022

Antonia Wehn

Prof. Dr. med. Nikolaus Plesnila (Supervisor)

Xiang Mao (first author of Paper I)

Shiqi Cheng (first author of Paper III)

2. Introduction

Traumatic brain injury (TBI) is one of the major challenges for medical care, public health, and the economy [1-3]. Cases occur across all ages, and the scarcity of therapeutic interventions makes TBI a major health problem worldwide. Amongst its survivors, TBI is a major cause of long-term disabilities and neurological disorders such as various forms of dementia and chronic traumatic encephalopathy, leading to a decrease in life expectancy and quality [4, 5]. The shortage of targeted therapeutic options stems from the fact that the exact pathomechanisms of posttraumatic brain injury are still not fully understood. Damage occurs in two different stages. The acute phase is marked by quickly evolving and irreversible cell death, causing the so-called primary injury, inaccessible to therapy. Thereafter, however, ongoing inflammation and vascular changes lead to potentiation of the initial injury [6]. This secondary injury is subject to numerous studies and caused by a variety of pathomechanisms initiated by the primary impact. Given the fact that secondary lesion progression occurs with a delay, this injury – which can be significantly larger than the initial lesion – is potentially amenable for therapeutic intervention and improvement of cognitive outcome of patients.

2.1 Epidemiology

In 2016, more than 27 million new cases of TBI were reported worldwide, marking a global increase of 3.6 % since 1990 [7]. These numbers, however, are thought to significantly underestimate the burden of TBI, since they do not take into account patients who did not seek or receive medical care. TBI has therefore been termed the ‘silent’ epidemic, since the actual impact of TBI on a global scale is probably much larger than assumed [8]. Moreover, TBI affects all age groups and represents the leading cause of death and disability in children and young adults [7]. However, a second peak can be observed in people aged 65 and older, as most trauma-related hospitalizations and deaths occur in patients of this subpopulation [9, 10]. With growing population density, aging and frequency in motorization, case numbers are expected to increase significantly in the coming decades [11]. Typical causes of TBI include falls, especially in the older population, road traffic accidents, assaults, and sporting accidents, the latter predominantly in younger patients [12]. The incidence of TBI is subject to considerable geographical and socioeconomic variation [7, 11]. Highest incidences for TBI are reported in countries with a higher sociodemographic index (SDI) such as central Europe with 857 cases per 100.000 inhabitants/year, whereas lower rates were observed in regions with a lower SDI such as Sub-Saharan Africa at 326 cases in 100.000 inhabitants/year [7]. However, these variations can be largely explained by reporting bias, since limited access to healthcare resources is expected to occur in less developed countries [7].

2.2 Classification and Clinical Outcome

TBI is a very heterogeneous disease. In general, it is a form of acquired brain injury characterized by an external mechanical impact to the head, leading to a disruption of normal brain function [13]. It can result from a blow to the head or by an object piercing the skull and entering brain tissue. Depending on whether the dura mater is disrupted or not, TBI can be classified as closed (dura is intact) or open (dura is torn) [14]. This distinction is primarily relevant for the initial care of the patient, because of the increased risk of infection in case of dural injury, but can also be important for the subsequent pattern of neurological deficits. Brain trauma can also be classified depending on areas affected by the impact, namely in a focal or diffuse manner. Focal injuries

Points	Eye opening	Verbal response	Motor response
1	None	None	None
2	To pressure	Sounds	Extension
3	To sound	Words	Abnormal flexion
4	Spontaneous	Confused	Normal Flexion
5		Oriented	Localizing
6			Obey commands
Total score = 3 – 15			

Table 1: Overview of the Glasgow Coma Scale.

are characterized by neurological deficits that depend on the affected region, while closed head injuries usually are of a more diffuse nature, also affecting remote regions of the central nervous system such as the spinal cord [15]. However, most TBIs show a mixture of both injury patterns, resulting in very heterogeneous clinical and neuropsychological presentations, depending on the intensity of the impact and the regions affected [16]. For example, it has previously been reported that loss of consciousness is one of the strongest predictors for adverse outcome and is a common symptom of most TBIs [17]. It is therefore very important to determine the severity of the injury in order to draw conclusions on outcome. The Glasgow Coma Scale (GCS) which was introduced in 1974 by Teasdale and Jennett is still the most common clinical scale used to assess TBI severity in adults, especially in an emergency setting, because of its high inter-observer reproducibility and good prognostic value [18].

TBI severity is most commonly assessed and classified according to the patient's GCS score at admission: mild TBI if the GCS score is 13-15, moderate TBI for GCS scores from 9-12, and severe TBI if initial GCS scores range from 3-8. However, this scoring system is also subject to an array of different confounders such as intoxication, sedation, intubation, and (previously existing) paralysis, restricting its application [19]. A number of alternative scores have been proposed to improve clinical assessment, e. g. the Brussels Coma Grades, Grady Coma Grades, Innsbruck Coma Scale, and the Full Outline of Unresponsiveness (FOUR) score. However some of these are quite complicated to perform and therefore not used as widely as the GCS [20].

Clinical characteristics and outcome of TBI may vary largely depending on injury mechanism and severity. In the acute stage, patients with mild TBI typically show physical, cognitive and behavioral symptoms, such as loss of consciousness, amnesia, slowed reaction times, headaches, emotional lability and irritability [21]. However, most subjects fully recover within the first weeks after trauma. Only around 15% of cases are associated with ongoing cognitive and behavioral deficits such as progressive memory loss and mood disorders [21]. In moderate and severe TBI, however, patients often present with impaired consciousness or coma, and up to 60% are expected to show a poor functional outcome, such as severe neurocognitive deficits, vegetative state, or death [22]. Typical long-term consequences of TBI include an increased risk for dementia and neurodegenerative syndromes (e. g. Alzheimer's disease, Parkinson's disease, amyotrophic lateral sclerosis), chronic traumatic encephalopathy, as well as psychiatric disorders such as depression [23].

2.3 Clinical Management

2.3.1 Emergency and ICU Treatment

Given the complexity and heterogeneity of its presentation and the incomplete knowledge of TBI pathophysiology (see 2.4), there are to date no causal treatment options in TBI. Current therapy mainly aims at treating symptoms, stabilizing the patient and preventing secondary events. Primary focus of the early (emergency and ICU) management of TBI is cardiopulmonary stabilization of the patient in order to obtain radiological as well as neurological baseline evaluation to plan further treatment and estimate outcome [24]. These measures aim at providing adequate oxygenation and perfusion of the brain by securing the airway/ventilation and stabilizing blood pressure, as (preclinical) hypotension and hypoxemia are known risk factors for adverse outcome [25-27]. Furthermore, patients are positioned with head elevation to promote venous outflow [28] in order to lower intracranial pressure (ICP), secure adequate brain perfusion and avoid herniation (transtentorial or transforaminal). According to the German Guidelines for the Treatment of TBI, as soon as patients have been admitted to a hospital and are cardiopulmonally stable, computed tomography should be performed to ascertain TBI extent and severity as well as to diagnose possible associated extracranial injuries [29]. Once the diagnosis of (severe) TBI has been established further steps depend on imaging findings. In case of localized pathologies such as epidural or subdural hematomas, prompt surgical evacuation is warranted. In case of diffuse lesion patterns and unconscious patients, ICP monitoring should be considered. In the presence of increased intracranial pressure, the Brain Trauma Foundations recommends staged therapeutic measures [30]. These include hyperosmolar therapy using osmotic diuretics, such as mannitol or hypertonic saline, to improve blood rheology [31], as well as permissive hypocapnia (pCO_2 between 30 and 35 mmHg) achieved by hyperventilation, which results in vasoconstriction and thus lowers ICP [32, 33]. Furthermore, the brain's energy demand can be lowered in order to preserve tissue [34]. One way is to place the patient into a medically induced comatose state through the use of

benzodiazepines such as midazolam or barbiturates such as phenobarbital [34]. Another option is therapeutic cooling, which also reduces brain metabolism [35].

In case of intractable intracranial hypertension, surgical therapy may be necessary. The standard tool to surgically alleviate intracranial pressure is decompressive craniectomy (DC). However, the effects of DC with regard to long-term patient outcome have to be viewed critically. In the DECRA study, the first randomized controlled trial (RCT) investigating the effects of bifrontotemporoparietal DC in patients with moderately increased ICP and no mass lesion, a lowering of ICP values during ICU stay was observed, however, DC was also associated with a more unfavorable outcome 6 months after TBI [36]. In a follow up study, no differences between DC and standard medical care could be observed after 12 months [37]. In contrast, the RESCUE ICP study found that DC was associated with a lower 6-month mortality, but also resulted in higher rates of vegetative state and severe disability compared to conservative medical treatment [38]. Due to these ambivalent findings, the indication and timing for DC has to be critically evaluated [39].

To date, no causal therapeutic strategies have been established to prevent the long-term consequences, e. g. ongoing neurodegeneration and chronic neurological impairment, after TBI, which will be critically discussed below. While many studies have shown promising approaches in a preclinical setting, translation into the clinical field has, so far, failed [40, 41].

2.3.2 Imaging

Following TBI early diagnosis of factors associated with adverse outcome is crucial for proper management and assessment of prognosis. Imaging is the most important tool to quickly and comprehensively investigate and assess TBI sequelae and thus to potentially improving patient morbidity and mortality. Different imaging tools are available in the clinical setting to determine severity of injury, possibly treatable complications as well as serve as indicator for further treatment. In addition, it has also become indispensable for surgical planning, since it provides precise non-invasive information on anatomical structures [42].

Conventional computed tomography (CT) is the imaging modality of choice in the acute setting because of its broad availability, short imaging time and cost effectiveness [43]. In addition, bone structures and hemorrhagic formations can be better evaluated using CT scans [44]. Within the first 24 hours after TBI, CT can be used to evaluate acute complications [45]. However, it also has its limitations: CT scanning at early stages (within 3 hours) after injury has been shown to underestimate contusion size [46]. In addition, repetitive CT scans to evaluate progression in absence of neurological changes are heavily under debate, not least because every CT scan means exposure to radiation [47-49].

Magnetic resonance imaging (MRI) is considered to be generally more sensitive for anatomical imaging of the brain tissue and provides better accuracy for diagnosis [50]. Especially in the sub-acute timeframe after TBI, namely 48 to 72 hours after TBI, ability of blood detection increases for MRI while it decreases for CT. As blood composition changes and permanent iron deposits, also called hemosiderin, start forming, MRI proves to be superior in detecting smaller hemorrhagic

foci [42]. In addition, MRI can also show diffuse axonal injury through alteration of the white matter signal [45]. Finally, anatomical structures such as the basal ganglia, thalamus and brain stem can be assessed better by MR imaging [51]. However, long acquisition times, low availability, and high costs are disadvantageous in the acute setting. The duration of the procedure also requires a long horizontal positioning of the patient, which can be detrimental in case of increased intracranial pressure.

2.4 Pathophysiology

Brain damage associated with TBI can be classified into two groups according to the timing of their emergence. The first is the primary injury, which represents the initial insult caused by outside mechanical forces. It occurs within seconds upon impact, is irreversible and as such cannot be influenced therapeutically. Following this initial damage, the so-called secondary injury develops and represents a delayed but progressive further tissue loss in response to primary injury; actively expanding secondary tissue loss has been described to occur for years and even decades after TBI [52-54]. Because of its deferred emergence, secondary brain injury offers a time-window to therapeutically intervene and thereby to potentially slow down or even stop further damage.

2.4.1 Primary Brain Damage

Depending on TBI severity and mechanism, the initial impact can result in two types of primary brain damage: focal or diffuse injuries. In response to concussion and compression forces, the area directly impacted by the mechanical force often exhibits a focal lesion characterized by necrosis of neurons and glial cells, as well as hematoma and potentially epidural, subdural or intracerebral hemorrhages [55]. Diametrically opposite of this so-called 'coup', another contusion may develop, called "contre-coup", due to compression and rebound of the tissue against the skull or bony protruberances [34]. Depending on their localization, these focal injuries can lead to changes in behavior, sensomotoric dysfunction and/or cognitive deficits [56]. In contrast, diffuse brain injury is a result of shearing and stretching of tissue due to rapid acceleration and deceleration [57]. These strong non-contact forces induce damage of the cytoskeleton of astrocytes, blood vessels, and oligodendrocytes, resulting in disruption of the blood-brain-barrier, ionic imbalance, osmotic changes [58], as well as axonal damage. This results in myelin sheath disruption and degradation, leading to severe malfunction of axonal transport and neuron interconnection, primarily affecting subcortical and deep white matter tissue such as the brain stem and corpus callosum [59]. The resulting damage leads to very heterogeneous symptoms depending on the severity of the impact and manifests in wider regions of the brain as well as bilateral neurological deficits [60].

2.4.2 Secondary Brain Damage

Following the primary injury, a number of downstream processes occur, leading to a deterioration and enlargement of the initial lesion, the so-called secondary damage. The pathophysiology behind this lesion expansion is still not completely understood; however, several factors have been identified as contributors. In general, edema formation and intracranial hypertension reduce brain perfusion, thus increasing ischemic and hypoxic stress, which in turn promotes further brain swelling. This vicious circle leads to ischemia-induced dysregulation of the tissue surrounding the necrotic area, resulting in ionic dysbalance, long-lasting chronic neuroinflammation and cell death [61]. These chronic processes cause progressive neuronal death and worsen functional outcome in return. The following paragraphs discuss major pathomechanisms of secondary brain damage relevant for the present thesis (see figure 1).

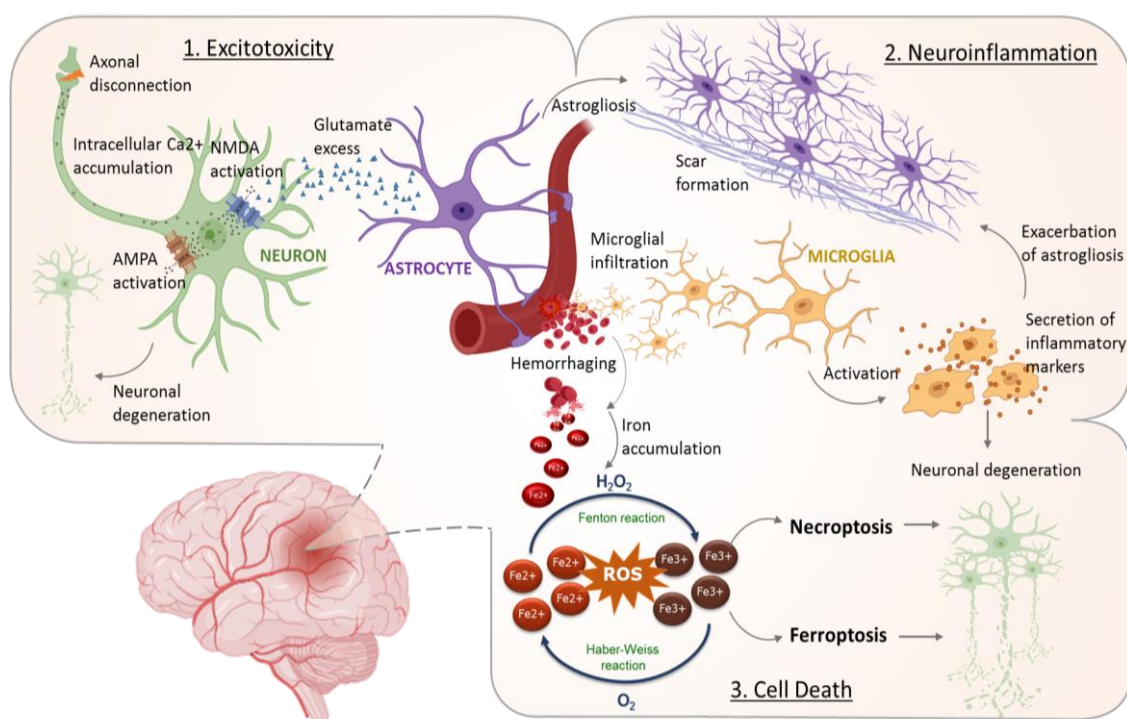


Figure 1: Visual representation of pathomechanisms in secondary brain damage after TBI. Created with BioRender.com.

2.4.2.1 Excitotoxicity

Several studies have defined excitotoxicity as one of the main promoters of secondary neuronal loss after brain injury [62, 63]. This process is mediated by an increased sodium and calcium influx into cells through the following pathomechanisms: due to injury and energy failure, a sudden simultaneous burst of depolarizing neurons leads to a release of large amounts of aspartate and glutamate into the extracellular space and a subsequent activation of glutamate N-Methyl-D-Aspartate (NMDA) or α -Amino-3-hydroxy-5-methyl-4-isoxazol-Propionic Acid (AMPA) receptors, which in return induce sodium and calcium influx into neurons [64, 65]. This intracellular calcium-overload then leads to cell damage via caspase activation and induction of apoptosis

[66]. Previously, astrocytes have been shown to take up the excessive glutamate, convert it to glutamine and redistribute it amongst neighboring astrocytes [67]. However, TBI has been associated with cessation of this clearing mechanism [68] or even reversed efflux into surrounding tissue [69]; astrocytes may thus exacerbate excitotoxic injury. Additionally, a decrease in pH levels due to lactate production can also directly activate specific proton-gated ion channels and increase calcium conductivity through the so-called acid sensing ion channels (ASIC) [70]. Accordingly, calcium influx leads to cell damage and, eventually, cell death.

2.4.2.2 Neuroinflammation

TBI has been shown to induce a wide variety of different inflammatory responses, which can either promote regeneration or exacerbate injury [71]. For instance, tissue damage leads to the release of an array of different inflammatory mediators, such as prostaglandins, cytokines, complement factors or free radicals [72]. In return, those lead to the mobilization of immune cells and innate glial cells through stimulation of other chemokines and upregulation of adhesion molecules [73]. For example, studies have shown the accumulation of CD8-positive phagocytes on the border of pan-necrotic tissue and infiltration into surrounding tissue, on the one hand clearing necrotic material and helping scar formation, on the other hand increasing inflammatory cytokines such as the inducible nitric oxide synthase (iNOS), nitric oxide (NO), tumor necrosis factor- α (TNF- α), and interleukin-1 β (IL-1 β) [71, 74]. Their infiltration is facilitated by upregulation of specific adhesion molecules, such as intracellular adhesion molecules (ICAM-1), vascular adhesion molecules (VCAM-1) and P-selectin [75]. Furthermore, secretion of vasoconstrictors, such as leukotrienes and prostaglandins, promote ischemic injury and lead to microvasculature damage, thus promoting blood-brain-barrier (BBB) disruption [74]. This vicious cycle of constant reorganization promotes chronic inflammation and leads to lesion progression. In addition, microglia activation can also benefit recovery through phagocytosis, but also promotes injury through increased cytokine secretion and thus extend inflammatory response [76]. Studies in the past have shown the regenerative role of microglia through targeted distribution of growth factors to damaged neurons and removal of excitatory input to protect cells of over-excitation and promote regeneration [77, 78]. However, prolonged microglial activation and chronic cytokine release also exacerbates inflammation, as described above [71]. Through all these processes, necrotic and adjacent tissue is eliminated and astrocytes finally start producing neurotrophins and microfilaments to initiate scar formation [79].

2.4.2.3 Cell death

Cell death may play a pathological as well as physiological role in the living organism. During the aging process, various cell death pathways are required for regulating cell turnover and maintain homeostasis [80]. In a pathological context however, cell death occurs as a result of disturbances in cell homeostasis [81]. Previously, cell death processes following TBI have been dichotomized into necrosis as an immediate response to mechanical damage, and into apoptosis as a programmed and delayed mechanism [82]. Necrosis results in ionic imbalance, thus morphologically leading to cell swelling and membrane rupture [83]. Subsequently, the excessive release of

amino acid neuro-transmitters and metabolic dysfunction activates caspases and apoptosis in neighboring cells as well as an inflammatory response [84]. In contrast to necrosis, apoptosis is characterized by condensation and fragmentation of the cell, eventual phagocytosis by neighboring cells and lack of inflammation [85]. In recent years however, studies have shown that necrosis can also be regulated, meaning the morphological processes of necrosis can be triggered by different molecules that lead to membrane disruption. In the ensuing years, many more cell death pathways have been described to occur following TBI. One of these new pathways is necroptosis, a caspase independent regulated form of necrosis [86]. Necroptosis is the best described form of regulated apoptosis. It is triggered by activation of several death receptors, such as the TNF receptor superfamily, which leads to the deubiquitylation of the receptor interacting protein (RIP) 1 by the ubiquitin carboxyl-terminal hydrolase CYLD and the subsequent necrosome complex formation, consisting of RIP1 and RIP3. This complex then induces phosphorylation of the mixed lineage kinase domain like pseudokinase (MLKL), which in return results in membrane damage and loss of cell integrity [87]. An inhibitor of RIP1, necrostatin-1, has previously been described to attenuate tissue loss and improve cognitive outcome in mice [88]. Similarly, ferrostatin-1 has shown similar effects and thus, ferroptosis, an iron-linked form of cell death, has also been shown to play a role in the development of posttraumatic secondary brain injury [89]. Due to vessel rupture after mechanical impact, as well as disruption of the blood-brain-barrier, iron in a heme and non-heme form is known to extravasate into the tissue and accumulate there, triggering neuronal loss. However, this type of cell death does differ greatly from the previously described mechanisms, both in terms of induction and of morphology. The underlying mechanism of ferroptosis is an accumulation of iron in the cell and the subsequent production of reactive oxygen species (ROS). These are normally reduced via the Fenton reaction or by various other mechanisms, such as the cystine-glutamate antiporter (Xc-), the glutathione peroxidase (GPX) 4 or mitochondrial voltage-dependent anion channels (VDAC) [90]. However, in the event of oversaturation of these mechanisms, ROS can accumulate and induce cell death. Morphologically, the only distinguishable characteristics are shrunken mitochondria and increased membrane density [91]. However, even though these various mechanisms have been described and characterized previously, still much is unknown about their role in TBI. Therefore, elucidating their role in the development of posttraumatic brain damage and how they are interconnected on a molecular scale may help to better understand the mechanisms of secondary brain injury after TBI and may facilitate the development of causal treatment strategies.

2.5 Animal Models

2.5.1 TBI models

In order to be able to study TBI pathophysiology in an experimental setting, animal models are required for investigating the underlying physiological, biomechanical, and cellular mechanisms and find potential therapeutic targets. Even though larger animals, such as primates and swine,

are more closely related to humans in terms of physiology, rodent species have long dominated the field of research given their small size, relatively low maintenance costs, as well as the possibility for generating genetically modified specimens. In order to be able to replicate the heterogeneous nature of TBI in humans, several different models have been established. Among the most common TBI paradigms are the controlled cortical impact (CCI) model [92], weight-drop injury [93, 94], fluid percussion injury [95] and blast injury [96].

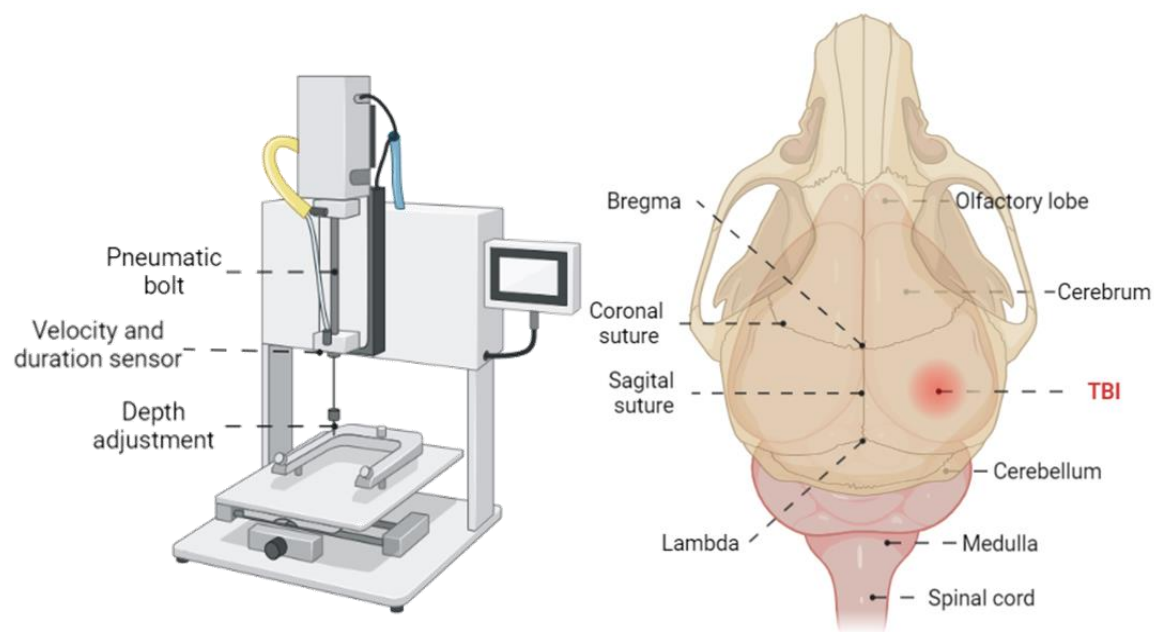


Figure 2: Schematic image of CCI setup (left) and surgical site (right). Created with BioRender.com.

For the CCI model, a craniotomy is performed over the right parietal cortex and trauma induced via a pneumatic bolt at constant, predetermined parameters (see figure 2). Typical characteristics of this model of injury are therefore cortical contusion, intraparenchymal hemorrhage, axonal injury and subsequent tissue loss [97]. The main advantage of this model is its high reproducibility, since the highly controlled parameters create a consistently sized lesion in all animals. In addition, the severity of injury can very reliably be adjusted by increasing or decreasing any of the given parameters, depending on experimental requirements. Due to positioning of the piston over the right parietal cortex, damage can be seen depending on severity of the injury in several regions of the brain, including cortex, hippocampus, thalamus, and corpus callosum [98], thus allowing to not only assess biochemical but also behavioral changes in animals. However, this high consistency also has the disadvantage of only representing one small part of the heterogeneous spectrum of TBI induced pathology. Several factors, including damage to the skull, diffuse spinal injury as a result of whiplash forces and multifocal injuries cannot be adequately simulated in CCI. Mouse studies themselves also have limitations which need to be considered. Starting on a macroscopic level, brain anatomy differs between humans and rodents in terms of brain geometry, craniospinal axis, and gyral complexity, largely determining structural and functional outcome [99]. Furthermore, differences can also be found on a microscopic level, namely alterations in brain cell proportions, laminar distributions, gene expression and morphology [100].

2.5.2 Structural analysis

In order to evaluate TBI severity and draw conclusions as to how these changes on the microscopic level relate to behavioral deficits, anatomical and histological characterizations of the lesion are necessary. Firstly, the extent of tissue damage via lesion volume needs to be established. Previously, brain damage has been routinely assessed by histology, more specifically in Nissl stained sections [101-103]. This method established by Franz Nissl in 1894 [104] is used to mark the endoplasmic reticulum and nucleus of neuronal cells. After brain injury, dying neurons lose their structural integrity and the basic dyes cannot bind to DNA and RNA [105], therefore delineating the lesion site. However, this method has limitations, since lesion volume analysis can only be done post-mortem. Therefore, a separate group of animals needs to be bred and prepared for each individual time point at which lesion size is assessed. This encompasses a large number of animals, time and substantial costs for long-term studies of chronic TBI. In addition, correlation of structural changes and behavioral deficits is rendered more difficult, since different groups of animals are to be compared. New imaging techniques such as MRI offer a solution to these limitations. Since it is a non-invasive imaging modality, anatomical structures can be evaluated repeatedly in the live animal, reducing the number of animals needed for assessment, especially in chronic experiments. Moreover, the same group of mice can be used for behavioral analysis, allowing researchers to relate structural changes with neuropsychiatric performance. However, repetitive MR imaging also comes with its own set of disadvantages and limitations. While the repeated exposure to magnetic fields was shown to have no adverse effects on locomotion, memory or fetal development, it still requires multiple exposures to anesthesia which can cause mild distress and impairment of well-being in the animals as well as have adverse effects on the immune response, which in turn might influence important healing processes [106, 107]. In addition, the relatively low resolution of MRI compared to other imaging modalities can be a hindrance for detailed anatomical evaluation, however, in the context of lesion assessment in TBI, we could show with correlative analysis of light microscopy and MRI that the resolution of the latter is fully sufficient [108]. Therefore, the advantages of MRI outweigh the limitations by far.

2.5.3 Behavioral assessment

TBI is associated with a number of neurobehavioral sequelae in humans, which are crucial for the long-term quality of life [109, 110]. Therefore, translating these pathologies into animal research is crucial for a better understanding of pathology and evaluation of potential therapeutic options. However, planning and execution of such experiments needs to be highly standardized and validated across laboratories in order to acquire interpretable and reliable data. Several internal as well as external factors contribute to behavioral responses in mice, classified as “trait, state and technical factors” [111]. Trait factors describe genetic and developmental effects such as maternal behavior, stress, handling, housing, and social interaction. State factors relate to the timing of the experiments, the experience of the researcher, animal characteristics like health, hormonal sta-

tus, pharmacological treatment, as well as the testing environment. Finally, technical factors characterize the process of data acquisition and analysis [111]. This part is especially challenging to standardize and represents the main reason for poor reproducibility across different laboratories [112]. It is therefore crucial to establish standard operating procedures within laboratories and insure strict adherence and exact reporting for unbiased, reproducible data [113].

Primarily, behavioral testing has to be relevant with regard to outcome in humans. The most common long-term residual impairments include deficits in motor function, cognitive ability such as memory loss, as well as mood disturbances and depression-like behavior [114]. However, translation of these deficits and monitoring of specifically higher cognitive functions in rodent models can be challenging. For the CCI model specifically, careful considerations must be made as to which behavioral deficits have to be expected from the brain injury produced. In case of a right parietal lesion (at 3 mm from bregma), affection of the motor cortex resulting in motor deficits of the left hind limb are therefore to be expected. Below the cortical surface, the hippocampus is located in this area of the mouse brain. Damage to this area leads to impairment of spatial and memory function. Finally, through expansion of the lesion due to previously described secondary processes, progression towards the neighboring frontal cortex can lead to mood disorders similar to the depression-like behavior reported in humans.

2.6 Aims of the Present Thesis

As described above, the current lack of causal therapeutic options for the treatment of TBI is still a hurdle to overcome. Therefore, deciphering the underlying pathophysiological mechanisms may help to develop new and improved therapeutic approaches. Previous research on TBI focuses on the acute effects of TBI, but very little is known about the pathomechanisms of chronic sequelae. The present studies aim to characterize the role and mechanisms of secondary brain damage following traumatic brain injury, its long-term effects on functional outcome and investigate possible therapeutic targets. First, in a proof-of-principle study, chronic neuropathological and behavioral sequelae were characterized in C57Bl/6 mice to establish a baseline for future reference. For this, the animals were subjected to either a highly standardized and widely used model of TBI, the controlled cortical impact model or to sham surgery and followed up to 12 months after injury. Behavioral tests measuring motor deficits, depression-like behavior and neurocognitive impairment were performed to evaluate functional outcome after TBI, and histomorphological analysis of the lesion was done to assess neuropathological changes such as chronic inflammation and ongoing neurodegeneration. These findings provide comprehensive data on time course and extent of long-term/chronic posttraumatic brain damage in the murine CCI model (see Publication I, p. 25) [115]. The author of this thesis was involved in performing experiments, data acquisition and analysis for subsets of this study.

After functional, radiological, and histomorphological characterization of long-term outcome after CCI-TBI, the mechanisms mediating chronic posttraumatic brain damage were evaluated in order

to identify relevant pathomechanisms and thus potential therapeutic strategies. In a first study, we investigated the role of necroptosis, a form of regulated cell death described above (see 2.4.2), on the development of secondary brain damage. We used two different knockout mouse lines lacking either RIP1 or RIP3, the key effectors of this pathway, and subjected these mice as well as their wild type littermates to the CCI model. These animals were then followed up to three months after TBI and neuro-behavioral as well as histopathological outcomes were assessed. Sham-operated as well as naïve animals were simultaneously assessed to normalize for phenotypic changes. The results of this study were published in Publication II (see p. 46) [108]. The author of this dissertation was responsible for all data acquisition and was constantly involved in the planning, data analysis and writing of the paper.

In a second study, we assessed the role of an intracellular mechanism of cell death via the acid-sensing ion channel (ASIC) 1a. Again, knockout animals lacking ASIC1a as well as heterozygous and wild type littermates were subjected to the described CCI protocol and chronic outcome was evaluated up to 18 months after injury. These results were published in Publications III (see p. 71) [70]. The author of the dissertation was involved in the data acquisition and analysis of certain aspects of this study.

3. Summary

Traumatic brain injury represents the leading cause of death and long-term disability in children and young adults worldwide and is associated with a wide range of posttraumatic complications including neurocognitive, behavioral and psychosocial deficits. As such, it continues to impose a heavy burden on the individual as well as the healthcare system due to high health care expenditures. So far, causal therapies to treat and reduce posttraumatic brain damage are at want. TBI related brain damage develops in two stages: the primary injury, representing the damage caused by the initial impact on the head, is irreversible and cannot be influenced therapeutically. The secondary injury however, which develops months to years after the initial impact due to vascular changes, chronic inflammation, and ongoing neurodegeneration provides a therapeutic window for intervention. However, the mechanisms underlying these changes are still not fully understood. The aim of the present study was to characterize chronic functional and neuropathological outcome of TBI in mice and investigate molecular mechanisms underlying the development of secondary brain damage following TBI in order to identify potential therapeutic targets.

First, male C57BL/6N mice (n=10 per group) were subjected to either TBI using the highly standardized control cortical impact model (CCI) or sham surgery. Motor function using the beam walk, depression-like behavior using the tail suspension test and memory function via Barnes maze were then assessed together with naïve animals 30, 90, 180, and 360 days after TBI. TBI animals presented a significant decrease in motor and memory function as well as progressive depressive behavior compared to the sham-operated and naïve groups. Histopathological changes were evaluated through immunohistochemistry and showed continuous enlargement of the lesion as well as progressive atrophy of the white matter and hippocampus area, indicating chronic neurodegeneration (see Publication I, p. 25).

Next, potential pathophysiological mechanisms underlying this chronic secondary brain damage were investigated. We firstly focused on a form of regulated cell death, necroptosis, which is mediated by the necrosome, a complex formed by the receptor interacting proteins (RIP) 1 and 3. Transgenic RIP3 and RIP1 neuronal transgenic male mice (n=8-10 per group) as well as wild type controls were subjected to CCI trauma or sham surgery and observed together with naïve animals (n= 4-5/group) at 15 minutes, 1, 7, 30, 60 and 90 days after injury. Serial MR imaging was used to characterize posttraumatic brain damage and motor function, depression-like behavior and memory function were assessed using the same paradigms detailed in Publication I. At 90 days after TBI, brains were harvested for histopathological evaluation. RIP1 and RIP3 deficient animals had significantly smaller lesion volumes compared to their wild type littermates, as well as less hippocampal atrophy. This translated into significant improvement of memory and learning function, however not into better motor function or motivational behavior. Immunohistochemical analysis revealed a reduction of reactive astrogliosis and less activation of microglia in knockout animals, suggesting an attenuation of chronic inflammation. There were hints that this neuroprotection is due to a reduction of blood-related toxicity (see Publication II, p. 46).

Finally, we looked at an intracellular mechanism of cell death mediated by the acid sensing ion channel (ASIC) 1a. After TBI, the pH in the brain tissue drops due to hypoxia and electrolyte dysbalance; this leads to a calcium influx into adjacent neuronal cells via ASIC1a and causes further cell death. We used male ASIC1a knockout mice as well as heterozygous and wildtype littermates (n=10 per group) to investigate chronic outcome after TBI. Animals were subjected to CCI and serial MR imaging was performed at 1, 7, 30, 60, 90 and 180 days after TBI to assess posttraumatic damage. Again, functional outcome was evaluated and histopathological analysis was performed. We found a significant reduction in posttraumatic brain damage as well as improved neurocognitive and motor outcome. This was associated with a reduction of chronic inflammatory processes in the brain (see Publication III, p. 71).

In conclusion, we established a standardized protocol for morphological, neurobehavioral and histopathological evaluation of chronic outcome after experimental TBI and investigated two molecular pathways in the context of secondary brain injury that could serve as potential therapeutic targets.

4. Zusammenfassung

Das Schädel-Hirn-Trauma (SHT) ist weltweit die Hauptursache für Tod und Langzeitbehinderung bei Kindern und jungen Erwachsenen und ist mit einem breiten Spektrum posttraumatischer Komplikationen verbunden, darunter neurokognitiven, motorischen und psychosozialen Defiziten. Somit stellt es nach wie vor eine schwere Belastung, sowohl für den Einzelnen als auch für das Gesundheitssystem dar, zum einen aufgrund der hohen Behandlungskosten in der akuten, aber auch der chronischen Erkrankungsphase. Ein schwerwiegendes Problem stellt der Mangel an kausalen Therapien dar, insbesondere die chronischen klinischen Verschlechterungen können derzeit nicht behandelt werden. Der posttraumatische Hirnschaden entwickelt sich in zwei Stadien: Der Primärschaden, der durch den mechanischen Schaden innerhalb von wenigen Sekunden bis Minuten entsteht, ist irreversibel und kann dementsprechend therapeutisch nicht beeinflusst werden. Der Sekundärschaden hingegen, der als Reaktion auf die Primärverletzung aufgrund vaskulärer Veränderungen, chronischer Entzündung und fortschreitender Neurodegeneration entsteht, entwickelt sich über Monate bis Jahre nach dem eigentlichen SHT. Diese zeitliche Verzögerung bietet prinzipiell ein therapeutisches Fenster für Interventionen, um diesen zu reduzieren. Die Mechanismen, die der Entstehung des Sekundärschadens zugrunde liegen, sind jedoch immer noch nicht vollständig geklärt. Ziel der vorliegenden Arbeit ist es, den langfristigen funktionellen und neuropathologischen Verlauf des SHT in Mäusen zu charakterisieren und die molekularen Mechanismen zu untersuchen, die der Entstehung von sekundärem Hirnschaden nach SHT zugrunde liegen. Ziel ist einerseits die Charakterisierung der Pathophysiologie, andererseits die Identifikation potenzieller therapeutischer Angriffspunkte.

Zunächst wurden männliche C57BL/6N-Mäuse (n=10 pro Gruppe) entweder einem SHT unter Verwendung des hoch standardisierten Controlled Cortical Impact Models (CCI) oder einer Schein-Operation (Kraniotomie ohne Trauma) unterzogen. Anschließend wurde die Feinmotorik mittels des Beam-Walk-Tests, depressives Verhalten mit dem Tail-Suspension-Test und die Gedächtnisfunktion anhand des Barnes Maze gemessen. Die SHT-Mäuse wurden zusammen mit schein- und nicht-operierten Tieren zu den Zeitpunkten 30, 90, 180 und 360 Tage nach SHT untersucht. Die SHT Tiere zeigten im Vergleich zu den scheinoperierten und nichtoperierten Tieren eine signifikante Abnahme der Motorik und der Gedächtnisfunktion sowie ein progressiv depressives Verhalten. Histopathologische Veränderungen wurden immunhistochemisch ausgewertet und zeigten eine kontinuierliche Zunahme der Läsionsgröße sowie eine fortschreitende Atrophie der weißen Substanz und des Hippocampus, was auf eine durch das Trauma induzierte und langfristig aktive chronische Neurodegeneration hinweist (siehe Publikation I, S. 25).

Des Weiteren wurden mögliche pathophysiologische Mechanismen untersucht, welche diesem sekundären Hirnschaden zugrunde liegen könnten. Zunächst konzentrierten wir uns auf die Nekroptose, eine Form des regulierten Zelltods, die durch das sogenannte Nekrosom vermittelt wird, einem Eiweiß-Komplex der von den Rezeptor-Interaktionsproteinen (RIP) 1 und 3 gebildet wird. Männliche transgene RIP3, sowie RIP1 neuronale transgene Mäuse (n=8-10 pro Gruppe) und ihre entsprechenden Wildtyp-Kontrollen wurden einer CCI Trauma- oder Scheinoperation unterzogen und zusammen mit naiven Tieren zu den Zeitpunkten 15 Minuten, 1, 7, 30, 60 und 90 Tage

nach der Verletzung beobachtet. Zur Charakterisierung der posttraumatischen Hirnschädigung wurden repetitive serielle MRTs durchgeführt. Auf funktioneller Ebene wurden motorische Defizite mit dem Beam Walk Test untersucht, zudem wurden depressives Verhalten und die Gedächtnisfunktion wie zuvor beschrieben mehrfach im Verlauf beurteilt. Nach 90 Tagen wurden die Gehirne für die histopathologische Auswertung entnommen. Wir konnten zeigen, dass RIP1- und RIP3-defiziente Tiere im Vergleich zu ihren Wildtyp-Geschwistern signifikant geringere Läsionsvolumina sowie weniger Atrophie im Bereich des Hippocampus aufwiesen. Dies führte zu einer signifikanten Verbesserung der Gedächtnis- und Lernfunktion, hatte jedoch keinen Einfluss auf motorische Defizite oder das Motivationsverhaltens. Auf mikroskopischer Ebene zeigte sich eine Verringerung von reaktiver Astrogliose und Mikroglia-Aktivierung bei Knockout-Tieren, was darauf hindeutet, dass die beobachtete Protektion auf eine Abschwächung der chronischen Entzündung durch die RIP-Elimination zurückzuführen ist. Zusätzlich bot die Studie Hinweise darauf, dass die beobachteten Effekte mit einer geringeren Empfindlichkeit gegenüber blut-induzierter bedingter Toxizität zusammenhängen könnte (siehe Publikation II, S. 46).

In einem weiteren Projekt wurde ein intrazelluläre Zelltod-Mechanismus untersucht, der durch den acid sensing ion channel (ASIC) 1a vermittelt wird. Nach SHT kommt es aufgrund von Hypoxie und Elektrolyt-Störungen zu einer Absenkung des pH-Wertes im Hirnparenchym; dies wiederum aktiviert ASIC1a, was zum Kalziumeinstrom in neuronale Zellen führt und letztlich zusätzliche Zelltod-Mechanismen in Gang setzt. Männliche ASIC1a-Knockout-Mäuse sowie heterozygote und Wildtyp Geschwistertiere (n=10 pro Gruppe) wurden einem CCI Trauma unterzogen; 1, 7, 30, 60, 90 und 180 Tage nach SHT wurden MRT-Bildgebungen durchgeführt zur Beurteilung der posttraumatischen Schädigung. Auch hier wurde der funktionelle Status der Tiere mittels der oben genannten Test-Paradigmen bewertet und am Ende des Beobachtungszeitraums eine histopathologische Analyse der Gehirne durchgeführt. Wir konnten hier eine signifikante Reduktion der posttraumatischen Hirnschädigung sowie ein verbessertes funktionelles Ergebnis zeigen. Dies war ebenfalls mit einer Reduktion der chronisch entzündlichen Prozesse im Gehirn verbunden (siehe Publikation III, S. 71).

Zusammenfassend konnte einerseits ein standardisiertes Protokoll für die Untersuchung des langfristigen funktionellen, neurokognitiven, MR-morphologischen und histologischen Verlaufs nach experimentellem SHT etabliert werden. In zwei Folgeuntersuchungen wurden - basierend auf den so gewonnenen Erkenntnissen – zwei Pathomechanismen in Bezug auf ihre Wirkung auf den langfristigen Hirnschaden nach SHT untersucht. Diese Daten tragen zum besseren Verständnis der Pathophysiologie des posttraumatischen Hirnschadens bei und könnten in Zukunft helfen, die Schädigungsmechanismen besser zu verstehen und Moleküle oder Reaktionswege für zukünftige Therapien aufzudecken.

5. Paper I

Progressive Histopathological Damage Occurring Up to One Year after Experimental Traumatic Brain Injury Is Associated with Cognitive Decline and Depression-Like Behavior

Xiang Mao,^{1,2,*} Nicole A. Terpolilli,^{1-3,*} Antonia Wehn,^{1,2} Shiqi Cheng,^{1,2} Farida Hellal,^{1,2} Baiyun Liu,⁴ Burcu Seker,^{1,2} and Nikolaus Plesnila^{1,2}

¹Institute for Stroke and Dementia Research and ³Department of Neurosurgery, Munich University Hospital, Munich, Germany.

²Munich Cluster for Systems Neurology (SyNergy), Munich, Germany.

⁴Department of Neurosurgery, Beijing Tian Tan Hospital, Capital Medical University and China National Clinical Research Centre for Neurological Diseases, Beijing, China.

*The first two authors contributed equally.

Abstract

Increasing clinical and experimental evidence suggests that traumatic brain injury (TBI) is associated with progressive histopathological damage. The aim of the current study was to characterize the time course of motor function, memory performance, and depression-like behavior up to 1 year after experimental TBI, and to correlate these changes to histopathological outcome. Male C57BL/6N mice underwent controlled cortical impact (CCI) or sham operation, and histopathological outcome was evaluated 15 min, 24 h, 1 week, or 1, 3, 6, or 12 months thereafter (n = 12 animals per time point). Motor function, depression-like behavior, and memory function were evaluated concomitantly, and magnetic resonance imaging (MRI) was repeatedly performed. Naive mice (n = 12) served as an unhandled control group. Injury volume almost doubled within 1 year after CCI (p = 0.008) and the ipsilateral hemisphere became increasingly atrophic (p < 0.0001). Progressive tissue loss was observed in the corpus callosum (p = 0.007) and the hippocampus (p = 0.004) together with hydrocephalus formation (p < 0.0001). Motor function recovered partially after TBI, but 6 months after injury progressive depression-like behavior (p < 0.0001) and loss of memory function (p < 0.0001) were observed. The present study demonstrates that delayed histopathological damage that occurs over months after brain injury is followed by progressive depression and memory loss, changes also observed after TBI in humans. Hence, experimental TBI models in mice replicate long-term sequelae of brain injury such as post-traumatic dementia and depression.

Keywords: CCI; cognitive function; degeneration; head trauma; TBI

Introduction

Traumatic brain injury (TBI) is a major cause of death and permanent disability worldwide, especially in children and young adults.^{1,2} According to a World Health Organization (WHO) forecast, the incidence of severe TBI will significantly increase until 2030, further aggravating the huge socioeconomic burden caused by TBI.³

Because of improved emergency and critical care medicine, mortality after severe TBI is constantly declining in industrialized countries.^{4–6} However, it is increasingly recognized that TBI does not only acutely damage the brain, but has also long-term neurological and neuropsychiatric sequelae that sustainably affect the quality of life of TBI survivors.^{7,8} Symptom onset may occur years after the initial trauma, making correct diagnosis challenging and sometimes impeding patients from getting adequate medical support.⁹ Common symptoms are impaired fine motor skills, cognitive decline, and mood disorders.^{10,11} Further, it has been suggested that TBI predisposes patients to cognitive decline or even dementia.^{12–15} Mechanisms underlying these functional deficits in TBI patients may be progressive brain atrophy^{16,17} and hydrocephalus formation^{18–21} as a consequence of ongoing neuroinflammation.^{22,23} Post-mortem studies in athletes who sustained repetitive TBIs during their careers suggest that also extensive microfibrillary tangle formation caused by tau-protein aggregates and amyloid beta deposits may be involved in this process. So far, it has been established that inflammatory changes are one important factor for the development of chronic post-traumatic changes^{24–26}. The exact cellular and molecular mechanisms of chronic TBI are, however, not fully understood.

In contrast to research on humans, animal models of TBI are particularly suited for studying the mechanisms of chronic Injury severity can be tightly controlled, and injury progression can be studied not only in autopsy material, but also during the time course of the disease, thereby allowing mechanistic insight into the underlying pathophysiology. In fact, progressive neurodegeneration and tissue loss were elegantly demonstrated by magnetic resonance imaging (MRI) and by histopathology after controlled cortical injury (CCI), one of the most widely used TBI models.²⁶ However, compared with the extensively studied pathophysiological changes in the early post-traumatic period, comparatively little is known about the long-term functional consequences following experimental TBI. Therefore, the aim of the current study was to investigate whether functional deficits frequently observed in TBI patients months and years after injury, such as motor dysfunction, memory loss, or mood disorders, also occur after experimental TBI in mice.

Methods

All surgical procedures were performed in accordance with the guidelines of the animal care institutions of the University of Munich, and approved by the Bavarian government (protocol number 55.2-1-2532-44-2017). Results are reported according to the Animal Research: Reporting of *In Vivo* Experiments (ARRIVE) guidelines.²⁷ Animal care, husbandry, and health checks were performed according to the Federation for Laboratory Animal Science Associations (FELASA) recommendations.²⁸ Mice were randomly assigned to experimental groups. Surgical preparation, trauma, neurological testing, MRI scanning, and data analysis were performed by investigators blinded to the treatment of the animals. The following experimental groups and time points were examined: naive animals (non-traumatized; $n = 12$), sham surgery ($n = 12$), and post-traumatic groups evaluated at 15 min, 1, 7, 30, 90, 180, or 360 days after CCI ($n = 12$ each). Figure 1A shows a graphic summary of the experimental groups.

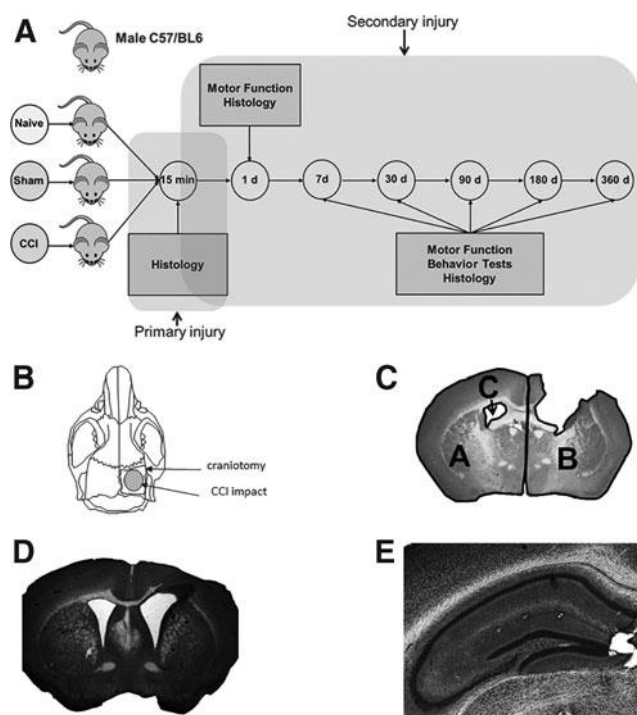


FIG. 1. Methodology. (A) Experimental design. (B) Position and size of craniotomy and controlled cortical impact (CCI). (C) Calculation of defect volume. (D) Exemplary section used for quantification of corpus callosum thickness. (E) Exemplary slide used for hippocampal volume determination.

CCI

TBI was induced by the previously described CCI method.^{29–31} Anesthesia was induced after injection of buprenorphine (100 mg/kg i.p., 30 min prior to surgery) by 1.2% isoflurane in 30% oxygen/70% air in spontaneously breathing animals. Briefly, after right parietal craniotomy (4 x 5 mm), the impact (tip size 3 mm) of our custom made CCI device (L. Kopacz, University of Mainz, Germany) was directly applied to the dura with 8 m/sec velocity, 1 mm impact depth, and 150 ms contact time (see Fig. 1B for schematic drawing). The craniotomy was closed immediately afterwards using histoacrylic glue. All surgical procedures were performed on a feedback-controlled heating pad (FHC, Bowdoin-ham, USA) that maintained core body temperature 37°C. In order to avoid post-operative hypothermia, animals were kept in an incubator heated to 32°C for 2 h. In the sham group, craniotomy was performed without applying the impact.

Outcome measures

Body weight. Body weight was measured immediately before CCI and every day after trauma for the first 7 days, then every month after trauma. Body weight is expressed in percent of pre-trauma body weight.

Beam walk assessment. As previously reported, the beam walking test is an adequate tool to test motor function after CCI, either alone³² or as part to the Neurological Severity Score.^{30, 31} The number of missteps of the hind paw and the time needed to cross the 1 m beam were recorded starting 3 days before trauma, and at 1, 3, and 7 days after trauma; subsequently, mice were tested every month until the end of the observation period.

Tail suspension test. The tail suspension test has been widely used to study depression-like behavior in mice^{33, 34}. The animal is suspended head down by the tail for 3 m under continuous video monitoring (EthoVision®XT, Noldus Information Technology, The Netherlands). The time the mouse moves in order to recover balance (mobility time) and the time the mouse does not move

any more (immobility time) are recorded. Longer immobility time indicates depression-like behavior. The test was performed 90, 180, 270, and 360 days after CCI.

Barnes maze test. The Barnes maze test is a paradigm to study spatial learning and memory in rodents.^{35,36} The test is performed on a brightly lit round platform (diameter 100 cm) that contains 20 identical holes (diameter 10 cm) spaced evenly around the perimeter of the platform. Below one of these apertures there is a box (20 · 5 · 3 cm) where the mouse can hide. The mouse learns where the box is located and the time the mouse needs to find the right aperture within the test duration of 180 sec is evaluated by video monitoring (EthoVision[®]XT, Noldus Information Technology, The Netherlands). Animals are trained daily for 5 days before the actual experiment.³⁶ The goal box location was the same in all testing runs. After CCI, the test is performed at days 90, 180, 270, and 360 after CCI.

MRI

MRI was performed in a small animal scanner (3T nanoScan[®] PET/MR, Mediso, Münster Germany with 25 mm internal diameter quadrature mouse head coil) at 15 min, 24 h, 7 days, and 1, 3, 6, 9, and 12 months after CCI. For scanning, mice were anesthetized with 1.2% isoflurane in 30% oxygen/70% air applied via a face mask. Respiratory rate and body temperature (37 – 0.5°C) were continuously monitored via an abdominal pressure-sensitive pad and rectal probe, and anesthesia was adjusted to keep them in a physiological range. The following sequences were obtained: coronal T2-weighted imaging (two-dimensional [2D] fast-spin echo [FSE], repetition time [TR]/echo time [TE] = 3000/57.1 ms, averages 14, resolution 167 x 100 x 500 μm^3), coronal T1-weighted imaging (2D FSE, TR/TE = 610/28,6 ms, averages 14, resolution 167 x 100 x 500 μm^3), and diffusion weighted imaging (DWI) (2D spin echo [SE], TR/TE = 1439/50 ms, averages 4, resolution 167 x 100 x 700 μm^3). MRI data were then post-processed using ImageJ; 14 sections surrounding the lesion were chosen for each data set, and the lesion area was measured using the polygon tool. Volume was then calculated using the equation $V = d \cdot (A_1/2 + A_2 + A_3 + A_n/2)$, with d being the distance between sections in mm and A being the measured area. Hemispheric volume was calculated by measuring the area of each hemisphere separately in all sections obtained; volume for each hemisphere was then calculated according the above-mentioned formula. Volume of the traumatized hemisphere is expressed as percentage of ipsilateral total hemispheric volume.

Histopathology

For histological evaluation 15 min, 24 h, 7 days, 1, 3, 6, and 12 months after CCI, coronal floating sections of the brain were prepared as previously described.³⁷ After transcardial perfusion with 0.9% NaCl followed by 4% paraformaldehyde (PFA) using a pressure-controlled perfusion system (Perfusion One, Leica Biosystems, Richmond, VA), brains were removed and stored in 4% PFA at 4°C for 12–16 h for post-fixation. Brains were stored in phosphate buffered saline (PBS) until further use. Fifty micrometer thick coronal sections were prepared using a vibratome (Leica VT1200S, Nussloch, Germany), starting 1000 μm behind the olfactory bulb; a total of 12 sequential coronal 50 μm thick sections were collected every 600 μm and stained with Cresyl violet.

Evaluation of defect volume. Gross examination revealed that tissue is lost in the contused area 7 days after CCI. Therefore, we did not determine contusion volume as previously described,^{30,32} but the defect area (Fig. 1C)^{32, 38} according to the following formula was: Defect Area (DA) = A (area contralateral hemisphere) – C (area contralateral ventricle) – B (area ipsilateral hemisphere).

The defect volume was then determined using the formula $V = d \cdot (DA1/2 + DA2 + DA3 + DA/2)$ with $d = 0.6$ (distance between two sections in mm).

Determination of gray and white matter atrophy, hydrocephalus, and hippocampal volume. Quantification of white matter/corpus callosum atrophy and hydrocephalus was performed as previously described.³⁹ Maximum corpus callosum thickness was assessed in a coronal section at bregma level by histomorphometry (see Fig. 1D for exemplary picture). Hemispheric atrophy was determined using one coronal section (bregma +1.0 mm) and expressing the area of the ipsilateral hemisphere as a percentage of contralateral hemisphere area. For assessment of hippocampal damage underneath the contusion, one coronal brain section (bregma -2.0 mm) was used to measure the total hippocampal area (see Fig. 1E for exemplary picture). Ventricle enlargement was assessed at the level of the lateral ventricles by histomorphometry (see Fig. 2A for exemplary pictures at 6 and 12 months after TBI).

Statistical analysis

Sample size calculations were performed using SigmaPlot (Version 13.0, Jandel Scientific, Erkrath, Germany) with the following parameters: α error = 0.05, β error = 0.2, standard deviation 22%, and a target effect size of 30%. Because of the group size, non-parametrical tests were used for further analysis. Hence, the Mann–Whitney rank sum test was used for comparisons between two groups and the Kruskal–Wallis test with Student–Newman–Keuls post-hoc test was performed for multi-group comparisons. Differences between groups were considered statistically significant at $p < 0.05$. All data are expressed as mean – standard deviation (SD).

Results

Histopathological changes

Brains sampled 15 min and 24 h after TBI showed a hemorrhagic contusion upon macroscopic inspection, whereas brains from naïve or sham-operated mice (data not shown) had no damage (Fig. 3A). Already 7 days after TBI the contused tissue was removed and replaced by a cyst filled with cerebrospinal fluid (CSF). The volume of this cyst was significantly smaller than the initial contusion and the contusion observed 7 days after injury (Fig. 3A). This finding is well in line with previous reports from our laboratory and with the literature.^{26,38} With time, the volume of the cyst increased, and 1 year after TBI the volume and the depth of the cyst increased so much that white matter structures became visible at the bottom of the cavity (Fig. 3A). When quantified by histological analysis, the volume of the defect was found to significantly increase in an almost linear fashion until 1 year after trauma (Fig. 3B, see Supplementary Fig. S1 for exemplary coronal sections; 7 days vs. 30 days, 90 days, 180 days, and 360 days: $p < 0.05$; 180 days vs. 7 days, 30 days, and 90 days: $p < 0.05$). Although the cyst increased in size, we observed a pronounced atrophy of the whole traumatized hemisphere over time (Fig. 3C) at 7 days after trauma (83 – 1% of the contralateral hemisphere) which continued to 74 – 5% at 180 days and 68 – 3% at 360 days after TBI (day 7 vs. all later time points: $p < 0.05$; 30 days, 90 days, and 180 days vs. 360 days: $p < 0.05$). At the same time the size of the ipsilateral ventricle enlarged significantly (Fig. 2A). At 7 days after TBI, there was asymmetrical hydrocephalus resulting in enlargement of the

ventricle area ipsilateral to the trauma (Fig. 2B). The thickness of the corpus callosum ipsilateral to the injury also decreased significantly over time (Fig. 2C).

Ninety days after the trauma only a slight asymmetry between the left and the right corpus callosum was visible, but at later time points the ipsilateral corpus callosum became significantly narrower than the contralateral one (180 days after CCI: $p = 0.024$, 360 days after CCI: $p = 0.007$). Lastly, we evaluated hippocampal damage as a potential morphological correlate for memory deficits (Fig. 4). Although in most cases the hippocampus is well preserved within the first 24 h after TBI (data not shown), the ipsilateral hippocampus was completely absent 360 days after TBI (Fig. 4A). This process was initiated within the 1st week after trauma, because already at this

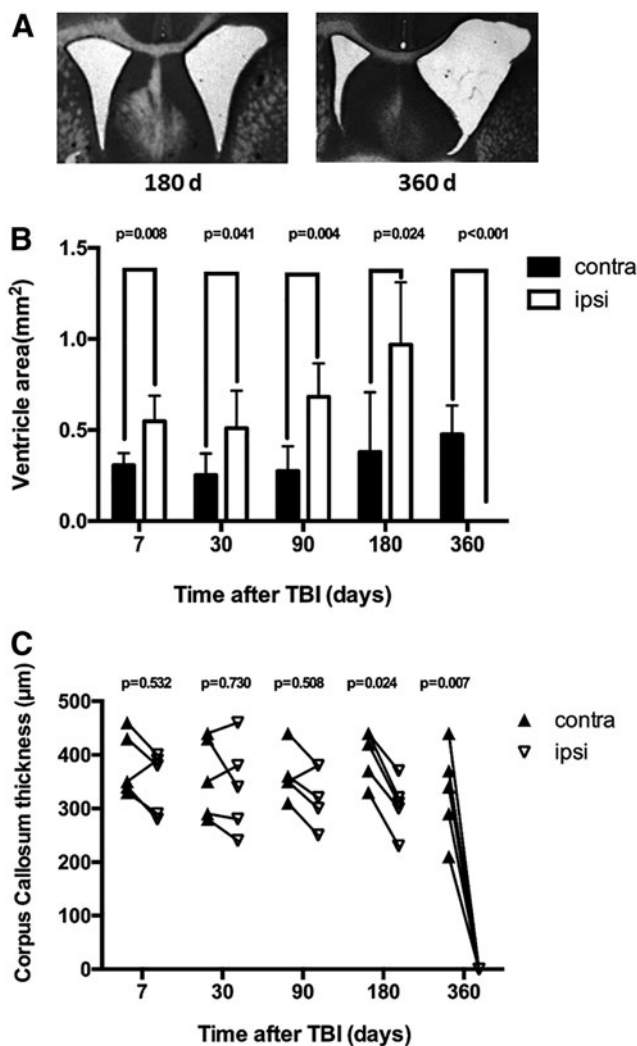


FIG. 2. Controlled cortical impact (CCI) leads to progressive ventricular enlargement/ hydrocephalus *ex vacuo* and white matter atrophy. (A) Exemply slides demonstrating progressive and asymmetrical ventricular expansion in the traumatized hemisphere 180 or 360 days after CCI. (B) As early as 7 days after CCI, the ipsilateral ventricle is significantly enlarged compared with the non-traumatized side; this asymmetry increases over time until the ventricle merges with the defect zone in most cases. (C) Corpus callosum width in the traumatized hemisphere decreases over time; this atrophy, however, takes longer to develop than global hemispheric atrophy: significant reduction of corpus callosum thickness occurs at 6 and 12 months after CCI.

early time point the area of the ipsilateral hippocampus was significantly reduced by *75% ($p < 0.0001$). Hippocampal atrophy aggravated over time until no ipsilateral hippocampal tissue could be detected 360 days after CCI (7 days vs. 360 days, $p = 0.007$, Fig. 4B). Concomitantly, the contralateral hippocampus also became atrophic, but to a far lesser degree than the ipsilateral one ($p = 0.004$ 7 vs. 360 days).

MRI

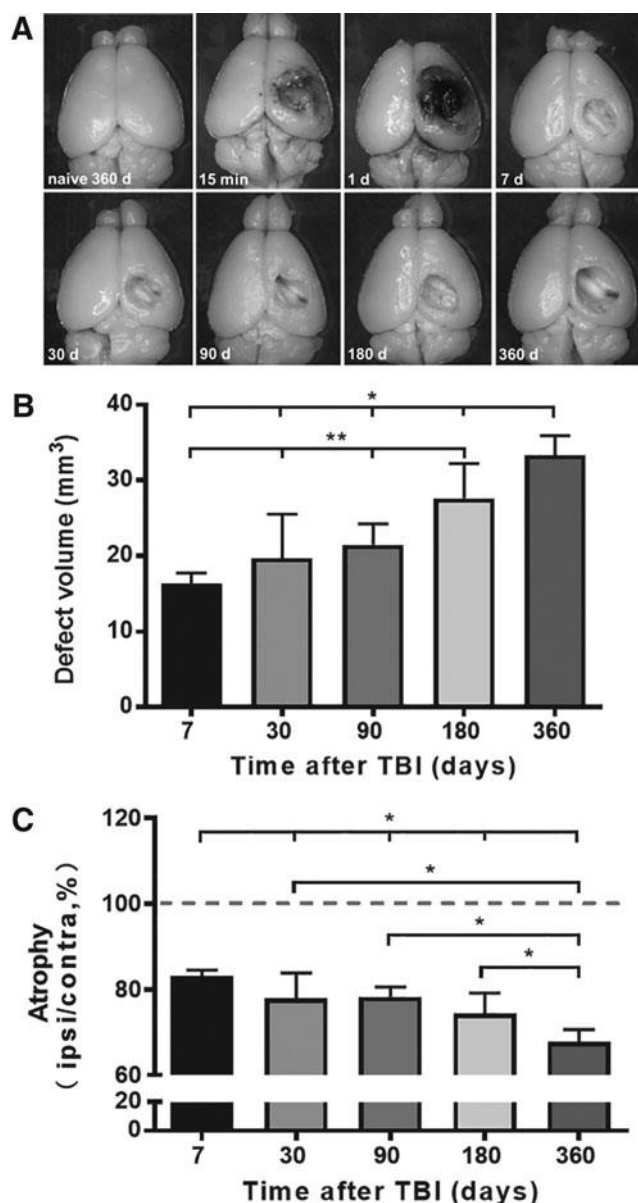


FIG. 3. Defect volume and whole brain atrophy over time.

(A) Exemplary brains. (B) Defect volume almost linearly increases over time reaching a maximum at 360 days. (C) Further, the traumatized hemisphere is undergoing significant atrophy over time. ($n = 12$ each, mean – standard deviation (SD), $*p < 0.05$ vs. 360 days; $**p < 0.05$ vs. 180 days).

MRI scanning closely mirrored the results obtained by histology. The exemplary timeline of T2-weighted scans obtained from 15 min until 12 months after CCI displayed in Figure 5A shows an increasing defect formation over time. Quantification (Fig. 5B) reveals differences compared with histological examination. Although at earlier time points lesion quantification is complicated because of tissue necrosis, edema, and hemorrhage resulting in volumes higher than those in histology, from 1 month after TBI on, the same progression of defect size was evident (1 months vs. 6, 9, and 12 months: $p < 0.01$). Atrophy of the traumatized hemisphere was also visible on MRI scans. After initial brain edema formation with subsequent swelling, which led to an increase of the ipsilateral versus the non-traumatized hemisphere, there was progressive atrophy to approximately the same level observed in histology (71 – 2.6% of contralateral hemisphere volume, 7 days, 1 month, and 3 months vs. 360 days: $p < 0.01$).

Functional outcome

No epileptic seizures were observed during routine checkups, handling, or neurological testing of traumatized, sham-operated, or naive animals. All animals survived until the end of the respective observation period.

Naive animals continuously gained weight during the observation period of 1 year (Supplementary Fig. S2). Sham-operated and traumatized mice, however, gained significantly less weight and only sham-operated mice started to recover their body weight 270 days after TBI and reached the level of naive mice at the end of the observation period; traumatized animals had a flatter weight gain curve and did not reach the body weight of naive or sham-operated mice (naive: 41.3 – 1.9 g, sham: 40.4 – 2.3 g, CCI: 34.4 – 1.5 g; $p < 0.0001$ vs. naive, $p < 0.0001$ vs. sham).

Motor function as assessed by the beam walk paradigm was not different among groups before surgery (Fig. 6A and B). After TBI, the time needed to cross the beam (Fig. 6A) as well as the number of missteps (Fig. 6B), increased massively in traumatized animals, whereas naive mice and sham-operated animals performed as before trauma. The performance of traumatized animals improved substantially within 1 month after CCI; however, motor function was still significantly impaired as compared with pre-trauma levels and with both control groups. Thirty days after TBI, the initial phase of improvement ended and traumatized animals suffered a residual and stable motor dysfunction until the end of the observation period (CCI vs. own pre-trauma baseline, $p < 0.0001$; CCI 360 days vs. naive 360 days, $p < 0.0001$; CCI 360 days vs. sham 360 days, $p < 0.0001$).

In order to detect and quantify depression-like behavior, we used the Tail Hanging Test (Fig. 7). Before trauma, there was no difference in mobility time among groups (naive: 33.0 – 22.2 sec, sham: 31.0 – 9.7 sec, CCI: 32.6 – 7.4 sec). Over the course of the experiment, mobility time declined in all groups, most probably as a result of habituation and/or weight gain; however, sham-operated as well as traumatized animals displayed shorter mobility times 90 days after TBI (sham

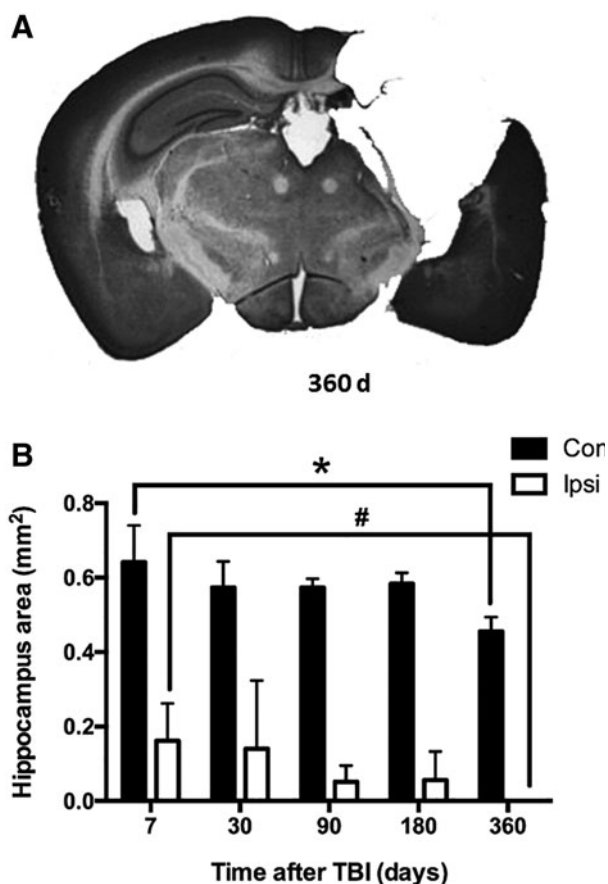


FIG. 4. Hippocampal damage. (A) Exemplary slide 360 days after traumatic brain injury (TBI) with highly atrophied hippocampus. (B) Quantification. As early as 7 days after controlled cortical impact (CCI) there is significant asymmetry between the hippocampus areas; this asymmetry further develops until the ipsilateral hippocampus almost vanishes.

vs. naive, $p = 0.05$; CCI vs. naive, $p = 0.05$). As with body weight, sham-operated animals recovered to the level of naive mice 1 year after injury, but mobility time of mice subjected to TBI further declined over time, and 360 days after trauma

all traumatized mice remained completely immobile when hung head-down by the tail (CCI vs. sham, $p < 0.0001$; CCI vs. naive, $p = 0.0002$).

Finally, we assessed orientation, memory, and learning using the Barnes Maze paradigm. Exemplary heat maps of the movement of single mice obtained 270 days after TBI illustrate that naive (top panel) and sham-operated animals (middle panel) were able to find the home-box quickly and with no delay. In contrast, the traumatized mouse (bottom panel) found the home box only after extensive, random searching (Fig. 8A). This loss of memory function is also represented by the quantitative analysis: naive and sham-operated mice showed normal memory function in terms of the time needed to find the home-box (latency), the distance travelled to find the home-box (distance traveled), and the search speed (velocity), whereas traumatized mice showed a significantly reduced performance of all investigated parameters already 3 months after injury (Fig. 8B–D). Despite the fact that the distance travelled remained almost stable over time, the latency to find the home-box increased 180 days after TBI and reached a maximum 1 year after injury, suggesting progressive loss of memory function in brain injured mice starting 6 months after trauma.

Discussion

In the current study, we assessed the behavioral and histopathological effects of a single cortical contusion up to 1 year after experimental TBI in mice. On the histopathological level, we described the time course of gray and white matter atrophy, the loss of hippocampal tissue, and the formation of hydrocephalus. This was corroborated by MRI; the differences observed, especially in the early phase after TBI, most probably are caused by residual brain swelling, possible hemorrhagic tissue within the contusion, and the fact that MRI scans were performed on many more levels than histology. On the functional level, we demonstrated improvement of motor dysfunction over time, but loss of memory and depression-like behavior beginning 6 months after and progressing up to 1 year after TBI. Because brain atrophy, progressive loss of memory function, and delayed depression are also features of TBI in humans, the current study underpins the clinical and translational value of experimental TBI models in rodents, provided sufficiently long observation periods are used.

For decades, acute pathophysiological processes were the main focus of clinical and experimental TBI research, as it was believed that acute traumatic brain damage is the main determinant of clinical outcome. In recent years, however, there is increasing experimental and clinical evidence that an acute injury to the brain may also be the trigger for delayed processes that may result in additional and long-lasting sequelae. The most common neurological manifestations after TBI are motor and cognitive deficits.^{40–44} Neuropsychological disorders after TBI are more common when TBI occurred in early adulthood, and seems to depend on trauma severity.^{43–45} Further, a single history of TBI seems to be a predisposing factor for neurodegenerative disorders such as Parkinson's disease and dementia.^{7,13,14} In some cases post-traumatic dementia was linked to tau and *b*-amyloid deposits,^{12,46,47} specifically in contact-sports athletes^{48–50} and military veterans;^{51,52} however, amyloid plaques were also found in one third of long-term survivors of a single severe TBI.⁴⁷

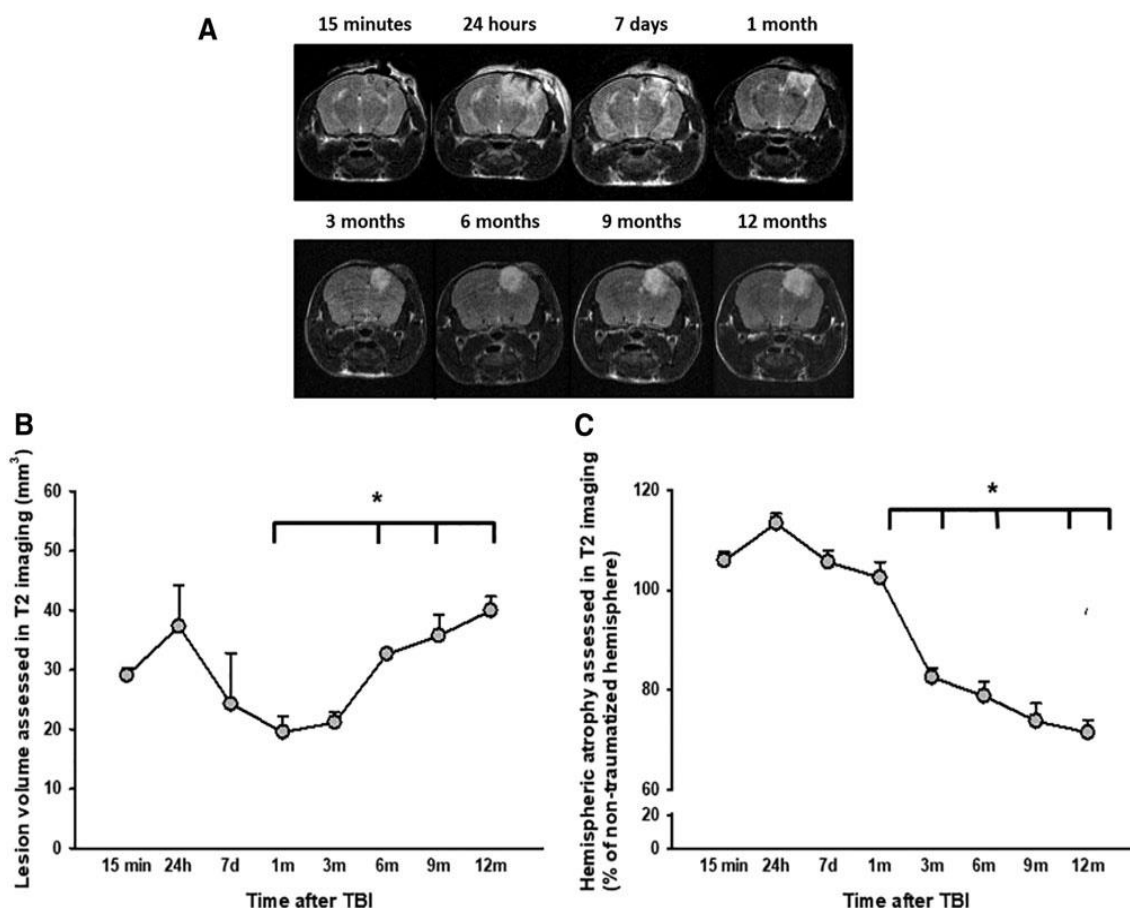


FIG. 5. Magnetic resonance imaging (MRI). (A) Exemplary coronal T2 scans at different time points after traumatic brain injury (TBI). (B) Quantification of lesion volume in T2 weighed imaging. Although at early time points after controlled cortical impact (CCI) T2 quantified lesion volume differs from histological evaluation, MRI scanning also shows significant enlargement of lesion/defect volume ($n = 12$ each, mean – standard deviation (SD), $*p < 0.01$ vs. 1 month) (C) MR-morphological assessment of hemispheric volume of the traumatized versus the contralateral side ($n = 12$ each, mean – SD, $*p < 0.01$).

Despite this clear epidemiological and clinical evidence, most knowledge about chronic traumatic encephalopathy (CTE), chronic post-traumatic brain damage, and related long-term sequelae of TBI derives from human autopsy material which, however, allows only limited insight into pathophysiological mechanisms. Hence, specifically when trying to establish novel therapeutic approaches, experimental studies are the only possible approach.⁵³ Of the >1400 experimental studies assessing outcome listed in PubMed, however, only a minority evaluated post-traumatic brain damage long-term (> 7–30 days after insult); that is, over periods of time covering a significant proportion of the animal's lifespan.^{26,54–69} Recent promising studies already detected important roles for inflammatory processes^{55,64,65} and *cis*-phosphorylated tau^{62,66–68,70} and identified potential target pathways for a possible chronic TBI treatment.

In order to expand our knowledge about the chronic sequelae of TBI, the current study was therefore not only designed to evaluate histopathological parameters up to 1 year after TBI, but also to assess behavioral changes in traumatized, sham-operated, and age-matched naive animals. This approach allowed us to correlate the time course of histopathological and behavioral changes after TBI and to dissect these changes from findings that occurred only as a result of surgery or anesthesia.

The most pronounced histopathological observation we made was progressive loss of brain tissue not only at the lesion, but also in brain areas farther away from the contusion, such as the rostral corpus callosum. Atrophy is a well-known feature of chronic post-traumatic brain damage in patients,^{16,17} and its severity correlates with the development and severity of cognitive deficits,^{16,44,71} as also shown in the current study. The same seems to be true for white matter damage, which also correlates with the occurrence and severity of cognitive defects.⁷² In our study, we detected not only atrophy of the ipsilateral hemisphere, but also atrophy of *trans*-hemispheric white matter tracts as evidenced by corpus callosum shrinkage. This finding is in line with radiomorphological and histopathological findings in humans, and is also supported by previous experimental series.^{55,60,61} Hemispheric atrophy, which was detected in the present study from day 7 on, seems to precede corpus callosum/white matter defects, which became evident only later than 6 months after the insult. A similar time course of brain tissue atrophy was also reported after mild experimental TBI,⁶² and recently by diffusion tensor imaging (DTI) after CCI.⁵⁵

Ventricular enlargement/hydrocephalus is a common finding after TBI.^{18,19} In the early phase after TBI, hydrocephalus occurs mainly because of obstruction of CSF passage or impaired absorption caused by hemorrhage. Later after TBI, ventricular enlargement is most often considered to be an *ex vacuo* phenomenon caused by tissue atrophy. This is the most likely reason why late hydrocephalus after TBI is associated with adverse neurological outcome.^{21,71} In our model, we detected ventricular asymmetry starting as early as 1 week after TBI and progressing until the end of the observation period. In our severe lesion model, tissue loss was quite pronounced toward the end of the experiment, supporting the *ex vacuo* theory. Further, we did not detect any midline shift indicating increased intracranial pressure (ICP) at any time after TBI. A very severe loss of brain tissue was also observed in the ipsi- and contralateral hippocampus, a finding also commonly present in TBI survivors⁷³ and in previous experimental studies.^{55,56,60} Post-traumatic hippocampal atrophy has been linked to memory deficits⁷⁴⁻⁷⁷ as well as to the occurrence of mood disorders,⁷⁸ and may therefore be the (most relevant) pathophysiological correlate for the progressive behavioral abnormalities observed in the Barnes Maze and the Tail Suspension tests seen in this study. As cognitive deficits and mood disorders are among the main reasons for TBI patients not to return to their previous occupations,⁷⁹ it is of the utmost importance that an experimental model of chronic TBI reproduce such a deficit.

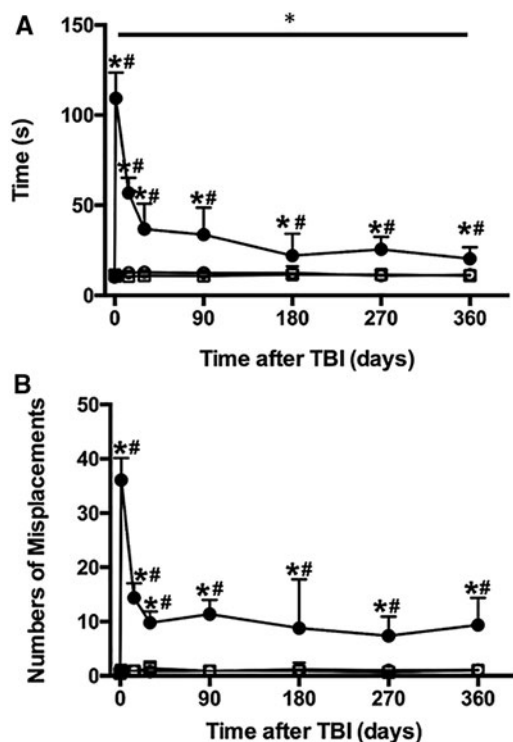


FIG. 6. Motor function after experimental traumatic brain injury (TBI) as assessed by the Beam Walk test. (A) Directly after trauma there is a massive increase in the time needed to cross the beam and (B) in the number of missteps; the initial massive deterioration recovers within 1 month, but controlled cortical impact (CCI) animals neither reach their pre-trauma baseline levels nor can they match the naive or sham control animals. There is a significant difference to both control groups that can be observed until 12 months after TBI. ($n = 12$ each, mean – standard deviation (SD); * $p < 0.05$)

Memory functions are frequently impaired after TBI in humans.^{40–42} Accordingly, cognitive tests are frequently performed in experimental studies investigating long-term outcome after TBI. Among the most widely used and accepted tests to assess memory function in rodents are the Morris Water Maze⁸⁰ and the Barnes Maze.^{81,82} Multiple reports described short-term memory impairments 4–6 weeks after CCI, starting as early as 2 weeks after CCI, but only a few studies provide data for time points later than 6 months or perform repetitive and long-term investigations over time in the same cohort of animals. Albayram and coworkers,⁶⁷ Luo and coworkers,⁶³ Ferguson and coworkers,⁷⁰ and Pischiutta⁵⁵ found neurocognitive deficits 6 months after TBI. Significant memory impairments were reported 205 days after CCI⁸³ and for up to 1 year after experimental trauma.^{57,84,85} In a very recent study, cognitive impairment as assessed by contextual fear conditioning was absent at 2 weeks, but present in untreated CCI mice 20 months after TBI compared with sham animals;⁶⁹ however, there is no information about the time course of memory decline between these two time points. In the present study, we detected a significantly increased latency to find the target area 3 months after CCI. In the further course of the experiment (at 6, 9, and 12 months after CCI) memory function further deteriorated in the same cohort of animals, indicating progressive memory deficits.

Motor function was assessed by the Beam Walk Test and deteriorated most pronouncedly during the 1st week after TBI, but recovered quickly thereafter as also observed by others.^{83,86,87} Recovery was not complete, and persistent motor deficits were observed for up to 1 year after TBI. These motor deficits are in line with observations in patients, where motor deficits are also most pronounced in the early phase after TBI, but may persist at a lesser degree together with postural instability for years.^{88–91}

Depressive symptoms, mood instability, and lack of impetus are common symptoms after TBI of all severities in humans. Neuro- behavioral deficits have been increasingly reported to occur already after mild TBI and may significantly affect quality of life and decrease the frequency of patients' returning to work.^{92,93} Although quite common in humans, depression and depressive symptoms occurring later than 4 weeks after trauma have been less studied in experimental TBI models than other, more easily quantifiable deficits (e. g., paresis)

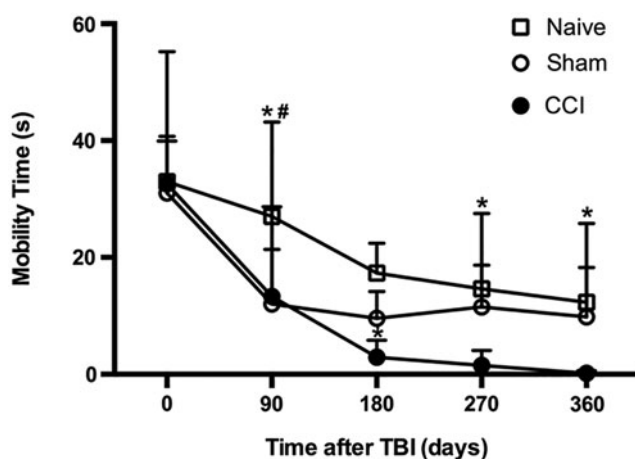


FIG. 7. Depression-like behavior after controlled cortical impact (CCI) as assessed by the Tail Suspension Test. Mobility time, the surrogate for depressive behavior, is reduced over time in all groups (most probably a habituation phenomenon). All operated animals spend less time mobile than the naive controls 3 months after surgery; however, whereas sham-operated mice recover and reach the levels of non-traumatized animals by day 180 after trauma, CCI mice further deteriorate to significantly worse levels than the sham and naive controls. (n = 12 each, mean – standard deviation (SD); *p < 0.05 vs. naive, #p < 0.05 vs. sham group).

as depressive symptoms are challenging to assess.⁹⁴ So far, depression-like behavior was not consistently found up to 3 months after TBI;^{95–102} as with motor and cognitive symptoms, time points later than 3 months have been little investigated and yielded conflicting results,^{100,103,104} perhaps facilitated by small group sizes and single point investigations. In the present study, we found significant depression-like behavior in our mice beginning 6 months after TBI. Six and 9 months after TBI the mobility time was reduced; however, 1 year after TBI, traumatized mice did not try at all to straighten up when suspended by the tail. These results suggest that mice exhibit progressive and severe depression-like behavior after TBI. Further, these results stress the importance and necessity of a long observation period in order to achieve stable and reproducible results and to adequately assess the role of neurobehavioral symptoms.

Conclusion

In conclusion, the present study observing mice up to 1 year after induction of a cortical contusion adequately reproduces key behavioral and histopathological features of TBI in humans, such as progressive loss of memory function, progressive depression-like behavior, sustained motor deficits, progressive brain and hippocampal atrophy, and progressive white matter damage. For this, we used a large cohort of animals that were assessed repetitively over time; further, each time point when neurobehavioral deficits were assessed (15 min until 12 months) is correlated with histopathological findings for each time point. Our results suggest that the mechanisms of long-term sequelae of TBI, so far unrecognized to be present in animal models, such as progressive memory loss and progressive depression, can be investigated experimentally in the future.

Funding Information

The study was supported by the Friedrich Baur Foundation (#60/ 17, NAT) and by the Federal Ministry for Education and Research (Bundesministerium für Bildung und Forschung, BMBF, grant # 01EW1502A, NP). X.M. was supported by the China Scholarship Council (grant #201508080072) and the National Natural Science Cultivate Foundation of China (grant #2016KJ12).

Author Disclosure Statement

No competing financial interests exist.

References

1. Nguyen, R., Fiest, K.M., McChesney, J., Kwon, C.S., Jette, N., Frolkis, A.D., Atta, C., Mah, S., Dhaliwal, H., Reid, A., Pringsheim, T., Dykeman, J., and Gallagher, C. (2016). The international incidence of traumatic brain injury: a systematic review and meta-analysis. *Can. J. Neurol. Sci.* 43, 774–785.
2. Thurman, D.J. (2016). The epidemiology of traumatic brain injury in children and youths: a review of research since 1990. *J. Child Neurol.* 31, 20–27.
3. World Health Organization (2018). Projections of mortality and causes of death, 2015 and 2030. <https://www.who.int/healthinfo/globalburdendisease/projections20152030/en/> (last accessed July 24, 2018).
4. Nagata, I., Abe, T., Uchida, M., Saitoh, D., and Tamiya, N. (2018). Ten-year in-hospital mortality trends for patients with trauma in Japan: a multicentre observational study. *BMJ Open* 8, e018635.
5. Di, S.S., Gambale, G., Coccolini, F., Catena, F., Giorgini, E., Ansaloni, L., Amadori, N., Coniglio, C., Giugni, A., Biscardi, A., Magnone, S., Filicori, F., Cavallo, P., Villani, S., Cinqantini, F., Annicchiarico, M., Gordini, G., and Tugnoli, G. (2014). Changes in the outcomes of severe trauma patients from 15-year experience in a Western European trauma ICU of Emilia Romagna region (1996–2010). A population cross-sectional survey study. *Langenbecks Arch. Surg.* 399, 109–126.
6. Curtis, K.A., Mitchell, R.J., Chong, S.S., Balogh, Z.J., Reed, D.J., Clark, P.T., D'Amours, S., Black, D.A., Langcake, M.E., Taylor, C.B., McDougall, P., and Cameron, P.A. (2012). Injury trends and mortality in adult patients with major trauma in New South Wales. *Med. J. Aust.* 197, 233–237.
7. Wilson, L., Stewart, W., Dams-O'Connor, K., Diaz-Arrastia, R., Horton, L., Menon, D.K., and Polinder, S. (2017). The chronic and evolving neurological consequences of traumatic brain injury. *Lancet Neurol.* 16, 813–825.
8. Masel, B.E., and DeWitt, D.S. (2010). Traumatic brain injury: a disease process, not an event. *J. Neurotrauma* 27, 1529–1540.
9. Schulz-Heik, R.J., Poole, J.H., Dahdah, M.N., Sullivan, C., Adamson, M.M., Date, E.S., Salerno, R., Schwab, K., and Harris, O. (2017). Service needs and barriers to care five or more years after moderate to severe TBI among Veterans. *Brain Inj.* 31, 1287–1293.
10. Perry, D.C., Sturm, V.E., Peterson, M.J., Pieper, C.F., Bullock, T., Boeve, B.F., Miller, B.L., Guskiewicz, K.M., Berger, M.S., Kramer, J.H., and Welsh-Bohmer, K.A. (2016). Association of traumatic brain injury with subsequent neurological and psychiatric disease: a meta-analysis. *J. Neurosurg.* 124, 511–526.
11. Bryant, R.A., O'Donnell, M.L., Creamer, M., McFarlane, A.C., Clark, C.R., and Silove, D. (2010). The psychiatric sequelae of traumatic injury. *Am. J. Psychiatry* 167, 312–320.

12. Guo, Z., Cupples, L.A., Kurz, A., Auerbach, S.H., Volicer, L., Chui, H., Green, R.C., Sadvnick, A.D., Duara, R., DeCarli, C., Johnson, K., Go, R.C., Growdon, J.H., Haines, J.L., Kukull, W.A., and Farrer, L.A. (2000). Head injury and the risk of AD in the MIRAGE study. *Neurology* 54, 1316–1323.
13. Vespa, P. (2017). Traumatic brain injury is a longitudinal disease process. *Curr. Opin. Neurol.* 30, 563–564.
14. Rasmusson, D.X., Brandt, J., Martin, D.B., and Folstein, M.F. (1995). Head injury as a risk factor in Alzheimer's disease. *Brain Inj.* 9, 213–219.
15. Fleming, S., Oliver, D.L., Lovestone, S., Rabe-Hesketh, S., and Giora, A. (2003). Head injury as a risk factor for Alzheimer's disease: the evidence 10 years on; a partial replication. *J. Neurol. Neurosurg. Psychiatry* 74, 857–862.
16. Reider-Groswasser, I., Cohen, M., Costeff, H., and Groswasser, Z. (1993). Late CT findings in brain trauma: relationship to cognitive and behavioral sequelae and to vocational outcome. *AJR Am. J. Roentgenol.* 160, 147–152.
17. MacKenzie, J.D., Siddiqi, F., Babb, J.S., Bagley, L.J., Mannon, L.J., Sinson, G.P., and Grossman, R.I. (2002). Brain atrophy in mild or moderate traumatic brain injury: a longitudinal quantitative analysis. *AJNR Am. J. Neuroradiol.* 23, 1509–1515.
18. Cardoso, E.R. and Galbraith, S. (1985). Posttraumatic hydrocephalus—a retrospective review. *Surg. Neurol.* 23, 261–264.
19. Guyot, L.L., and Michael, D.B. (2000). Post-traumatic hydrocephalus. *Neurol. Res.* 22, 25–28.
20. Honeybul, S., and Ho, K.M. (2012). Incidence and risk factors for post-traumatic hydrocephalus following decompressive craniectomy for intractable intracranial hypertension and evacuation of mass lesions. *J. Neurotrauma* 29, 1872–1878.
21. Mazzini, L., Campini, R., Angelino, E., Rognone, F., Pastore, I., and Oliveri, G. (2003). Post-traumatic hydrocephalus: a clinical, neuro-radiologic, and neuropsychologic assessment of long-term outcome. *Arch. Phys. Med. Rehabil.* 84, 1637–1641.
22. Ramlackhansingh, A.F., Brooks, D.J., Greenwood, R.J., Bose, S.K., Turkheimer, F.E., Kinnunen, K.M., Gentleman, S., Heckemann, R.A., Gunanayagam, K., Gelosa, G., and Sharp, D.J. (2011). Inflammation after trauma: microglial activation and traumatic brain injury. *Ann. Neurol.* 70, 374–383.
23. Johnson, V.E., Stewart, J.E., Begbie, F.D., Trojanowski, J.Q., Smith, D.H., and Stewart, W. (2013). Inflammation and white matter degeneration persist for years after a single traumatic brain injury. *Brain* 136, 28–42.
24. Ritzel, R.M., Doran, S.J., Barrett, J.P., Henry, R.J., Ma, E.L., Faden, A.I., and Loane, D.J. (2018). Chronic alterations in systemic immune function after traumatic brain injury. *J. Neurotrauma* 35, 1419–1436.
25. Faden, A.I., and Loane, D.J. (2015). Chronic neurodegeneration after traumatic brain injury: Alzheimer disease, chronic traumatic encephalopathy, or persistent neuroinflammation? *Neurotherapeutics* 12, 143–150.
26. Loane, D.J., Kumar, A., Stoica, B.A., Cabatbat, R., and Faden, A.I. (2014). Progressive neurodegeneration after experimental brain trauma: association with chronic microglial activation. *J. Neuro-pathol. Exp. Neurol.* 73, 14–29.
27. Kilkenney, C., Browne, W.J., Cuthill, I.C., Emerson, M., and Altman, D.G. (2010). Improving bioscience research reporting: the ARRIVE guidelines for reporting animal research. *PLoS Biol* 8, e1000412.

-
28. Guillen, J. (2012). FELASA Guidelines and Recommendations. *J. Am. Assoc. Lab. Anim. Sci.* 51, 311–321.
 29. Engel, D.C., Mies, G., Terpolilli, N.A., Trabold, R., Loch, A., De Zeeuw, C.I., Weber, J.T., Maas, A.I., and Plesnila, N. (2008). Changes of cerebral blood flow during the secondary expansion of a cortical contusion assessed by ¹⁴C-iodoantipyrine autoradiography in mice using a non-invasive protocol. *J. Neurotrauma* 25, 739–753.
 30. Terpolilli, N.A., Zweckberger, K., Trabold, R., Schilling, L., Schinzel, R., Tegtmeier, F., and Plesnila, N. (2009). The novel nitric oxide synthase inhibitor 4-amino-tetrahydro-L-biopterine prevents brain edema formation and intracranial hypertension following traumatic brain injury in mice. *J. Neurotrauma*. Terpolilli, N.A., Kim, S.W., Thal, S.C., Kuebler, W.M., and Plesnila, N. (2013). Inhaled nitric oxide reduces secondary brain damage after traumatic brain injury in mice. *J. Cereb. Blood Flow Metab.* 33, 311–318.
 31. Zweckberger, K., Stoffel, M., Baethmann, A., and Plesnila, N. (2003). Effect of decompression craniotomy on increase of contusion volume and functional outcome after controlled cortical impact in mice. *J. Neurotrauma* 20, 1307–1314.
 32. Steru, L., Chermat, R., Thierry, B., and Simon, P. (1985). The tail suspension test: a new method for screening antidepressants in mice. *Psychopharmacology (Berl)* 85, 367–370.
 33. Cryan, J.F., Mombereau, C., and Vassout, A. (2005). The tail suspension test as a model for assessing antidepressant activity: review of pharmacological and genetic studies in mice. *Neurosci. Biobehav. Rev.* 29, 571–625.
 34. Fox, G.B., Fan, L., LeVasseur, R.A., and Faden, A.I. (1998). Effect of traumatic brain injury on mouse spatial and nonspatial learning in the Barnes circular maze. *J. Neurotrauma* 15, 1037–1046.
 35. Attar, A., Liu, T., Chan, W.T., Hayes, J., Nejad, M., Lei, K., and Bitan, G. (2013). A shortened Barnes maze protocol reveals memory deficits at 4-months of age in the triple-transgenic mouse model of Alzheimer's disease. *PLoS. One* 8, e80355.
 36. Ghosh, M., Balbi, M., Hellal, F., Dichgans, M., Lindauer, U., and Plesnila, N. (2015). Pericytes are involved in the pathogenesis of cerebral autosomal dominant arteriopathy with subcortical infarcts and leukoencephalopathy. *Ann. Neurol.* 78, 887–900.
 37. Zweckberger, K., Eros, C., Zimmermann, R., Kim, S.W., Engel, D., and Plesnila, N. (2006). Effect of early and delayed decompressive craniectomy on secondary brain damage after controlled cortical impact in mice. *J. Neurotrauma* 23, 1083–1093.
 38. Buhler, D., Azghandi, S., Schuller, K., and Plesnila, N. (2015). Effect of decompressive craniectomy on outcome following subarachnoid hemorrhage in mice. *Stroke* 46, 819–826.
 39. Willmott, C., Ponsford, J., Hocking, C., and Schonberger, M. (2009). Factors contributing to attentional impairments after traumatic brain injury. *Neuropsychology* 23, 424–432.
 40. Selassie, A.W., Zaloshnja, E., Langlois, J.A., Miller, T., Jones, P., and Steiner, C. (2008). Incidence of long-term disability following traumatic brain injury hospitalization, United States, 2003. *J. Head Trauma Rehabil.* 23, 123–131.
 41. Dymowski, A.R., Owens, J.A., Ponsford, J.L., and Willmott, C. (2015). Speed of processing and strategic control of attention after traumatic brain injury. *J. Clin. Exp. Neuropsychol.* 37, 1024–1035.
 42. Draper, K., and Ponsford, J. (2008). Cognitive functioning ten years following traumatic brain injury and rehabilitation. *Neuropsychology* 22, 618–625.
 43. Dikmen, S.S., Corrigan, J.D., Levin, H.S., Machamer, J., Stiers, W., and Weisskopf, M.G. (2009). Cognitive outcome following traumatic brain injury. *J. Head Trauma Rehabil.* 24, 430–438.

44. Sariaslan, A., Sharp, D.J., D'Onofrio, B.M., Larsson, H., and Fazel, S. (2016). Long-term outcomes associated with traumatic brain injury in childhood and adolescence: a nationwide Swedish cohort study of a wide range of medical and social outcomes. *PLoS Med.* 13, e1002103.
45. Johnson, V.E., Stewart, W., and Smith, D.H. (2010). Traumatic brain injury and amyloid-beta pathology: a link to Alzheimer's disease? *Nat. Rev. Neurosci.* 11, 361–370.
46. Johnson, V.E., Stewart, W., and Smith, D.H. (2012). Widespread tau and amyloid-beta pathology many years after a single traumatic brain injury in humans. *Brain Pathol.* 22, 142–149.
47. Omalu, B., Bailes, J., Hamilton, R.L., Kambou, M.I., Hammers, J., Case, M., and Fitzsimmons, R. (2011). Emerging histomorphologic phenotypes of chronic traumatic encephalopathy in American athletes. *Neurosurgery* 69, 173–183.
48. Saing, T., Dick, M., Nelson, P.T., Kim, R.C., Cribbs, D.H., and Head, E. (2012). Frontal cortex neuropathology in dementia pugilistica. *J. Neurotrauma* 29, 1054–1070.
49. Mez, J., Daneshvar, D.H., Kiernan, P.T., Abdolmohammadi, B., Alvarez, V.E., Huber, B.R., Alosco, M.L., Solomon, T.M., Nowinski, C.J., McHale, L., Cormier, K.A., Kibilus, C.A., Martin, B.M., Murphy, L., Baugh, C.M., Montenigro, P.H., Chaisson, C.E., Tripathi, Y., Kowall, N.W., Weuve, J., McClean, M.D., Cantu, R.C., Goldstein, L.E., Katz, D.I., Stern, R.A., Stein, T.D., and McKee, A.C. (2017). Clinicopathological evaluation of chronic traumatic encephalopathy in players of American football. *JAMA* 318, 360–370.
50. Goldstein, L.E., Fisher, A.M., Tagge, C.A., Zhang, X.L., Velisek, L., Sullivan, J.A., Upreti, C., Kracht, J.M., Ericsson, M., Wojnarowicz, M.W., Goletiani, C.J., Maglakelidze, G.M., Casey, N., Moncaster, J.A., Minaeva, O., Moir, R.D., Nowinski, C.J., Stern, R.A., Cantu, R.C., Geiling, J., Blusztajn, J.K., Wolozin, B.L., Ikezu, T., Stein, T.D., Budson, A.E., Kowall, N.W., Chargin, D., Sharon, A., Saman, S., Hall, G.F., Moss, W.C., Cleveland, R.O., Tanzi, R.E., Stanton, P.K., and McKee, A.C. (2012). Chronic traumatic encephalopathy in blast-exposed military veterans and a blast neurotrauma mouse model. *Sci. Transl. Med.* 4, 134R460.
51. McKee, A.C., Stern, R.A., Nowinski, C.J., Stein, T.D., Alvarez, V.E., Daneshvar, D.H., Lee, H.S., Wojtowicz, S.M., Hall, G., Baugh, C.M., Riley, D.O., Kibilus, C.A., Cormier, K.A., Jacobs, M.A., Martin, B.R., Abraham, C.R., Ikezu, T., Reichard, R.R., Wolozin, B.L., Budson, A.E., Goldstein, L.E., Kowall, N.W., and Cantu, R.C. (2013). The spectrum of disease in chronic traumatic encephalopathy. *Brain* 136, 43–64.
52. Osier, N.D., Carlson, S.W., DeSana, A., and Dixon, C.E. (2015). Chronic histopathological and behavioral outcomes of experimental traumatic brain injury in adult male animals. *J. Neurotrauma* 32, 1861–1882.
53. Pierce, J.E., Smith, D.H., Trojanowski, J.Q., and McIntosh, T.K. (1998). Enduring cognitive, neurobehavioral and histopathological changes persist for up to one year following severe experimental brain injury in rats. *Neuroscience* 87, 359–369.
54. Pischitta, F., Micotti, E., Hay, J.R., Marongiu, I., Sammal, E., Tolomeo, D., Vegliante, G., Stocchetti, N., Forloni, G., De Simoni, M.G., Stewart, W., and Zanier, E.R. (2018). Single severe traumatic brain injury produces progressive pathology with ongoing contralateral white matter damage one year after injury. *Exp. Neurol.* 300, 167–178.
55. Smith, D.H., Chen, X.H., Pierce, J.E., Wolf, J.A., Trojanowski, J.Q., Graham, D.I., and McIntosh, T.K. (1997). Progressive atrophy and neuron death for one year following brain trauma in the rat. *J. Neurotrauma* 14, 715–727.
56. Dixon, C.E., Kochanek, P.M., Yan, H.Q., Schiding, J.K., Griffith, R.G., Baum, E., Marion, D.W., and DeKosky, S.T. (1999). One-year study of spatial memory performance, brain morphology, and cholinergic markers after moderate controlled cortical impact in rats. *J. Neurotrauma* 16, 109–122.

-
57. Nonaka, M., Chen, X.H., Pierce, J.E., Leoni, M.J., McIntosh, T.K., Wolf, J.A., and Smith, D.H. (1999). Prolonged activation of NF- κ B following traumatic brain injury in rats. *J. Neurotrauma* 16, 1023–1034.
 58. Mannix, R.C., Zhang, J., Park, J., Zhang, X., Bilal, K., Walker, K., Tanzi, R.E., Tesco, G., and Whalen, M.J. (2011). Age-dependent effect of apolipoprotein E4 on functional outcome after controlled cortical impact in mice. *J. Cereb. Blood Flow Metab.* 31, 351–361.
 59. Bramlett, H.M., and Dietrich, W.D. (2002). Quantitative structural changes in white and gray matter 1 year following traumatic brain injury in rats. *Acta Neuropathol.* 103, 607–614.
 60. Rodriguez-Paez, A.C., Brunschwig, J.P., and Bramlett, H.M. (2005). Light and electron microscopic assessment of progressive atrophy following moderate traumatic brain injury in the rat. *Acta Neuro-pathol.* 109, 603–616.
 61. Mouzon, B.C., Bachmeier, C., Ferro, A., Ojo, J.O., Crynen, G., Acker, C.M., Davies, P., Mullan, M., Stewart, W., and Crawford, F. (2014). Chronic neuropathological and neurobehavioral changes in a repetitive mild traumatic brain injury model. *Ann. Neurol.* 75, 241–254.
 62. Luo, J., Nguyen, A., Villeda, S., Zhang, H., Ding, Z., Lindsey, D., Bieri, G., Castellano, J.M., Beaupre, G.S., and Wyss-Coray, T. (2014). Long-term cognitive impairments and pathological alterations in a mouse model of repetitive mild traumatic brain injury. *Front. Neurol.* 5, 12.
 63. Erturk, A., Mentz, S., Stout, E.E., Hedehus, M., Dominguez, S.L., Neumaier, L., Krammer, F., Llovera, G., Srinivasan, K., Hansen, D.V., Liesz, A., Searce-Levie, K.A., and Sheng, M. (2016). Interfering with the chronic immune response rescues chronic degeneration after traumatic brain injury. *J. Neurosci.* 36, 9962–9975.
 64. Sargin, D., Hassouna, I., Sperling, S., Siren, A.L., and Ehrenreich, H. (2009). Uncoupling of neurodegeneration and gliosis in a murine model of juvenile cortical lesion. *Glia* 57, 693–702.
 65. Kondo, A., Shahpasand, K., Mannix, R., Qiu, J., Moncaster, J., Chen, C.H., Yao, Y., Lin, Y.M., Driver, J.A., Sun, Y., Wei, S., Luo, M.L., Albayram, O., Huang, P., Rotenberg, A., Ryo, A., Goldstein, L.E., Pascual-Leone, A., McKee, A.C., Meehan, W., Zhou, X.Z., and Lu, K.P. (2015). Antibody against early driver of neurodegeneration cis P-tau blocks brain injury and tauopathy. *Nature* 523, 431–436.
 66. Albayram, O., Kondo, A., Mannix, R., Smith, C., Tsai, C.Y., Li, C., Herbert, M.K., Qiu, J., Monuteaux, M., Driver, J., Yan, S., Gormley, W., Puccio, A.M., Okonkwo, D.O., Lucke-Wold, B., Bailes, J., Meehan, W., Zeidel, M., Lu, K.P., and Zhou, X.Z. (2017). Cis P-tau is induced in clinical and preclinical brain injury and contributes to post-injury sequelae. *Nat. Commun.* 8, 1000.
 67. Yoshiyama, Y., Uryu, K., Higuchi, M., Longhi, L., Hoover, R., Fujimoto, S., McIntosh, T., Lee, V.M., and Trojanowski, J.Q. (2005). Enhanced neurofibrillary tangle formation, cerebral atrophy, and cognitive deficits induced by repetitive mild brain injury in a transgenic tauopathy mouse model. *J. Neurotrauma* 22, 1134–1141.
 68. Campos-Pires, R., Hirnet, T., Valeo, F., Ong, B.E., Radyushkin, K., Aldhoun, J., Saville, J., Edge, C.J., Franks, N.P., Thal, S.C., and Dickinson, R. (2019). Xenon improves long-term cognitive function, reduces neuronal loss and chronic neuroinflammation, and improves survival after traumatic brain injury in mice. *Br. J. Anaesth.* 123, 60–73.
 69. Ferguson, S., Mouzon, B., Paris, D., Aponte, D., Abdullah, L., Stewart, W., Mullan, M., and Crawford, F. (2017). Acute or delayed treatment with anatabine improves spatial memory and reduces pathological sequelae at late time-points after repetitive mild traumatic brain injury. *J. Neurotrauma* 34, 1676–1691.

-
70. Himanen, L., Portin, R., Isoniemi, H., Helenius, H., Kurki, T., and Tenovuo, O. (2005). Cognitive functions in relation to MRI findings 30 years after traumatic brain injury. *Brain Inj.* 19, 93–100.
 71. Kraus, M.F., Susmaras, T., Caughlin, B.P., Walker, C.J., Sweeney, J.A., and Little, D.M. (2007). White matter integrity and cognition in chronic traumatic brain injury: a diffusion tensor imaging study. *Brain* 130, 2508–2519.
 72. Ariza, M., Serra-Grabulosa, J.M., Junque, C., Ramirez, B., Mataro, M., Poca, A., Bargallo, N., and Sahuquillo, J. (2006). Hippocampal head atrophy after traumatic brain injury. *Neuropsychologia* 44, 1956–1961.
 73. Squire, L.R. (1992). Memory and the hippocampus: a synthesis from findings with rats, monkeys, and humans. *Psychol. Rev.* 99, 195–231.
 74. Moser, E., Moser, M.B., and Andersen, P. (1993). Spatial learning impairment parallels the magnitude of dorsal hippocampal lesions, but is hardly present following ventral lesions. *J. Neurosci.* 13, 3916–3925.
 75. Bohbot, V.D., Allen, J.J., and Nadel, L. (2000). Memory deficits characterized by patterns of lesions to the hippocampus and para-hippocampal cortex. *Ann. N. Y. Acad. Sci.* 911, 355–368.
 76. Reed, J.M., and Squire, L.R. (1997). Impaired recognition memory in patients with lesions limited to the hippocampal formation. *Behav. Neurosci.* 111, 667–675.
 77. Jorge, R.E., Acion, L., Starkstein, S.E., and Magnotta, V. (2007). Hippocampal volume and mood disorders after traumatic brain injury. *Biol. Psychiatry* 62, 332–338.
 78. Grauwmeijer, E., Heijenbrok-Kal, M.H., Haitisma, I.K., and Ribbers, G.M. (2012). A prospective study on employment outcome 3 years after moderate to severe traumatic brain injury. *Arch. Phys. Med. Rehabil.* 93, 993–999.
 79. Morris, R. (1984). Developments of a water-maze procedure for studying spatial learning in the rat. *J. Neurosci. Methods* 11, 47–60.
 80. Harrison, F.E., Reiserer, R.S., Tomarken, A.J., and McDonald, M.P. (2006). Spatial and nonspatial escape strategies in the Barnes maze. *Learn. Mem.* 13, 809–819.
 81. Barnes, C.A. (1979). Memory deficits associated with senescence: a neurophysiological and behavioral study in the rat. *J. Comp. Physiol. Psychol.* 93, 74–104.
 82. Pottker, B., Stober, F., Hummel, R., Angenstein, F., Radyushkin, K., Goldschmidt, J., and Schafer, M.K.E. (2017). Traumatic brain injury causes long-term behavioral changes related to region-specific increases of cerebral blood flow. *Brain Struct. Funct.* 222, 4005–4021.
 83. Sell, S.L., Johnson, K., DeWitt, D.S., and Prough, D.S. (2017). Persistent behavioral deficits in rats after parasagittal fluid percussion injury. *J. Neurotrauma* 34, 1086–1096.
 84. Lindner, M.D., Plone, M.A., Cain, C.K., Frydel, B., Francis, J.M., Emerich, D.F., and Sutton, R.L. (1998). Dissociable long-term cognitive deficits after frontal versus sensorimotor cortical contusions. *J. Neurotrauma* 15, 199–216.
 85. Lighthall, J.W. (1988). Controlled cortical impact: a new experimental brain injury model. *J. Neurotrauma* 5, 1–15.
 86. Fox, G.B., and Faden, A.I. (1998). Traumatic brain injury causes delayed motor and cognitive impairment in a mutant mouse strain known to exhibit delayed Wallerian degeneration. *J. Neurosci. Res.* 53, 718–727.
 87. Swaine, B.R., and Sullivan, S.J. (1996). Longitudinal profile of early motor recovery following severe traumatic brain injury. *Brain Inj.* 10, 347–366.

-
88. Walker, W.C., and Pickett, T.C. (2007). Motor impairment after severe traumatic brain injury: A longitudinal multicenter study. *J. Rehabil. Res. Dev.* 44, 975–982.
 89. Geurts, A.C., Ribbers, G.M., Knoop, J.A., and van, L.J. (1996). Identification of static and dynamic postural instability following traumatic brain injury. *Arch. Phys. Med. Rehabil.* 77, 639–644.
 90. Dehail, P., Petit, H., Joseph, P.A., Vuadens, P., and Mazaux, J.M. (2007). Assessment of postural instability in patients with traumatic brain injury upon enrolment in a vocational adjustment programme. *J. Rehabil. Med.* 39, 531–536.
 91. Kim, E., Lauterbach, E.C., Reeve, A., Arciniegas, D.B., Coburn, K.L., Mendez, M.F., Rummans, T.A., and Coffey, E.C. (2007). Neuropsychiatric complications of traumatic brain injury: a critical review of the literature (a report by the ANPA Committee on Research). *J. Neuropsychiatry Clin. Neurosci.* 19, 106–127.
 92. Alway, Y., Gould, K.R., Johnston, L., McKenzie, D., and Ponsford, J. (2016). A prospective examination of Axis I psychiatric disorders in the first 5 years following moderate to severe traumatic brain injury. *Psychol. Med.* 46, 1331–1341.
 93. Malkesman, O., Tucker, L.B., Ozl, J., and McCabe, J.T. (2013). Traumatic brain injury – modeling neuropsychiatric symptoms in rodents. *Front. Neurol.* 4, 157.
 94. Tucker, L.B., Burke, J.F., Fu, A.H., and McCabe, J.T. (2017). Neuropsychiatric symptom modeling in male and female c57bl/6j mice after experimental traumatic brain injury. *J. Neurotrauma* 34, 890–905.
 95. Washington, P.M., Forcelli, P.A., Wilkins, T., Zapple, D.N., Parsadanian, M., and Burns, M.P. (2012). The effect of injury severity on behavior: a phenotypic study of cognitive and emotional deficits after mild, moderate, and severe controlled cortical impact injury in mice. *J. Neurotrauma* 29, 2283–2296.
 96. Zohar, O., Rubovitch, V., Milman, A., Schreiber, S., and Pick, C.G. (2011). Behavioral consequences of minimal traumatic brain injury in mice. *Acta Neurobiol. Exp. (Wars.)* 71, 36–45.
 97. Bajwa, N.M., Halavi, S., Hamer, M., Semple, B.D., Noble-Haeusslein, L.J., Baghchechi, M., Hiroto, A., Hartman, R.E., and Obenaus, A. (2016). Mild concussion, but not moderate traumatic brain injury, is associated with long-term depression-like phenotype in mice. *PLoS One* 11, e0146886.
 98. Collins-Praino, L.E., Arulsamy, A., Katharesan, V., and Corrigan, F. (2018). The effect of an acute systemic inflammatory insult on the chronic effects of a single mild traumatic brain injury. *Behav. Brain Res.* 336, 22–31.
 99. Davies, M., Jacobs, A., Brody, D.L., and Friess, S.H. (2018). Delayed hypoxemia after traumatic brain injury exacerbates long-term behavioral deficits. *J. Neurotrauma* 35, 790–801.
 100. Arulsamy, A., Teng, J., Colton, H., Corrigan, F., and Collins-Praino, L. (2018). Evaluation of early chronic functional outcomes and their relationship to pre-frontal cortex and hippocampal pathology following moderate-severe traumatic brain injury. *Behav. Brain Res.* 348, 127–138.
 101. Titus, D.J., Wilson, N.M., Freund, J.E., Carballosa, M.M., Sikah, K.E., Furones, C., Dietrich, W.D., Gurney, M.E., and Atkins, C.M. (2016). Chronic cognitive dysfunction after traumatic brain injury is improved with a phosphodiesterase 4B inhibitor. *J. Neurosci.* 36, 7095–7108.
 102. Rowe, R.K., Ziebell, J.M., Harrison, J.L., Law, L.M., Adelson, P.D., and Lifshitz, J. (2016). Aging with traumatic brain injury: effects of age at injury on behavioral outcome following diffuse brain injury in rats. *Dev. Neurosci.* 38, 195–205.

-
103. Cheng, J.S., Craft, R., Yu, G.Q., Ho, K., Wang, X., Mohan, G., Mangnitsky, S., Ponnusamy, R., and Mucke, L. (2014). Tau reduction diminishes spatial learning and memory deficits after mild repetitive traumatic brain injury in mice. *PLoS One* 9, e115765.

6. Paper II

RIPK1 or RIPK3 deletion prevents progressive neuronal cell death and improves memory function after traumatic brain injury

Antonia Clarissa Wehn^{1,2}, Igor Khalin^{1,2}, Marco Duering^{1,2,9}, Farida Hellal^{1,2}, Carsten Culmsee^{3,4}, Peter Vandenabeele^{5,6}, Nikolaus Plesnila^{1,2,7*†} and Nicole Angela Terpolilli^{1,2,8*†}

¹ Institute for Stroke and Dementia Research (ISD), Munich University Hospital, Munich, Germany

² Munich Cluster of Systems Neurology (Synergy), Munich, Germany.

³ Institute for Pharmacology and Clinical Pharmacy, Biochemical-Pharmacological Center Marburg, University of Marburg, Marburg, Germany

⁴ University of Marburg, Marburg, Germany

⁵ Molecular Signaling and Cell Death Unit, VIB Inflammation Research Center, Ghent, Belgium

⁶ Department of Biomedical Molecular Biology, Ghent University, Ghent, Belgium

⁷ Graduate School of Systemic Neurosciences (GSN), Ludwig-Maximilians University Munich, Munich, Germany

⁸ Department of Neurosurgery, Munich University Hospital, Munich, Germany.

⁹ Medical Image Analysis Center (MIAC AG) and Qbig, Department of Biomedical Engineering, University of Basel, Basel, Switzerland

*Correspondence: nikolaus.plesnila@med.uni-muenchen.de; nicole.terpolilli@med.uni-muenchen.de

†Nikolaus Plesnila and Nicole Angela Terpolilli authors are equally contributed to this work.

Abstract

Traumatic brain injury (TBI) causes acute and subacute tissue damage, but is also associated with chronic inflammation and progressive loss of brain tissue months and years after the initial event. The trigger and the subsequent molecular mechanisms causing chronic brain injury after TBI are not well understood. The aim of the current study was therefore to investigate the hypothesis that necroptosis, a form of programmed cell death mediated by the interaction of Receptor Interacting Protein Kinases (RIPK) 1 and 3, is involved in this process. Neuron-specific RIPK1- or RIPK3-deficient mice and their wild-type littermates were subjected to experimental TBI by controlled cortical impact. Posttraumatic brain damage and functional outcome were assessed longitudinally by repetitive magnetic resonance imaging (MRI) and behavioral tests (beam walk, Barnes maze, and tail suspension), respectively, for up to three months after injury. Thereafter, brains were investigated by immunohistochemistry for the necroptotic marker phosphorylated mixed lineage kinase like protein (pMLKL) and activation of astrocytes and microglia. WT mice showed progressive chronic brain damage in cortex and hippocampus and increased levels of

pMLKL after TBI. Chronic brain damage occurred almost exclusively in areas with iron deposits and was significantly reduced in RIPK1- or RIPK3-deficient mice by up to 80%. Neuroprotection was accompanied by a reduction of astrocyte and microglia activation and improved memory function. The data of the current study suggest that progressive chronic brain damage and cognitive decline after TBI depend on the expression of RIPK1/3 in neurons. Hence, inhibition of necroptosis signaling may represent a novel therapeutic target for the prevention of chronic post-traumatic brain damage.

Keywords: Traumatic brain injury, Chronic posttraumatic brain damage, Magnetic resonance imaging, Necroptosis, Ferroptosis, Neuroprotection

Introduction

With an estimated case load of 69 million per year [1], traumatic brain injury (TBI) represents a leading cause of death and disability in all age groups worldwide, especially in children and young adults. The incidence of TBI is expected to increase in the coming decades, as the number of the two main etiologies—motor vehicle accidents and falls—are expected to rise due to an increase in motorization and an aging population, respectively [2]. The socio-economic impact of TBI is vast, with estimated costs of approximately 400 billion US\$ annually [3]. This number does not only include the direct costs due to acute primary care, but also long-term follow-up costs since many TBI survivors suffer from mood changes, memory deficits, and loss of fine motor skills, have difficulties returning to their previous occupation, and therefore require lifelong support [4–6]. Consequently, TBI is increasingly recognized as a chronic neurological disorder with socio-economic implications comparable to conditions like Alzheimer's disease or other neurodegenerative disorders [7].

While the pathophysiology of acute brain damage has been investigated in detail in experimental animals and in humans over the past decades, relatively little is known about the mechanisms determining long-term outcome after TBI. Chronic functional deficits in TBI patients may be caused by progressive brain atrophy in cortex and hippocampus [8, 9] and hydrocephalus formation [10–13]. So far, clinical and experimental studies suggest that inflammation plays an important role for the development of chronic posttraumatic brain damage [14–18], however, the cellular and molecular mechanisms downstream of this process are not fully understood. Particularly, the trigger and the intracellular signaling cascades causing neuronal cell death weeks and months after TBI are still unknown.

Necroptosis is a form of necrotic regulated cell death, which involves the upstream assembly of the necroptosome complex formed by the interaction of receptor interacting protein kinase 1 and 3 (RIPK1 and 3) [19] and downstream RIPK3-mediated phosphorylation of mixed lineage kinase like protein (MLKL). Necroptosis can be initiated by activation of Toll-like receptors (TLR) 3 and 4, TNF-alpha receptor 1 or, as more recently shown by us and others, by cylindromatosis (CYLD)-mediated deubiquitination of RIPK1 [20]. CYLD is prone to activation by reactive oxygen species (ROS) [21]. Hence, necroptosis may be activated by several events, TNF release, TLR activation, inflammation and ROS production, which are all believed to occur in the brain following TBI [16, 22, 23]. Based on these findings, we hypothesize, that necroptosis may be a relevant intracellular mechanism which triggers chronic neurodegeneration after TBI. To address this issue, we used mice deficient for RIPK1 in neurons or RIPK3 and investigated lesion progression by longitudinal magnetic resonance imaging (MRI), behavioral outcome, and necroptotic signaling up to three months after TBI in a clinically relevant mouse model of TBI. Our results demonstrate that necroptosis is an important novel mediator of chronic neurodegeneration after TBI.

Material and methods

Ethical statement

All animal experiments were reviewed and approved by the Ethical Review Board of the Government of Upper Bavaria. The results of the study are reported in accordance with the ARRIVE guidelines [24]. Animal husbandry, health screens, and hygiene management checks were performed in accordance with Federation of European Laboratory Animal Science Associations (FELASA) guidelines and recommendations [25]. Only male mice between 6 and 8 weeks old mice were used. All surgical procedures, behavioral testing, imaging, and data analysis were performed in a randomized fashion by a researcher blinded to the genotype and group allocation of the animals. Group allocation was obtained by drawing lots by a third party not involved in the study or data analysis.

Animals

Inducible neuronal Ripk1 cKO mice were generated as previously described [26] and bred as Ripk1^{fl/fl} (WT) and Ripk1^{fl/fl}::Camk2a-Cre + /Cre (cKO) in our facility. For induction of neuronal RIPK1 deletion, Ripk1 cKO mice (starting at 4 weeks of age) received three intra-peritoneal injections of 2 mg Tamoxifen (Sigma-Aldrich, Taufkirchen, Germany, # T5648) in a 100 μ l Miglyol suspension (Caelo, Hilden, Germany, #3274) every 48 h (day 1, 3, 5). RIPK3-deficient mice were generated and kindly provided by V. M. Dixit, Genentech Inc., San Francisco, CA, [27] and bred heterozygously to obtain Ripk3^{-/-} (KO) and Ripk3^{+/+} (WT) cohorts. The genotype of each RIPK1 and RIPK3 deficient mouse was proven by genotyping (Additional file 1: Figure S1a and b). PCR was performed using the AccuStartTM II Mouse Genotyping Kit (Quanta Biosciences, Beverly, MA, #95,135–500) according to the manufacturer's instructions. Primers were obtained by Metabion (metabion GmbH Planegg, Germany). Neuronal specific conditional knock-out of Ripk1 was further proven by immunohistochemistry for RIPK1 (Additional file 1: Figure S1c). Induction of neuronal specific Cre recombinase resulted in an 80% reduction of RIPK1 expression in cortical neurons (Additional file 1: Figure S1d). Neither neuronal RIPK1 nor global RIPK3 deficient mice had any obvious phenotype and were born at normal Mendelian distributions.

Controlled Cortical Impact model of traumatic brain injury Animals were subjected to experimental traumatic brain injury using the previously described Controlled Cortical Impact (CCI) method [23, 28–30]. CCI induces a highly reproducible focal lesion and causes progressive brain damage and cognitive decline thereby replicating many acute and chronic characteristics of human TBI [23]. In short, after induction of anesthesia with buprenorphine (0.1 mg/kg Bw) and isoflurane (4%, 30 s), animals were sedated with 1.5–2.5% isoflurane in 30% oxygen and 70% nitrogen under continuous monitoring of body temperature and heart rate. After right parietal craniotomy, the impact was directly applied to the intact dura with a pressure-driven steel piston with a diameter of 3 mm (L. Kopacz, University of Mainz, Germany; 8 m/s impact velocity, 1 mm penetration depth, 150 ms contact time). For sham-surgery, the piston was placed on the dura, but no impact was applied. The craniotomy was resealed with tissue glue (VetBond, 3 M animal care products, St. Paul, MN) and animals were kept in an incubator at 34 °C and 60% air humidity until they regained full motor activity in order to prevent hypothermia. Carprofen (4 mg/kg every 24 h) was administered i.p. for the following 72 h for analgesia.

Experimental time-line

Motor function, depression-like behavior, and memory function were evaluated three days before trauma to obtain baseline values and up to three months thereafter. Lesion volume and tissue iron was evaluated by repetitive MRI up to three months after injury and validated by histology.

At the end of the observation time brains were removed for immunohistochemical analysis of lesion volume, tissue iron, astrocyte activation, and microglia morphology (Fig. 1).

Body weight and general condition

Animals were weighed daily from three days before CCI until day 7 after trauma, then weekly. General condition, surgery wounds, behavior, nutrition, and fluid balance were checked daily in the early postoperative period, then weekly.

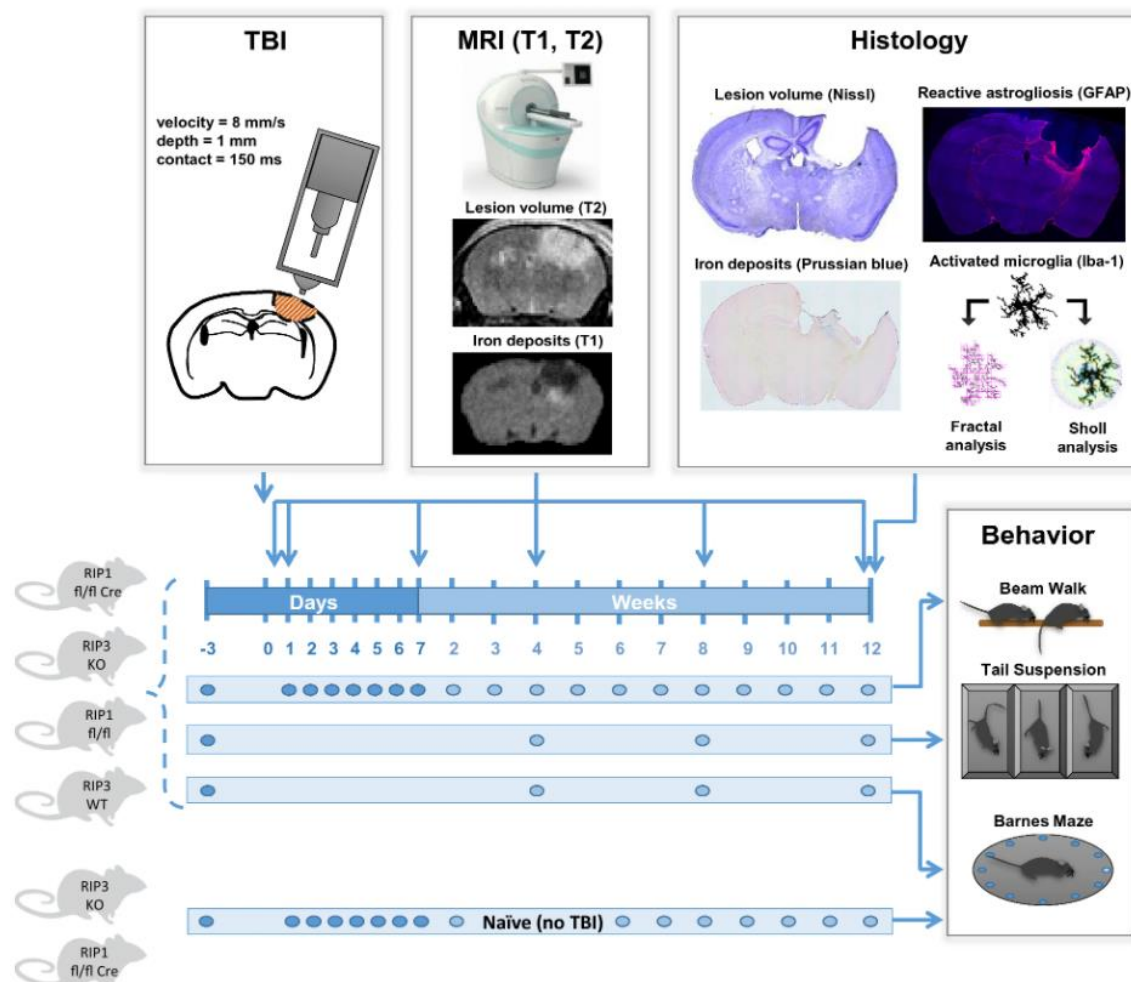


Figure 1: Experimental groups, methods, and time line

Magnetic resonance imaging and analysis

For longitudinal determination of lesion volume, MRI measurements were performed 15 min, 24 h, 7 days, one, two, and three months after TBI. For all animals, T1 weighted, T2 weighted, and diffusion weighted imaging (DWI) sequences were collected as previously described [23] under isoflurane anesthesia (1–1.5% in 30% oxygen/70% nitrogen) and multimodal monitoring of physiological parameters using a 3 T nanoScan® PET/MR (Mediso, Münster Germany). Sequences were collected in the following order: T2-weighted imaging (2D fast-spin echo (FSE), TR/TE = 3000/57.1 ms, averages 14, matrix size = 96 × 96; field of view = 16 mm × 16 mm; slice thickness = 500 μm, inter-slice gap = 60 μm), T1-weighted imaging (2D fast-spin echo (FSE), TR/TE = 610/28.6 ms, averages 14, matrix size = 96 × 96; field of view = 16 mm × 16 mm; slice thickness = 500 μm, interslice gap = 60 μm). Total imaging time was approximately 35 min per mouse and time-point. Lesion volume was measured using ImageJ software (Rasband, W.S., ImageJ, U. S.

National Institutes of Health, Bethesda, Maryland, USA, [https:// imagej.nih.gov/ij/](https://imagej.nih.gov/ij/), 1997–2018) in T2 sequences. 14 slices surrounding the lesion were chosen for each data- set and the area segmented using the polygon tool. Volume was then calculated using the following equation:

$$V = d * (A1/2 + A2 + A3 . . . + An/2)$$

with d being the distance between slices in mm (slice thickness + interslice gap), and A being the measured area in mm³.

Hippocampal atrophy was assessed in T2-weighted images as previously described [23]. One section located in the center of the lesion containing the hippocampus was chosen at the same position for each animal. Areas of both hippocampi were segmented using the polygon tool and the ipsilesional area of the hippocampus was expressed as % of the area of the uninjured contralateral hippocampus.

Behavioral testing

To exclude age-related factors as a cause for behavioral changes during the observation period, all behavioral tests were performed with an additional control group of non-traumatized (naive) RIPK3 or RIPK1 deficient mice (Fig. 1).

Motor function—Beam Walk

The Beam Walk Test was performed as previously described [23, 28, 30] on a 1 m long and 1 cm wide suspended wooden rod. Time to cross the beam and the number of missteps was recorded. Animals with more than two missteps in pre-trauma testing were excluded from randomization.

Memory and learning behavior—Barnes Maze

The Barnes Maze test, a well-established paradigm for assessing memory function [31, 32], was performed 1, 2, and 3 months after CCI as previously described [23]. In short, the animal was placed on a brightly lit round platform with 20 identical holes along its outer rim and trained to locate a box affixed below one of the apertures (home cage) as fast as possible. Time to reach the home cage (latency) as well as distance travelled and walking speed were recorded and analyzed using a video tracking software (EthoVison XT®, Version 11, 2014 Noldus Information Technology). Animals were trained for four consecutive days and memory function was evaluated on the sixth day.

Tail Suspension test

The Tail Suspension test is a paradigm to assess depression-like behavior in rodents and was performed as previously described [23]. Briefly, animals were suspended by the tail for three minutes and their movements recorded and analyzed using a video tracking software (EthoVison XT®, Version 11, 2014, Noldus Information Technology). The time of inactivity was used as a proxy for depression- like behavior [33].

Histological assessment

Lesion volume/ hippocampus volume

Three months after TBI, animals were fixed with 4% PFA in deep anesthesia by transcardial perfusion. Four- teen sequential 50 µm thick coronal sections were cut at 500 µm intervals on a vibratome (Leica, Germany) in order to match the tissue volume investigated by MRI, stained with cresyl violet according to Nissl, and evaluated by histomorphometry for lesion volume using the following formula as previously described [23]:

$$V = d * (A1/2 + A2 + A3 \dots + An/2)$$

The volume of the hippocampus in the traumatized hemisphere was determined in six slices one mm anterior until four mm posterior to bregma and then normalized to the contralesional side.

Iron deposits

One section per animal was stained with Prussian blue (Iron Stain Kit, Sigma-Aldrich, # HT20) at -1.5 mm from bregma to visualize iron deposits using a light microscope (Axioscope, Carl Zeiss Microscopy GmbH, Jena Germany). Tile scans were then processed in ImageJ by using the color deconvolution tool to separate color channels. The blue channel was binarized and the integrated density was measured using the particle analysis plugin. Values of the traumatized hemisphere were expressed as percentage of the contralateral side.

Immunohistochemistry

Fifty micrometer thick floating coronal sections were prepared as previously described [34]. Blocking and incubation with the primary antibody was performed in 1% bovine serum albumin, 0.1% gelatin from cold water fish skin, 0.5% Triton X-100 in 0.01 M PBS at pH 7.2–7.4 for 72 h at 4 °C. The following primary antibodies were used: IBA-1 (rabbit, Wako, #019–19,741, 1:200), GFAP-Cy3 (mouse, Sigma Aldrich, #2905, 1:200), RIPK1 (rabbit, Novusbio, #NBP1-77077SS, 1:100), NeuN (guinea pig, Synaptic Systems, #266 004), and phosphorylated MLKL (rabbit, Cell signaling technology, # 91689S, 1:100). After incubation, sections were washed in PBS and incubated with the following secondary antibodies: anti-rabbit coupled to Alexa-fluor 594 (goat anti-rabbit, Thermo Fisher Scientific, #A-11012), anti-guinea pig coupled to Alexa-fluor 488 (goat anti-guinea pig, Thermo Fisher Scientific, # A-11073), and anti-mouse coupled to Alexa-fluor 647 (goat anti-mouse, Thermo Fisher Scientific, #A- 32,728) in 0.01 M PBS at pH 7.2–7.4 containing 0.05% Tween 20. Nuclei were stained with 4',6-Diamidin-2-phenylindol (DAPI, Invitrogen, #D1306) 1:10,000 in 0.01 M PBS.

Imaging was performed using a ZEISS LSM 900 confocal microscope (Carl Zeiss Microscopy GmbH, Jena Germany). GFAP staining was recorded using a 10× objective (EC Plan-Neofluar 10x/0.30 Pol M27) with an image matrix of 512 × 512 pixel, a pixel scaling of 0.2 × 0.2 μm and a depth of 8 bit. Whole brain images were collected in z-stacks as tile scans with a slice-distance of 2 μm and a total range of 14 μm [35]. For microglia analysis, images were acquired using a 40× objective (EC Plan-Neofluar 40x/1.30 Oil DIC M27) with an image matrix of 1024 × 1024 pixel, a pixel scaling of 0.2 × 0.2 μm and a depth of 8 bit. Specific regions of interest were collected in Z-stacks to include the entire slice thickness with a slice-distance of 0.4 μm at 100 μm away from the lesion in the hippocampus and at 300 μm in the cortex. For p-MLKL staining, a 5 × objective was used (EC Plan-Neofluar 5x/0.16 Pol M27) with an image matrix of 1434 × 1434 pixel, a pixel scaling of 3.321 × 3.321 μm and a depth of 8 bit. Whole brain images were collected in z-stacks as tile scans with a slice-distance of 5 μm and a total range of 25 μm. To demonstrate the intracellular localization of p-MLKL, a 100 × objective (Epiplan-Neofluar 100x/1.3 Oil Pol M27) was used with an image matrix of 512 × 512 pixel, a pixel scaling of 0.166 × 0.166 μm and a depth of 8 bit. Images were collected in z-stacks with a slice-distance of 0,280 μm and a total range of 5.6 μm. After obtaining a maximum intensity projection, images were imported into ImageJ [36] and intensity of p-MLKL measured in the rim of the lesion and normalized to the signal of DAPI to correct for differences in staining. The corrected signal was then normalized to the same sized region of interest on the contralateral hemisphere.

Analysis of astrocyte coverage

Assessment of astrocyte coverage was performed using ImageJ in sections stained for GFAP (see above). Z-stacks were imported into Fiji and split into individual channels. GFAP intensity in five ROI (250 × 250 μm; at 0, 250, 500, 750, and 1000 μm distance from the lesion in the striatum) was then measured using the mean grey value and normalized to the measurements of the contralesional hemisphere to adjust for possible differences in staining intensity.

Analysis of microglia coverage and morphology

Microglia coverage was manually assessed in maximum intensity projections of iba-1 stained sections. One section per animal was chosen at 1.5 mm from bregma and two ROIs chosen on the ipsilesional hemisphere, one in layer V of the cortex at 300 μm away from the lesion and one in the CA1a region of the hippocampus. The number of microglia was normalized to total DAPI positive cell count and expressed in as percentage of coverage in sham operated animals.

To assess microglia morphology, Sholl and fractal analysis were performed to indicate ramification, cell range, total cell size, and circularity using a modified protocol from Young and Morrison [37]. Z-stack images were converted to a maximum intensity projection and cells were individually cut out using the polygon selection tool in ImageJ [35]. Only cells fully captured within the z-stack were selected. After background subtraction, images were binarized and resized to 600 × 600 pixels keeping the original scale. Speckles or debris around the cells were removed using the paintbrush tool. Sholl analysis was performed using the Sholl analysis plugin in ImageJ [38]. Centered on the soma, concentric circles with an increasing radius of 2 μm were drawn, the number of intersections measured at each radius. After converting binary images to outlines, fractal analysis was performed using the FracLac plugin for ImageJ [39]. As described previously [37], the total number of pixels present in the cell image of either the filled or outlined binary image were calculated and later transformed to μm² (pixel area = 0.208 μm²). Cell circularity was calculated as $\text{Circularity} = 4 \pi \text{Area} / \text{Perimeter}^2$. Maximum span across the convex hull represents the maximum distance between two points in the convex hull.

Statistical analysis

Sample size was calculated with the following parameters: alpha error = 0.05, beta error = 0.2, calculated standard deviation ranged from 15 to 20% (depending on the parameter investigated), and biologically relevant difference = 30%. All data is given as mean ± standard deviation (SD) if not indicated otherwise. For comparison between groups, Student t-test was used for normally distributed data and Mann–Whitney Rank Sum test for non-normally distributed data according to the result of Shapiro–Wilk normality test. Measurements over time were tested between groups using One-way or Two-way ANOVA for Repeated Measurements, followed by Tukey's multiple comparisons test for normally and Holm-Sidak's multiple comparisons test for non-normally distributed data as post hoc test. Calculations were performed with Sigma Plot version 14.0 (Systat Software GmbH, Erkrath, Germany).

Results

A total of 33 male RIP1 deficient mice (naïve RIP1fl/fl Cre group: n = 4, RIP1fl/fl Cre and RIP1fl/fl sham groups = 5 each, CCI RIP1fl/fl group: n = 10, RIP1fl/fl Cre group: n = 9) and 32 male RIP3 deficient mice (naïve RIP3^{-/-}, RIP3^{+/+}, and n = 9, CCI RIP3 group n = 8) were operated, assessed, and analyzed for the present study. One RIP3^{+/+} animal was excluded from randomization and not used for the study due to its performance in the Beam Walk Test before TBI (more than 2 missteps at baseline).

Traumatic brain injury induces long-term necroptotic signaling in neurons

Phosphorylated MLKL (pMLKL) was used as a specific marker for necroptosis [40]. Three months after TBI large amounts of pMLKL were found in the rim of the traumatic cavity, the presumed site of progressive chronic post-trauma brain damage (Fig. 2a, upper panel). pMLKL was found by high resolution confocal imaging in the cytoplasm of selected neurons as small dots (RIP3^{-/-}-sham group: n 5 each, CCI RIP3^{+/+} group), suggesting that pMLKL is part of a protein complex such as the necrosome (Fig. 2a, lower panel, white arrowheads). pMLKL staining was almost absent in neuronal RIPK3 deficient mice suggesting that necroptotic signaling in neurons did essentially not occur in these animals (Fig. 2b). Quantification of pMLKL staining showed a highly significant increase of activated MLKL in wild type mice of both strains, while neuronal Ripk1 or global Ripk3 knock-out completely blunted this response (Fig. 2c and d).

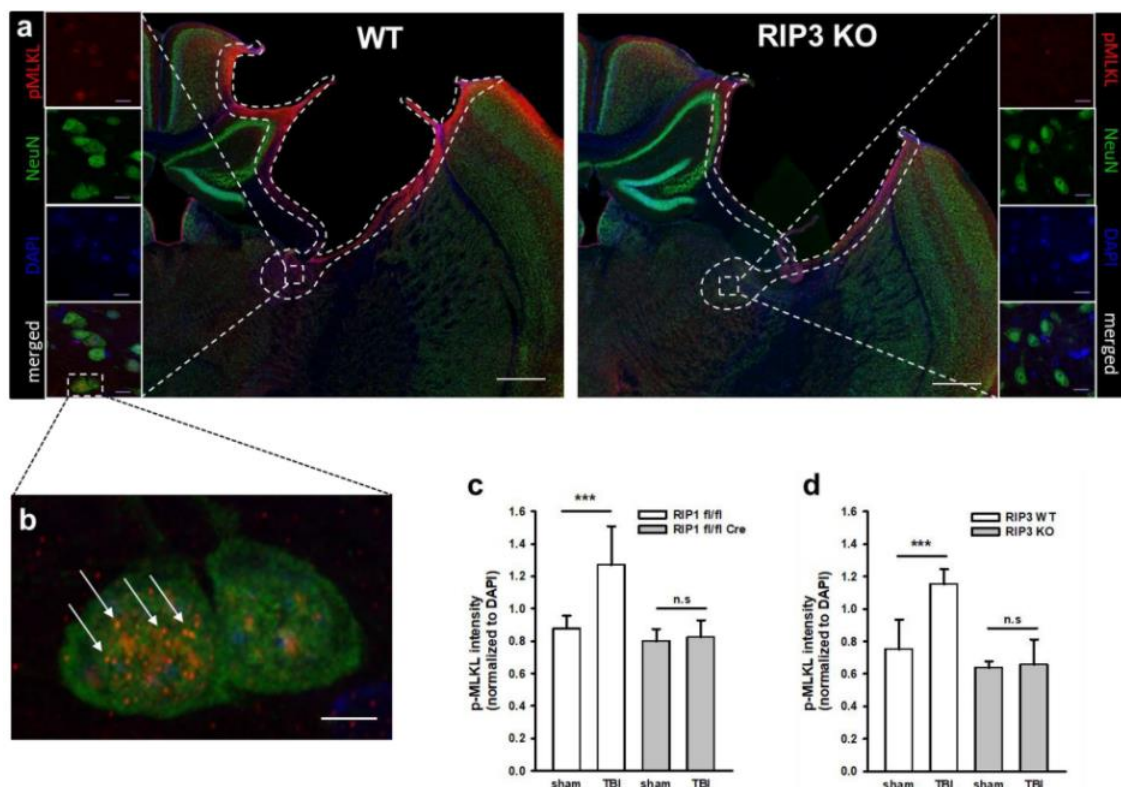


Figure 2: Phosphorylated MLKL, a marker of necroptosis is reduced in RIP knockout animals. a. Exemplary staining of pMLKL and NeuN (upper panel) and a pMLKL positive neuron at higher magnification (lower panel) in the rim of a traumatic contusion in a wild type mouse. b. pMLKL is significantly reduced in a RIPK3 deficient mouse. c and d p-MLKL signal intensity was significantly increased after TBI in wild type animals (white bars) compared to sham animals indicating significant presence of necroptosis three months after TBI; this increase was significantly blunted in RIPK1 (c) as well as in RIPK3 d mice where there was no difference between TBI and sham animals. Data are presented as mean \pm SD; n = 9–10 for RIPK1, n = 8–9 for RIPK3. Two-way RM ANOVA with Tukey's multiple comparisons test was used. ***p < 0.001, n.s. indicates no significant statistical difference between groups.

Chronic posttraumatic brain damage is reduced in RIPK1 or RIPK3 deficient mice

After demonstrating neuronal necroptotic signaling three months after TBI in wild type mice and showing that RIPK1 or 3 deficiency prevented this process, we evaluated lesion volume in cortex and hippocampus of wild type and RIPK deficient mice by longitudinal MR imaging. Two animals (one Ripk1 fl/fl::CamK2a Cre and one Ripk3 WT) of the study cohort died for unknown reasons before TBI and were excluded from analysis. All other animals completed the study. Anesthesia

and craniotomy did not have any influence on general outcome parameters: sham-operated and CCI animals recovered equally well from surgery in terms of bodyweight (Ripk1 cKO: Additional file 1: Figure S2a, Ripk3 KO: Additional file 1: Figure S2b) and general health score (Ripk1 cKO: Additional file 1: Figure S2c, Ripk3 KO: Additional file 1: Figure S2d). Exemplary three dimensional reconstructions of the brain showed a large lesion and a small hippocampus in the ipsilateral hemi- sphere of traumatized wild type mice three months after TBI, while the lesion was significantly smaller and the hippocampus significantly larger in neuronal RIPK1 deficient mice (Fig. 3a). Longitudinal investigation of lesion size and hippocampal volume by repetitive MRI showed that the primary damage measured 15 min after trauma was comparable in RIPK1 deficient mice and their respective wildtype controls (Fig. 3b, t= 15 min: Ripk1 cKO: 18.4 ± 2.6 mm³, wt: 18.4 ± 1.7 mm³) indicating that the initial trauma was similar in all investigated animals. In agreement with previous results in this model, lesion size peaked 24 h after TBI in both experimental groups (Ripk1 cKO: 27.0 ± 1.8 mm³, + 47% vs. 15 min; wt: 29.8 ± 4.3 mm³, + 61% vs. 15 min) as a representation of acute secondary brain damage. Lesion volume was not different between wild type and neuronal RIPK1 deficient mice at this time point indicating that necroptosis does not play a significant role for acute lesion progression. Within the first month after TBI, removal of necrotic tissue and scar formation resulted in an apparent shrinkage of the lesion. One to two months after TBI progressive loss of brain tissue started to occur, a process we previously demonstrated to continue for at least one year after experimental trauma [23]. Chronic post-trauma tissue injury was significantly reduced in neuronal RIPK1 deficient mice as compared to their wild type littermate controls (t = 1 month: Ripk1 cKO: 5.7 ± 1.6 mm³, wt 8.2 ± 1.9 mm³, p = 0.0355, t = 3 mon Ripk1 cKO: 6.5 ± 1.7 mm³, wt: 11.3 ± 2.0 mm³, p = 0.0002). A similar dynamic was seen in RIPK3 deficient animals. Acute injury was not affected by RIP 3 knock-out (Fig. 3c t = 24 h, Ripk3 KO: 24.8 ± 3.3 mm³, wt: 26.1 ± 5.3 mm³), while chronic lesion progression was significantly attenuated from one to three months after TBI (t = 1 month: Ripk3 KO: 8.8 ± 2.9 mm³, wt: 14.0 ± 1.9 mm³, p = 0.006; t = 3 months: Ripk3 KO: 7.3 ± 1.3 mm³, wt: 11.6 ± 3.6 mm³, p = 0.04). Individual traces for lesion volumes in each animal are given in Additional file 1: Figure S3a (RIP1 KO) and Additional file 1: Figure S3b (RIP3 KO). The MRI findings were corroborated by histopathological evaluations, i.e. acute brain damage 24 h after TBI was similar in RIP deficient and wild type animals (Additional file 1: Figure S4), while chronic brain damage three month after TBI correlated well with the injury assessed by MRI (Additional file 1: Figure S5a and b) and was significantly reduced in both knock-out strains (Additional file 1: Figure S5c and d).

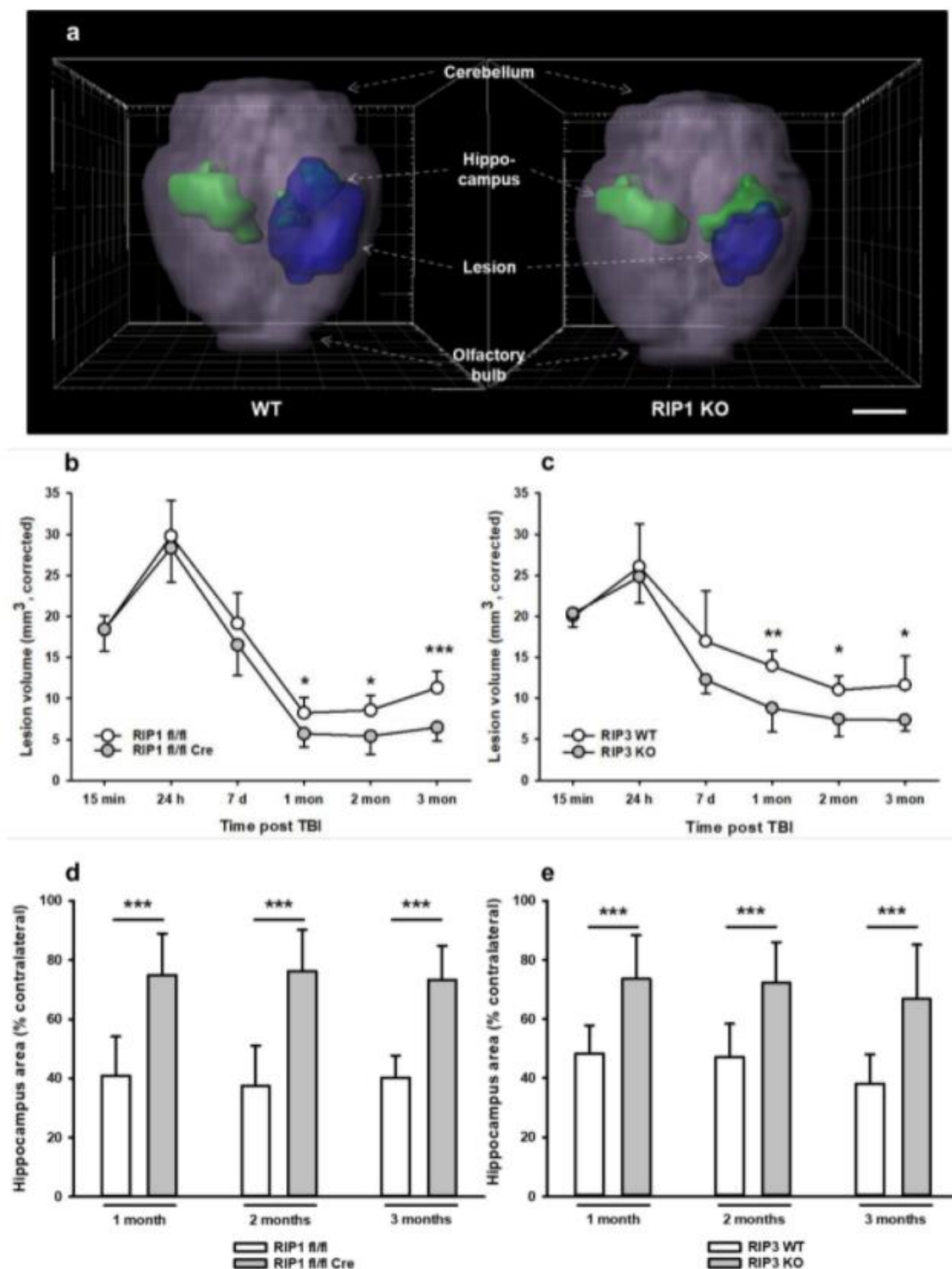


Figure 3: RIPK1 and RIPK3 deficiency significantly reduces posttraumatic brain damage. a 3D reconstruction of lesion volume (blue) in relation to ipsi- and contralateral hippocampus (green) for a RIPK3 wild type and a RIPK3 deficient mouse 3 months after TBI. Scale bar = 5 mm. b and c Lesion volume over time quantified by repetitive T2-weighted MR imaging in RIPK1 (b) and RIPK3 (c) knockout animal. d and e. Hippocampal atrophy over time assessed in longitudinal T2-weighted MRI. RIPK1 (d) and RIPK3 (e) knockout mice show better preservation of hippocampal tissue over time. Mean \pm SD; n = 9–10 for RIPK1, n = 8–9 for RIPK3. Two-way RM ANOVA with Sidak's multiple comparisons test was used. *p < 0.05, **p < 0.005, ***p < 0.001

Since memory deficits are a hallmark of chronic post-traumatic brain damage in mice and TBI patients [23, 41, 42], we next investigated long-term hippocampal damage by MRI. In the current TBI model, the hippocampus is only marginally injured acutely after TBI, but severely affected by progressive chronic damage as previously shown [23]. All wild type mice showed significant loss of hippocampal tissue in the traumatized hemisphere already one month after TBI (Fig. 3d and e, open bars). Starting one month after trauma, hippocampal loss was significantly less pronounced in neuronal RIPK1 and global RIPK3 deficient mice (Fig. 3d, RIPK1: reduction to $74.9 \pm 18.5\%$, wt: reduction to $40.3 \pm 18.7\%$ of contralateral hippocampus, $p = 0.0004$; Fig. 3e, RIPK3: reduction to $78.0 \pm 30.7\%$, wt: reduction to $48.2\% \pm 19.6\%$ of contralateral hippocampus, $p = 0.01$). This significant difference persisted until the end of the observation period three months after TBI and was corroborated by histology (Additional file 1: Figure S5e and f).

Astrogliosis and microglial activation are reduced in RIPK1 and RIPK3 deficient mice

The formation of a glial scar and the activation of microglia are other hallmarks of chronic brain damage after TBI [43, 44]. Indeed, we observed a marked increase in glial fibrillary acid protein (GFAP), an astrocyte marker, in the rim of the traumatic cavity and in perilesional tissue in wild type mice three months after TBI (Fig. 4a, left panel). Quantification of GFAP expression showed an almost four-fold increase in the rim of the lesion with a decreasing intensity towards perilesional areas (Fig. 4b and c, open bars). GFAP expression was far less pronounced in neuronal specific RIPK1 deficient mice (Fig. 4a, right panel). Quantification of astrocyte density by pixel-based analysis corroborated these findings and revealed that activation of astrocytes was significantly decreased by 25–35% in neuronal specific RIPK1 and in global RIPK3 deficient mice (Fig. 4b and c, closed bars).

cavity, while only subtle changes were observed in areas 300 μm away from the lesion site (Fig. 5, WT). The density of iba-1 staining was heavily reduced in neuronal specific RIPK1 deficient mice (Fig. 5, Ripk1 cKO). To quantify these changes, we assessed tissue coverage, area, circularity, and maximal span of microglia in the rim (100 μm) and in the vicinity (300 μm) of the traumatic lesion (Fig. 5b–i). In wild type mice all investigated parameters pointed towards a significant activation of microglia near the rim of the lesion, i.e. the coverage and circularity increased, while the area and the maximal span of microglia decreased (Fig. 5b–i, open bars).

Microglia activation and the number of microglial branch points were significantly reduced and partly normalized in neuronal specific RIPK1 and in global RIPK3 deficient mice (Fig. 5b–m, closed symbols), suggesting that less neuronal cell death was associated with less microglial activation.

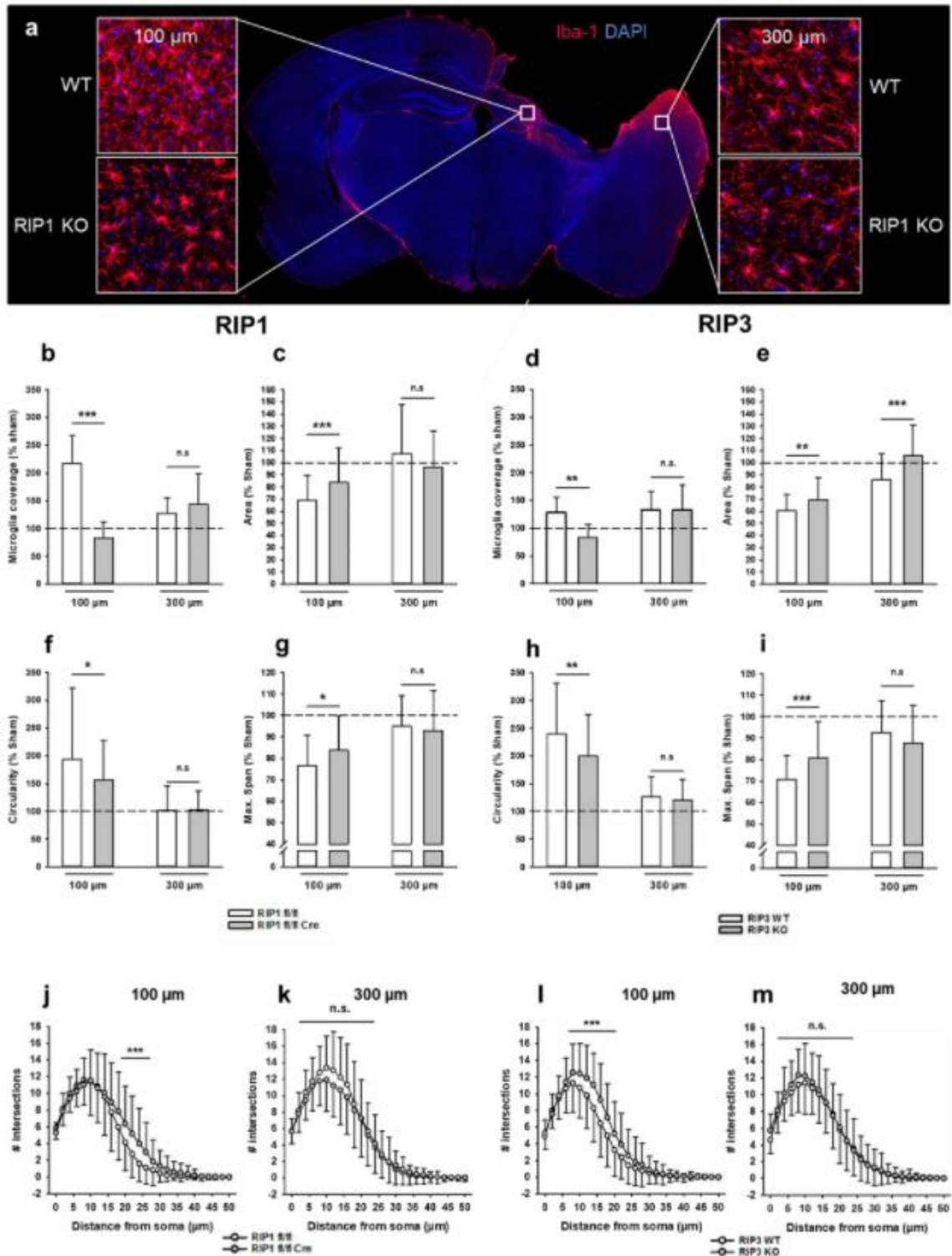


Figure 5: RIPK1 and RIPK3 deficiency reduces microglia activation. a. Exemplary stainings for the microglia marker *Iba1* in WT (upper inserts) and neuronal RIPK1 deficient mice (lower inserts) 100 μm (left inserts) and 300 μm (right inserts) from the rim of the lesion. b-i. Coverage and fractal analysis of microglia. In areas closer to the lesion site (100 μm , left side of each panel), knockout animals of both lines showed a decrease in microglia coverage (b. RIP 1, d. RIPK3) compared to their wild type littermates. Fractal analysis revealed that microglia of knockout animals in proximity to the lesion have less processes (c. RIP 1, e. RIPK3) are less circular (f. RIP 1, h. RIPK3), and overall smaller (g. RIP 1, i. RIPK3). In the more distal region, cells resembled those in sham

operated animals, with no differences between genotypes. j-m. Sholl analysis also shows increased ramification, i. e. more active cells, close to the lesion (j. RIP 1, l. RIPK3), but not further away from the lesion site (k. RIP 1, m. RIPK3). Data are presented as mean \pm SD; n = 9–10 for RIPK1, n = 8–9 for RIPK3. Student t-test for normalized and Man-Whitney-Rank-Sum-test for non-normalized data was used. *p < 0.05, **p < 0.005, ***p < 0.001. n.s. indicates no significant statistical difference between groups.

Neuronal RIPK1 and RIPK3 deficiency improves cognitive outcome three months after TBI

To investigate whether the reduction of lesion size, hippocampal damage, scar formation, and microglial activation had an effect of functional outcome, we investigated motor function by beam walk, depression-like behavior by the Tail Suspension test, and long-term memory using the Barnes Maze test. TBI significantly deteriorated motor function and induced depression-like behavior compared to pre-trauma performance as previously described [23], genetic deletion of RIPK1 or RIPK3, however, had no effect on these parameters (Fig. 6a–d). Long-term memory was normal in non-traumatized Ripk1 or Ripk3 knock-out mice; it was, however, significantly disturbed in traumatized animals, i.e. TBI increased the time needed to find the home cage, the latency to goal, by more than ten times and memory loss progressed over time (Fig. 6e and f, triangles and open circles). In neuronal specific RIPK1 and in global RIPK3 deficient mice, however, long-term memory function was almost completely preserved and resembled that of not traumatized animals (Fig. 6e and f, closed circles). Hence, protection of hippocampal neurons by genetic deletion of RIP 1 or RIPK3 resulted in preserved long-term memory function.

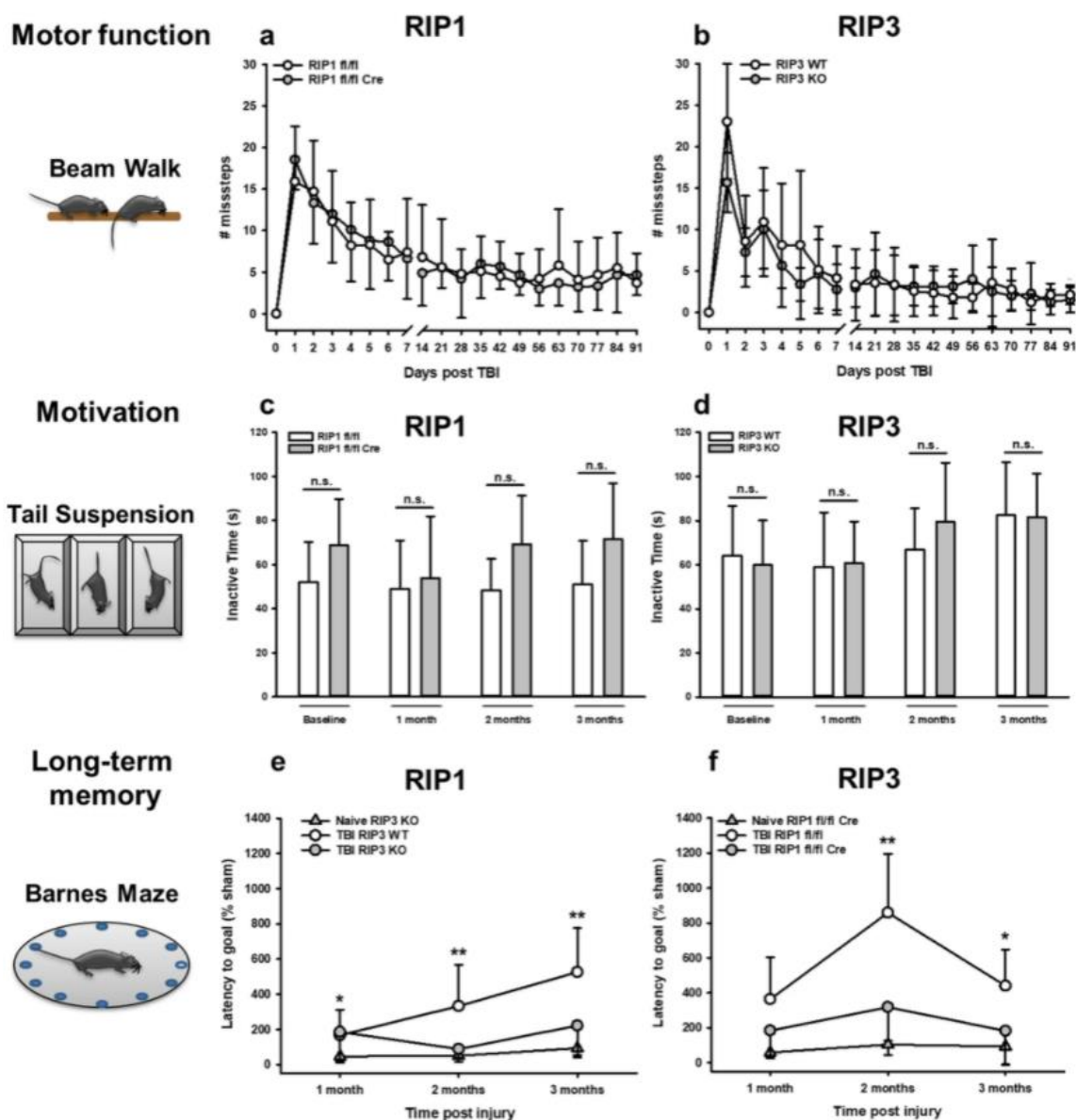


Figure 6: RIPK1 and RIPK3 deficiency improves neurocognitive performance three months after TBI. a and b Motor impairment after TBI. Beam Walk Test revealed long term impaired motor function of the left hind limb in TBI animals (missteps compared to respective baseline, # for WT, * for KO), but there were no differences between a RIPK1 or b RIPK3 knockout animals and their respective controls. c and d Depression-like behavior after TBI. Mice of both strains showed an increase of total immobility time throughout the time course of three months, however no significant differences could be detected between RIPK1 (c) and RIPK3 (d) knockout animals compared to wild type. e and f Learning and memory dysfunction after TBI. CCI induces severe long-term memory deficits in WT mice (open circles) while RIPK1 or RIPK3 knockout animals (grey circles) show similar long-term memory function as uninjured littermate controls. Data are presented as mean \pm SD; n = 9–10 for RIPK1, n = 8–9 for RIPK3. Two-way RM ANOVA with Tukey's multiple comparisons test was used. * $p < 0.05$, ** $p < 0.005$, *** $p < 0.001$, **** $p < 0.0001$.

Chronic lesion progression after TBI is associated with iron deposits and reduced in RIP-deficient mice

Since our data suggest that necroptotic signaling is important for chronic brain damage after TBI, we were interested to identify the mechanisms triggering this process. Traumatic contusions are

associated with hemorrhage and subsequent deposition of iron in perilesional brain parenchyma. Since free iron is well-known to trigger ferroptotic [45] and possibly necroptotic cell death signaling [46], we hypothesized that chronic post-traumatic brain damage may be associated with iron deposition. Since iron can alter MRI signals, we looked for signal alterations using MRI scans. Indeed, we found hyperintense signals at the border of the lesion one month after TBI by T1-weighted MRI (Fig. 7a, upper panel) and could demonstrate that these signals showed a close spatial correlation with iron deposits as identified by Prussian blue staining (Fig. 7a, lower panel and Fig. 7b). Comparison of the volume of iron deposits between wild type and RIP deficient mice revealed equal amounts of iron in all animals, suggesting that the amount of hemorrhage was equal in all experimental groups (Fig. 7c and d). In a next step, we investigated the spatial and temporal relationship between chronic lesion expansion and iron deposits. For this purpose, we recorded iron deposits one month and lesion area three months after TBI, a time point when the lesion already expanded. In wild type mice the rim of the lesion area, the site of lesion progression, colocalized with iron deposits, while in neuronal specific RIPK1 deficient mice colocalization was minimal (Fig. 7e). The quantification of lesion area and iron deposition in wild type, RIPK1 and RIPK3 deficient mice, demonstrated that tissue loss co-localizing with histopathological detection of iron was significantly reduced in RIP deficient animals, suggesting that free iron may be involved in the pathophysiology of chronic neuronal necroptosis following TBI (Fig. 7f and g).

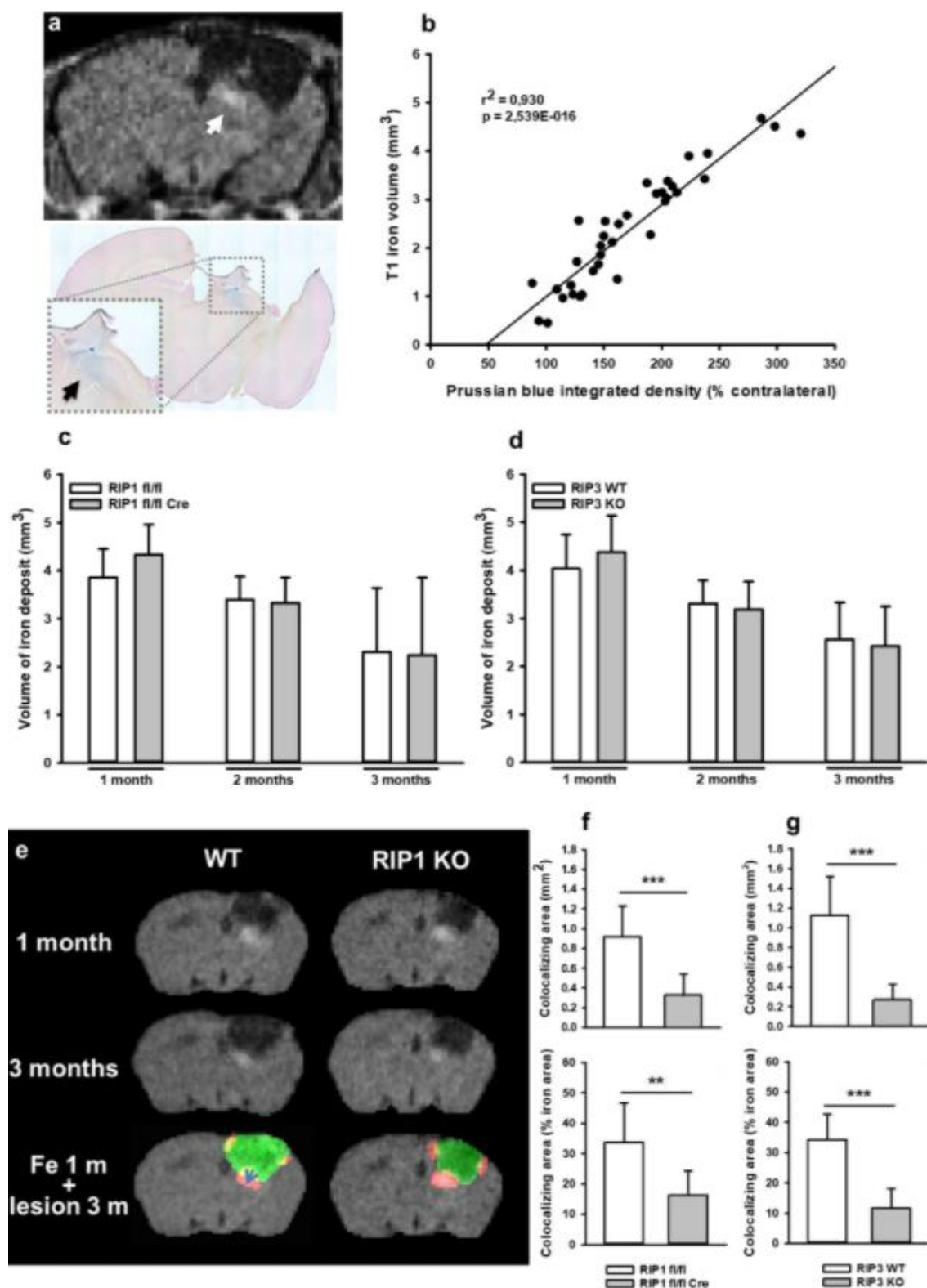


Figure 7: Lesion progression occurs in areas with iron deposits. a T1-weighted MRI (upper panel) and Prussian blue staining (lower panel) three months after injury. There is a close spatial correlation between the T1-hyperintense signal and iron staining (arrowheads). b There is high spatial correlation between the area of T1 hyperintensities and iron deposits as assessed by Prussian blue staining. Pearson product-moment correlation analysis. c and d Iron deposits in pericontusional brain tissue assessed by longitudinal MRI. Extent of hemorrhage is comparable in RIPK1 (c) and RIPK3 (d) knockout animals and controls, indicating no differences in hemorrhage size

after TBI between groups. T1 hyperintensities decreased over time in all groups, suggesting a very slow resorption of iron over time. e. Co-localization of iron deposits (red) observed at 1 month after TBI (upper panels) and lesion size assessed at the end of the observation period (3 months, middle row, green) suggests a progressive expansion of the lesion towards the regions with iron deposits. f and g Quantification of overlap between iron deposits and lesion. The higher the overlap of iron deposits and lesion size at three months, the higher the rate of tissue loss/ cell death in iron containing tissue. Co-localization is significantly less pronounced in RIPK1 (f) or RIPK3 (g) deficient mice, suggesting a reduced lesion growth in RIP knockouts due to toxic iron residues. Data are presented as mean \pm SD; n = 9–10 for RIPK1, n = 8–9 for RIPK3. Two-way RM ANOVA with Tukey's multiple comparisons test was used. **p < 0.005, ***p < 0.001.

Discussion

It is increasingly recognized that next to its acute sequelae, traumatic brain injury is a chronic disease [14]. Chronic post-trauma brain damage is associated with inflammation, persists for years after the initial insult, and may spread to areas initially not affected by the initial impact [47]. Affected patients often suffer from neuro- cognitive and mood disorders, personality changes, neurocognitive dysfunction, or even dementia [48–54]. So far, no therapeutic concepts targeting the long-term sequelae of TBI exist as the pathophysiology of chronic traumatic brain injury is still poorly understood.

Here, we propose, to our knowledge for the first time, that programmed cell death signaling mediates chronic neuronal injury after TBI. More specifically, we identified the necroptosis signaling molecules RIPK1 and RIPK3 to be major players in this process. Neurons affected by chronic traumatic damage showed necroptotic signaling as evidenced by enhanced levels of pMLKL. Moreover, Ripk3 global knockout animals as well as neuronal RIPK1 deficient mice were significantly protected from chronic brain injury and showed improved neurocognitive function up to three months after TBI. Of note, no protection was observed within the first days after TBI, suggesting that necroptosis is not involved in acute injury, but specifically mediates chronic traumatic brain damage. Hence, our data further suggest that mechanistically acute and chronic neuronal cell death seem to be mediated by different processes.

Longitudinal MRI and histological assessment revealed that lesion progression was associated with parenchymal iron deposition and that neuronal or global deletion of RIPK1 or RIPK3 prevented lesion progression. These findings suggest that chronic traumatic brain damage may be triggered by iron and mediated by necroptotic signaling. The association of lesion progression with iron deposits is intriguing and may indicate that iron plays an important role in this process, however, further experiments addressing this issue in more detail will need to further evaluate whether there is a causal or just a correlative relationship between iron deposition and neuronal necroptosis.

Hemorrhage and the subsequent degradation of red blood cells releases large amounts of hemoglobin, heme, and free iron, i.e. molecules with high cytotoxic activity, into brain tissue [55]. From numerous studies investigating intraparenchymal hemorrhage, a subtype of hemorrhagic stroke, it is well known that specifically free iron generates reactive oxygen species thereby damaging cell membranes and causing tissue damage and neurological dysfunction [36, 56–59]. Cerebral macro- and microhemorrhages are common after TBI [60–62]. Specifically, microbleeds have been shown to exert toxic effects on endothelial cells, astrocytes, neurons, oligodendrocytes, and microglia and may thus lead to blood–brain barrier damage, neuronal cell death, demyelination, and chronic inflammation [63]. The importance of blood degradation products for the pathophysiology of TBI is further demonstrated by the fact that the presence and extent of hemorrhage show

a close correlation with injury severity and long-term clinical outcome in TBI patients [63, 64]. In line with these clinical studies, we previously demonstrated that the TBI model used in current study shows acute macro-hemorrhage, which, however, resolves within the first week after injury [23]. In the current study we now show by MRI and Prussian blue staining that iron persists in pericontusional tissue for up to three months after the initial impact. Iron deposits identified in still viable pericontusional brain tissue one month after TBI co-localized with damaged tissue three months after injury, suggesting that chronic lesion progression preferably occurred in areas with previous hemorrhage and subsequent iron deposition. Since this process was significantly attenuated in neuronal Ripk1 and global Ripk3 knockout animals, our findings suggest that pericontusional iron may be involved in chronic posttraumatic lesion expansion and that this process is mediated by necroptotic signaling in neurons.

So far, neuroinflammation was believed to be the main cause of chronic brain damage after TBI [44]. However, the mechanisms by which microglial activation promotes neuronal injury and death remain elusive. Further, microglial activation after TBI may exert beneficial as well as detrimental effects, i.e. tissue regeneration versus accelerated damage, respectively. Therefore, disentangling these opposite functions of microglia may have important therapeutic consequences. Our current data suggest that the final steps causing neuronal cell death during chronic post-trauma brain damage depend on RIPK1 and RIPK3 activity. Based on these findings, we suggest a hypothetical scenario in which chronic post-trauma brain damage is initiated by the ongoing production of reactive oxygen species (ROS) by inflammatory cells. Physiological concentrations of ROS are usually well tolerated by cells since they are detoxified to water and oxygen by the glutathione system and catalases [65]. However, in the presence of iron, hydrogen peroxide is converted to highly reactive hydroxyl radicals by the Fenton reaction and may initiate a form of programmed cell death called ferroptosis [66, 67]. The link between ferroptosis and RIPK1/3-mediated necroptosis in neurons is not fully established, but may be mediated by cylindromatosis (CylD), a deubiquitinase able to activate RIPK1 and downstream necroptosome formation under conditions of oxidative stress as we recently demonstrated [21]. We showed that CYLD-dependent RIPK1/RIPK3 necrosome-formation occurred in neuronal cells exposed to ferroptosis activators and knockdown of the necroptosis-mediators CYLD, RIPK1 or RIPK3 attenuated cell death. Interestingly, the role for CYLD in ferroptosis also translated into neuroprotective effects *in vivo*, since CYLD knockout mice showed reduced secondary brain damage after TBI compared to controls [21]. These findings are corroborated by results in models of hemorrhagic stroke suggesting that necroptosis and ferroptosis are indeed interconnected under conditions of blood-induced tissue damage [68].

Despite its obvious strengths, the current study also has some notable limitations. We studied only young male animals and are therefore not able to make any statements on the role of necroptosis in the aged or female brain. Further, due to technical limitations, such as the lack of specific antibodies for the study of necroptosis in brain tissue, we were only able to demonstrate the involvement of a single signaling molecule downstream of RIPK activation, namely pMLKL. Thus, future studies using novel experimental tools will need to define necroptotic signaling after TBI in more detail. Another shortcoming of the current study is that we demonstrate only a spatial correlation between iron deposition and necroptosis. Thus, further studies are needed to further clarify whether there is a causal relationship between iron deposition and neuronal necroptosis. Finally, we want to point out that memory tests in mice are sometimes hard to interpret since results may be influenced by differences in motor function or the level of disinhibition which are well known to occur after TBI. We controlled for differences in motor function and the intensity of

exploratory behavior between groups and are confident that the presented data indeed reflect memory function, however, the results need nevertheless to be interpreted with caution.

In conclusion, the current study provides evidence that RIPK1 and RIPK3 are critically involved in chronic post-trauma brain damage. Further, our findings suggest that free iron may be involved in this process. Our results therefore help to better understand the mechanisms of chronic post-trauma brain damage and suggest that RIPK1- and RIPK3-mediated necroptosis may represent a novel therapeutic target for the treatment of patients suffering from the long-term sequels of TBI.

References

1. Dewan MC, Rattani A, Gupta S, Baticulon RE, Hung YC, Punchak M, Agrawal A, Adeleye AO, Shrivastava MG, Rubiano AM et al (2018) Estimating the global incidence of traumatic brain injury. *J Neurosurg*. <https://doi.org/10.3171/2017.10.JNS17352>
2. Injury GBDTB, Spinal Cord Injury C (2019) Global, regional, and national burden of traumatic brain injury and spinal cord injury, 1990-2016: a systematic analysis for the Global Burden of Disease Study 2016. *The Lancet Neurology* 18: 56-87 [https://doi.org/10.1016/S1474-4422\(18\)30415-0](https://doi.org/10.1016/S1474-4422(18)30415-0)
3. Maas AIR, Menon DK, Adelson PD, Andelic N, Bell MJ, Belli A, Bragge P, Brazinova A, Buki A, Chesnut RM et al (2017) Traumatic brain injury: integrated approaches to improve prevention, clinical care, and research. *Lancet Neurol* 16:987–1048. [https://doi.org/10.1016/S1474-4422\(17\)30371-X](https://doi.org/10.1016/S1474-4422(17)30371-X)
4. Rabinowitz AR, Levin HS (2014) Cognitive sequelae of traumatic brain injury. *Psychiatr Clin North Am* 37:1–11. <https://doi.org/10.1016/j.psc.2013.11.004>
5. Selassie AW, Zaloshnja E, Langlois JA, Miller T, Jones P, Steiner C (2008) Incidence of long-term disability following traumatic brain injury hospitalization, United States, 2003. *J Head Trauma Rehabil* 23:123–131. <https://doi.org/10.1097/01.HTR.0000314531.30401.39>
6. Silver JM, McAllister TW, Arciniegas DB (2009) Depression and cognitive complaints following mild traumatic brain injury. *Am J Psychiatry* 166:653–661. <https://doi.org/10.1176/appi.ajp.2009.08111676>
7. Ramos-Cejudo J, Wisniewski T, Marmar C, Zetterberg H, Blennow K, de Leon MJ, Fossati S (2018) Traumatic brain injury and Alzheimer's disease: the cerebrovascular link. *EBioMedicine* 28:21–30. <https://doi.org/10.1016/j.ebiom.2018.01.021>
8. MacKenzie JD, Siddiqi F, Babb JS, Bagley LJ, Mannon LJ, Sinson GP, Grossman RI (2002) Brain atrophy in mild or moderate traumatic brain injury: a longitudinal quantitative analysis. *AJNR Am J Neuror* 23:1509–1515
9. Reider-Groswasser I, Cohen M, Costeff H, Groswasser Z (1993) Late CT findings in brain trauma: relationship to cognitive and behavioural sequelae and to vocational outcome. *AJR Am J Roentgenol* 160:147–152. <https://doi.org/10.2214/ajr.160.1.8416613>
10. Cardoso ER, Galbraith S (1985) Posttraumatic hydrocephalus—a retrospective review. *Surg Neurol* 23:261–264. [https://doi.org/10.0090/3019\(85\)90092-8\[pil\]](https://doi.org/10.0090/3019(85)90092-8[pil])
11. Guyot LL, Michael DB (2000) Post-traumatic hydrocephalus. *Neurol Res* 22:25–28
12. Honeybul S, Ho KM (2012) Incidence and risk factors for post-traumatic hydrocephalus following decompressive craniectomy for intractable intracranial hypertension and evacuation of mass lesions. *J Neurotrauma* 29:1872–1878. <https://doi.org/10.1089/neu.2012.2356>
13. Mazzini L, Campini R, Angelino E, Rognone F, Pastore I, Oliveri G (2003) Posttraumatic hydrocephalus: a clinical, neuroradiologic, and neuropathologic assessment of long-term outcome. *Arch Phys Med Rehabil* 84:1637–1641

14. Faden AI, Loane DJ (2015) Chronic neurodegeneration after traumatic brain injury: Alzheimer disease, chronic traumatic encephalopathy, or persistent neuroinflammation? *Neurotherapeutics* 12:143–150. <https://doi.org/10.1007/s13311-014-0319-5>
15. Johnson VE, Stewart JE, Begbie FD, Trojanowski JQ, Smith DH, Stewart W (2013) Inflammation and white matter degeneration persist for years after a single traumatic brain injury. *Brain* 136:28–42. <https://doi.org/10.1093/brain/aws322>
16. Loane DJ, Kumar A, Stoica BA, Cabatbat R, Faden AI (2014) Progressive neurodegeneration after experimental brain trauma: association with chronic microglial activation. *J Neuro-pathol Exp Neurol* 73:14–29
17. Ramlackhansingh AF, Brooks DJ, Greenwood RJ, Bose SK, Turkheimer FE, Kinnunen KM, Gentleman S, Heckemann RA, Gunanayagam K, Gelsa
18. G et al (2011) Inflammation after trauma: microglial activation and traumatic brain injury. *Ann Neurol* 70:374–383. <https://doi.org/10.1002/ana.22455>
19. Ritzel RM, Doran SJ, Barrett JP, Henry RJ, Ma EL, Faden AI, Loane DJ (2018) Chronic alterations in systemic immune function after traumatic brain injury. *J Neurotrauma* 35:1419–1436. <https://doi.org/10.1089/neu.2017.5399>
20. Hitomi J, Christofferson DE, Ng A, Yao J, Degterev A, Xavier RJ, Yuan J (2008) Identification of a molecular signaling network that regulates a cellular necrotic cell death pathway. *Cell* 135:1311–1323. <https://doi.org/10.1016/j.cell.2008.10.044>
21. Moquin DM, McQuade T, Chan FK (2013) CYLD deubiquitinates RIP1 in the TNF α -induced necrosome to facilitate kinase activation and programmed necrosis. *PLoS ONE* 8:e76841. <https://doi.org/10.1371/journal.pone.0076841>
22. Ganjam GK, Terpolilli NA, Diemert S, Eisenbach I, Hoffmann L, Reuther C, Herden C, Roth J, Plesnila N, Culmsee C (2018) Cylindromatosis mediates neuronal cell death in vitro and in vivo. *Cell Death Differ* 25:1394–1407. <https://doi.org/10.1038/s41418-017-0046-7>
23. Krieg SM, Voigt F, Knuefermann P, Kirschning CJ, Plesnila N, Ringel F (2017) Decreased secondary lesion growth and attenuated immune response after traumatic brain injury in Tlr2/4(-/-) mice. *Front Neurol* 8:455. <https://doi.org/10.3389/fneur.2017.00455>
24. Mao X, Terpolilli NA, Wehn A, Chen S, Hellal F, Liu B, Seker B, Plesnila N (2019) Progressive histopathological damage occurring up to one year after experimental traumatic brain injury is associated with cognitive decline and depression-like behavior. *J Neurotrauma*: [Doi https://doi.org/10.1089/neu.2019.6510](https://doi.org/10.1089/neu.2019.6510)
25. Kilkenny C, Browne WJ, Cuthill IC, Emerson M, Altman DG (2010) Improving bioscience research reporting: the ARRIVE guidelines for reporting animal research. *PLoS Biol* 8:e1000412. <https://doi.org/10.1371/journal.pbio.1000412>
26. Guillen J (2012) FELASA guidelines and recommendations. *J Am Assoc Lab Anim Sci* 51:311–321
27. Takahashi N, Vereecke L, Bertrand MJ, Duprez L, Berger SB, Divert T, Gonçalves A, Sze M, Gilbert B, Kourula S et al (2014) RIPK1 ensures intestinal homeostasis by protecting the epithelium against apoptosis. *Nature* 513:95–99. <https://doi.org/10.1038/nature13706>
28. Newton K, Sun X, Dixit VM (2004) Kinase RIP3 is dispensable for normal NF- κ B signaling by the B-cell and T-cell receptors, tumor necrosis factor receptor 1, and Toll-like receptors 2 and 4. *Mol Cell Biol* 24:1464–1469. <https://doi.org/10.1128/mcb.24.4.1464-1469.2004>
29. Terpolilli NA, Zweckberger K, Trabold R, Schilling L, Schinzel R, Tegtmeyer F, Plesnila N (2009) The novel nitric oxide synthase inhibitor 4-amino-tetrahydro-L-biopterine prevents

- brain edema formation and intracranial hypertension following traumatic brain injury in mice. *J Neurotrauma* 26:1963–1975. <https://doi.org/10.1089/neu.2008-0853>
30. Zweckberger K, Eros C, Zimmermann R, Kim SW, Engel D, Plesnila N (2006) Effect of early and delayed decompressive craniectomy on secondary brain damage after controlled cortical impact in mice. *J Neurotrauma* 23:1083–1093. <https://doi.org/10.1089/neu.2006.23.1083>
 31. Zweckberger K, Stoffel M, Baethmann A, Plesnila N (2003) Effect of decompression craniotomy on increase of contusion volume and functional outcome after controlled cortical impact in mice. *J Neurotrauma* 20:1307–1314. <https://doi.org/10.1089/089771503322686102>
 32. Barnes CA (1979) Memory deficits associated with senescence: a neurophysiological and behavioral study in the rat. *J Comp Physiol Psychol* 93:74–104. <https://doi.org/10.1037/h0077579>
 33. Gawel K, Gibula E, Marszalek-Grabska M, Filarowska J, Kotlinska JH (2019) Assessment of spatial learning and memory in the Barnes maze task in rodents-methodological consideration. *Naunyn-Schmiedeberg's Arch Pharmacol* 392:1–18. <https://doi.org/10.1007/s00210-018-1589-y>
 34. Cryan JF, Mombereau C, Vassout A (2005) The tail suspension test as a model for assessing antidepressant activity: review of pharmacological and genetic studies in mice. *Neurosci Biobehav Rev* 29:571–625. <https://doi.org/10.1016/j.neubiorev.2005.03.009>
 35. Ghosh M, Balbi M, Hellal F, Dichgans M, Lindauer U, Plesnila N (2015) Pericytes are involved in the pathogenesis of cerebral autosomal dominant arteriopathy with subcortical infarcts and leukoencephalopathy. *Ann Neurol* 78:887–900. <https://doi.org/10.1002/ana.24512>
 36. Schindelin J, Arganda-Carreras I, Frise E, Kaynig V, Longair M, Pietzsch T, Preibisch S, Rueden C, Saalfeld S, Schmid B et al (2012) Fiji: an open-source platform for biological-image analysis. *Nat Methods* 9:676–682. <https://doi.org/10.1038/nmeth.2019>
 37. Hua Y, Xi G, Keep RF, Hoff JT (2000) Complement activation in the brain after experimental intracerebral hemorrhage. *J Neurosurg* 92:1016–1022. <https://doi.org/10.3171/jns.2000.92.6.1016>
 38. Young K, Morrison H (2018) Quantifying microglia morphology from photomicrographs of immunohistochemistry prepared tissue using ImageJ. *J Vis Exp: Doi* <https://doi.org/10.3791/57648>
 39. Ferreira TA, Blackman AV, Oyrer J, Jayabal S, Chung AJ, Watt AJ, Sjostrom PJ, van Meyel DJ (2014) Neuronal morphometry directly from bitmap images. *Nat Methods* 11:982–984. <https://doi.org/10.1038/nmeth.3125>
 40. Karperien A (1999–2013) *FracLac for ImageJ*.
 41. Sun L, Wang H, Wang Z, He S, Chen S, Liao D, Wang L, Yan J, Liu W, Lei X et al (2012) Mixed lineage kinase domain-like protein mediates necrosis signaling downstream of RIP3 kinase. *Cell* 148:213–227. <https://doi.org/10.1016/j.cell.2011.11.031>
 42. Ariza M, Serra-Grabulosa JM, Junque C, Ramirez B, Mataro M, Poca A, Bargallo N, Sahuquillo J (2006) Hippocampal head atrophy after traumatic brain injury. *Neuropsychologia* 44:1956–1961. <https://doi.org/10.1016/j.neuropsychologia.2005.11.007>
 43. Jorge RE, Acion L, Starkstein SE, Magnotta V (2007) Hippocampal volume and mood disorders after traumatic brain injury. *Biol Psychiatry* 62:332–338. <https://doi.org/10.1016/j.biopsych.2006.07.024>

44. Jassam YN, Izzy S, Whalen M, McGavern DB, El Khoury J (2017) Neuroimmunology of traumatic brain injury: time for a paradigm shift. *Neuron* 95:1246–1265. <https://doi.org/10.1016/j.neuron.2017.07.010>
45. Morganti-Kossmann MC, Semples BD, Hellewell SC, Bye N, Ziebell JM (2019) The complexity of neuroinflammation consequent to traumatic brain injury: from research evidence to potential treatments. *Acta Neuropathol* 137:731–755. <https://doi.org/10.1007/s00401-018-1944-6>
46. Dixon SJ, Lemberg KM, Lamprecht MR, Skouta R, Zaitsev EM, Gleason CE, Patel DN, Bauer AJ, Cantley AM, Yang WS et al (2012) Ferroptosis: an iron-dependent form of nonapoptotic cell death. *Cell* 149:1060–1072. <https://doi.org/10.1016/j.cell.2012.03.042>
47. Pasparakis M, Vandenabeele P (2015) Necroptosis and its role in inflammation. *Nature* 517:311–320. <https://doi.org/10.1038/nature14191>
48. Plesnila N (2016) The immune system in traumatic brain injury. *Curr Opin Pharmacol* 26:110–117. <https://doi.org/10.1016/j.coph.2015.10.008>
49. Al-Khindi T, Macdonald RL, Schweizer TA (2010) Cognitive and functional outcome after aneurysmal subarachnoid hemorrhage. *Stroke* 41:e519–e536. <https://doi.org/10.1161/STROKEAHA.110.581975>
50. Alghnam S, AlSayyari A, Albabtain I, Aldebasi B, Alkelya M (2017) Long-term disabilities after traumatic head injury (THI): a retrospective analysis from a large level-I trauma center in Saudi Arabia. *Inj Epidemiol* 4:29. <https://doi.org/10.1186/s40621-017-0126-7>[pii]
51. Andelic N, Howe EI, Hellstrom T, Sanchez MF, Lu J, Lovstad M, Roe C (2018) Disability and quality of life 20 years after traumatic brain injury. *Brain Behav*. <https://doi.org/10.1002/brb3.1018>
52. Draper K, Ponsford J (2008) Cognitive functioning ten years following traumatic brain injury and rehabilitation. *Neuropsychology* 22:618–625. <https://doi.org/10.1037/0894-4105.22.5.618>
53. Hackett ML, Anderson CS (2000) Health outcomes 1 year after subarachnoid hemorrhage: an international population-based study. The Australian cooperative research on subarachnoid hemorrhage study group. *Neurology* 55:658–662
54. Hart T, Whyte J, Polansky M, Millis S, Hammond FM, Sherer M, Bushnik T, Hanks R, Kreutzer J (2003) Concordance of patient and family report of neurobehavioral symptoms at 1 year after traumatic brain injury. *Arch Phys Med Rehabil* 84:204–213. <https://doi.org/10.1053/apmr.2003.50019>
55. Himanen L, Portin R, Isoniemi H, Helenius H, Kurki T, Tenovu O (2005) Cognitive functions in relation to MRI findings 30 years after traumatic brain injury. *Brain Inj* 19:93–100
56. Regan RF, Panter SS (1996) Hemoglobin potentiates excitotoxic injury in cortical cell culture. *J Neurotrauma* 13:223–231. <https://doi.org/10.1089/neu.1996.13.223>
57. Bhasin RR, Xi G, Hua Y, Keep RF, Hoff JT (2002) Experimental intracerebral hemorrhage: effect of lysed erythrocytes on brain edema and blood-brain barrier permeability. *Acta Neurochir Suppl* 81:249–251. https://doi.org/10.1007/978-3-7091-6738-0_65

-
58. Derry PJ, Vo ATT, Gnanansekaran A, Mitra J, Liopo AV, Hegde ML, Tsai AL, Tour JM, Kent TA (2020) The chemical basis of intracerebral hemorrhage and cell toxicity with contributions from eryptosis and ferroptosis. *Front Cell Neurosci* 14:603043. <https://doi.org/10.3389/fncel.2020.603043>
 59. Letarte PB, Lieberman K, Nagatani K, Haworth RA, Odell GB, Duff TA (1993) Hemin: levels in experimental subarachnoid hematoma and effects on dissociated vascular smooth-muscle cells. *J Neurosurg* 79:252–255. <https://doi.org/10.3171/jns.1993.79.2.0252>
 60. Wan J, Ren H, Wang J (2019) Iron toxicity, lipid peroxidation and ferroptosis after intracerebral haemorrhage. *Stroke Vasc Neurol* 4:93–95. <https://doi.org/10.1136/svn-2018-000205>
 61. Hasiloglu ZI, Albayram S, Selcuk H, Ceyhan E, Delil S, Arkan B, Baskoy L (2011) Cerebral microhemorrhages detected by susceptibility-weighted imaging in amateur boxers. *AJNR Am J Neuroradiol* 32:99–102. <https://doi.org/10.3174/ajnr.A2250>
 62. Park JH, Park SW, Kang SH, Nam TK, Min BK, Hwang SN (2009) Detection of traumatic cerebral microbleeds by susceptibility-weighted image of MRI. *J Korean Neurosurg Soc* 46:365–369. <https://doi.org/10.3340/jkns.2009.46.4.365>
 63. van der Horn HJ, de Haan S, Spikman JM, de Groot JC, van der Naalt J (2018) Clinical relevance of microhemorrhagic lesions in subacute mild traumatic brain injury. *Brain Imaging Behav* 12:912–916. <https://doi.org/10.1007/s11682-017-9743-6>
 64. Glushakova OY, Johnson D, Hayes RL (2014) Delayed increases in microvascular pathology after experimental traumatic brain injury are associated with prolonged inflammation, blood-brain barrier disruption, and progressive white matter damage. *J Neurotrauma* 31:1180–1193. <https://doi.org/10.1089/neu.2013.3080>
 65. Lawrence TP, Pretorius PM, Ezra M, Cadoux-Hudson T, Voets NL (2017) Early detection of cerebral microbleeds following traumatic brain injury using MRI in the hyper-acute phase. *Neurosci Lett* 655:143–150. <https://doi.org/10.1016/j.neulet.2017.06.046>
 66. Conrad M, Pratt DA (2019) The chemical basis of ferroptosis. *Nat Chem Biol* 15:1137–1147. <https://doi.org/10.1038/s41589-019-0408-1>
 67. Li Q, Han X, Lan X, Gao Y, Wan J, Durham F, Cheng T, Yang J, Wang Z, Jiang C et al (2017) Inhibition of neuronal ferroptosis protects hemorrhagic brain. *JCI insight* 2:e90777. <https://doi.org/10.1172/jci.insight.90777>
 68. Ratan RR (2020) The chemical biology of ferroptosis in the central nervous system. *Cell Chem Biol* 27:479–498. <https://doi.org/10.1016/j.chembiol.2020.03.007>
 69. Zille M, Karuppagounder SS, Chen Y, Gough PJ, Bertin J, Finger J, Milner TA, Jonas EA, Ratan RR (2017) Neuronal death after hemorrhagic stroke in vitro and in vivo shares features of ferroptosis and necroptosis. *Stroke* 48:1033–1043. <https://doi.org/10.1161/strokeaha.116.015609>

7. Paper III

Acid-Ion Sensing Channel 1a Deletion Reduces Chronic Brain Damage and Neurological Deficits after Experimental Traumatic Brain Injury

Shiqi Cheng,^{1,2,†} Xiang Mao^{1,2} Xiangjiang Lin,^{1,2} Antonia Wehn^{1,2} Senbin Hu^{1, 2} Uta Mamrak^{1, 2} Igor Khalin^{1, 2} Maria Wostrack,³ Florian Ringel,⁴ Nikolaus Plesnila^{1,2} and Nicole A. Terpolilli^{1,2,5,*}

¹Institute for Stroke and Dementia Research, ⁵Department of Neurosurgery, Munich University Hospital, Munich, Germany.

²Munich Cluster for Systems Neurology (SyNergy), Munich, Germany. ³Department of Neurosurgery, Technical University Munich, Munich, Germany. ⁴Department of Neurosurgery, University Medical Center Mainz, Mainz, Germany.

[†]Current Address: Department of Neurosurgery, The Second Affiliated Hospital of Nanchang University, Nanchang, China.

*Address correspondence to: Nicole A. Terpolilli, MD, Department of Neurosurgery, Munich University Hospital, Marchioninistraße 15, 81377 Munich, Germany E-mail: Nicole.Terpolilli@med.uni-muenchen.de

Abstract

Traumatic brain injury (TBI) causes long-lasting neurodegeneration and cognitive impairments; however, the underlying mechanisms of these processes are not fully understood. Acid-sensing ion channels 1a (ASIC1a) are voltage-gated Na⁺- and Ca²⁺-channels shown to be involved in neuronal cell death; however, their role for chronic post-traumatic brain damage is largely unknown. To address this issue, we used ASIC1a-deficient mice and investigated their outcome up to 6 months after TBI. ASIC1a-deficient mice and their wild-type (WT) littermates were subjected to controlled cortical impact (CCI) or sham surgery. Brain water content was analyzed 24 h and behavioral outcome up to 6 months after CCI. Lesion volume was assessed longitudinally by magnetic resonance imaging and 6 months after injury by histology. Brain water content was significantly reduced in ASIC1a^{-/-} animals compared to WT controls. Over time, ASIC1a^{-/-} mice showed significantly reduced lesion volume and reduced hippocampal damage. This translated into improved cognitive function and reduced depression-like behavior. Microglial activation was significantly reduced in ASIC1a^{-/-} mice. In conclusion, ASIC1a deficiency resulted in reduced edema formation acutely after TBI and less brain damage, functional impairments, and neuroinflammation up to 6 months after injury. Hence, ASIC1a seems to be involved in chronic neurodegeneration after TBI.

Keywords: animal studies; brain edema; cognitive function; controlled cortical impact; traumatic brain injury

Introduction

Traumatic brain injury (TBI) is a major cause of death and disability worldwide.¹⁻³ In past decades, most clinical and experimental studies concentrated on clarifying pathomechanisms occurring in

the first hours and days after trauma. It is, however, increasingly recognized that pathophysiological processes that aggravate post-traumatic brain damage, thus causing progressive neurocognitive and behavioral deficits, are not restricted to the first few days, but may be active for months and even years after TBI.^{4–9} Further, a history of TBI is a risk factor for the development of neurocognitive,^{10,11} neurodegenerative,^{12,13} and psychiatric disorders^{14–16} and increases all-cause mortality.^{17,18} These clinical symptoms were linked to progressive brain atrophy and persisting inflammatory changes,^{19,20} findings corroborated by experimental studies showing that progressive histological damage occurs up to 1 year after experimental TBI and is accompanied by cognitive dysfunction and depressive behavior.^{21–24} The exact mechanisms resulting in chronic post-traumatic brain damage are, however, not yet fully elucidated.

Acidosis is important in the development of acute post-traumatic brain damage and occurs after experimental as well as clinical TBI.^{25–27} The mechanisms of acidosis-induced neuronal damage in TBI are, however, not completely understood. Recently, acid-sensing ion channels (ASICs) have been proposed as important acid sensors^{28,29} and hypothesized to play an important role for acidosis-induced post-ischemic neuronal damage.^{30,31} ASICs are widely expressed in the central nervous system (CNS) and peripheral nervous system.^{32–35} ASIC1a, one of the most prevalent isoforms in the CNS,^{33,36,37} is permeable to Na⁺ and Ca²⁺ and results in neuronal (over)excitation when activated by extracellular acidosis.³⁸ Based on its potential role in amplifying excitotoxicity, ASIC1a has been investigated in a variety of cerebral diseases: its pharmacological inhibition or genetic disruption reduced infarct volume after cerebral ischemia,^{30,39,40} conferred neuroprotection in ischemic pre- and post-conditioning,⁴¹ reduced brain injury in models of autoimmune encephalomyelitis,⁴² and improved outcome in Huntington's disease models.⁴³ In TBI, ASIC1a-deficient mice showed attenuated neuronal cell death 24 h and partially improved memory function 4 days after the insult.⁴⁴ So far, however, the role of ASIC1a for chronic brain damage and long-term behavioral impairments after TBI is unknown.

Based on these previous results, we hypothesize that acidosis-induced pathomechanisms mediated by ASIC1a contribute to the development of chronic post-traumatic brain damage. To test this, we investigated post-traumatic neuropathological and -behavioral outcome in ASIC1a-deficient mice up to 6 months after experimental TBI.

Methods

Experimental animals

ASIC1a transgenic mice were purchased from Jackson Laboratories (strain #013733), male homo- and heterozygous mice and their wild-type (WT) littermates were bred heterozygously⁴⁵ for experiments.

Experimental protocol

All procedures were approved by the Animal Ethics Board of the Government of Upper Bavaria. Mice of all genotypes were randomly assigned to experimental groups by drawing lots. All procedures and analyses were performed by a researcher blinded to group allocation/genotype and reported according to the ARRIVE (Animal Research: Reporting of in Vivo Experiments) criteria. Mice not reaching the end of the study (i.e., 180 days after TBI) were excluded from analysis in order to avoid mortality bias.

Brain water content was assessed in 8- to 10-week-old male ASIC1a^{+/-} and WT littermates (sham, $n = 4$ per group; TBI groups, $n = 16$ per group). Long-term evaluation was performed in 8- to 10-week-old male ASIC1a^{+/-} ($n = 12$), ASIC1a^{-/-} ($n = 12$), and WT littermates ($n = 11$; Fig. 1).

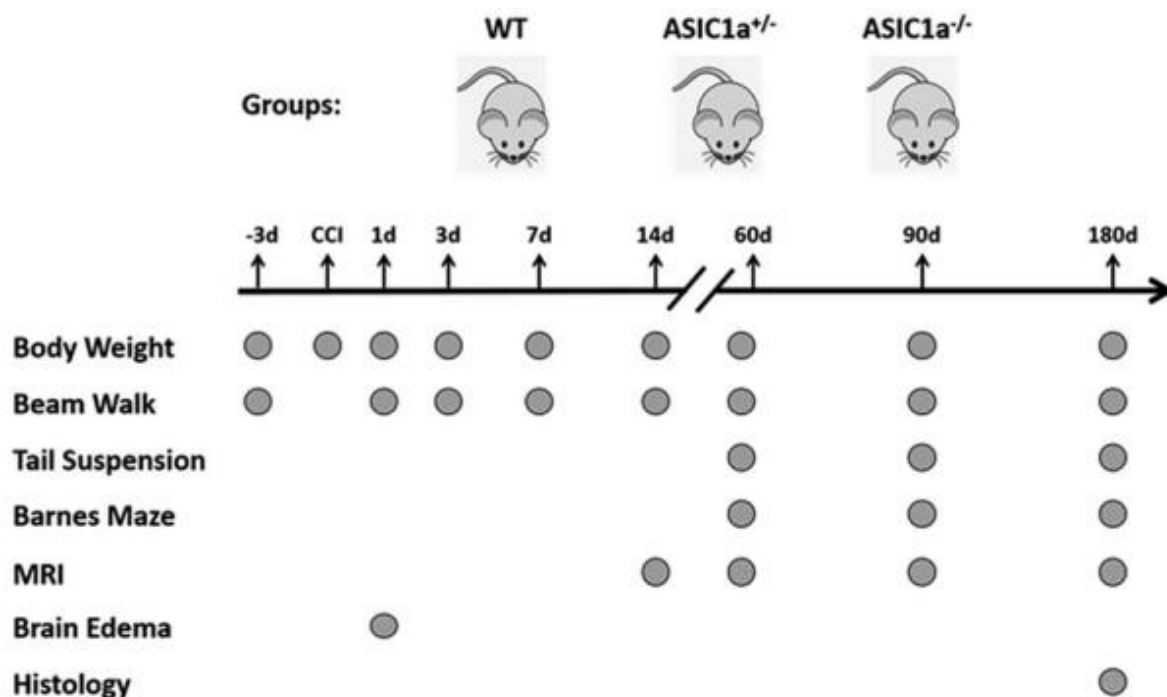


Figure 1: Schematic overview of the experimental protocol. MRI, magnetic resonance imaging; WT, wildtype.

Experimental traumatic brain injury

Controlled cortical impact (CCI) was induced as previously described.^{22,46–48} After a right parietal craniotomy, a CCI (impact depth, 1 mm; impact duration, 150 ms; impact velocity, 8 m/s) was performed onto the intact dura, then the bone flap was re-implanted. Sham operation consisted in craniotomy without CCI.

Body weight

Body weight was evaluated from 3 days before until 180 days after surgery using a scale with movement correction (OHAUS®; OHAUS Corporation, Munich, Germany).

Brain water content

Brain water content was measured 24 h after TBI by the wet-dry-weight method as previously described.^{22,46,47,49,50} Briefly, both hemispheres were dissected and weighed to obtain the wet weight. After drying (100°C, 24 h) to obtain the dry weight, brain water content was calculated using the following formula: $(\text{wet weight} - \text{dry weight}) / \text{wet weight} \cdot 100\%$. The difference between traumatized and non-traumatized hemisphere was calculated and plotted.

Beam walk test

The beam walk test for the evaluation of motor function was performed as previously described.^{22,51,52} Time to cross the beam and number of missteps were assessed from 3 days before until 180 days after CCI.

Tail suspension test

The tail suspension test is a widely used behavioral test for the evaluation of depression-like behavior in rodents.^{22,53,54} Animals were fixed by the tail and suspended head down in a custom-made frame; movement patterns were digitally recorded for 3 min on days 60, 90, and 180 after

TBI. Mobility/immobility times were automatically analyzed (EthoVision®XT; Noldus Information Technology, Wageningen, Netherlands).

Barnes maze test

The Barnes maze test is a test paradigm evaluating spatial learning and memory.^{22,55,56} The animal is placed on a brightly lit circular platform and trained to locate the home cage placed under one of the 20 holes at the platform rim. Mice were trained twice-daily for 4 days. On day 6, the time to reach the home cage (latency), distance, and speed traveled were evaluated by automated image analysis (EthoVision®XT).

Analysis of cortical and hippocampal lesion volume

Floating sections were prepared using a vibratome as previously described.⁵⁷ Briefly, thirteen 50- μ m-thick coronal brain sections were prepared at 500- μ m intervals. Sections were stained according to Nissl and digitized at 12.5-fold magnification (Zeiss Axio Imager M2; Carl Zeiss, Oberkochen, Germany). The area of the non-traumatized (A) and the traumatized hemisphere (B) were determined (Supplementary Fig. S1A), and the lesion area (C) was calculated ($A - B = C$) for each level. Lesion volume was then calculated according to the following formula: Lesion volume = $0.5 \text{ mm} \times (C1/2 + C2 + \dots + C13/2)$.²² Six sections containing the hippocampus (1.5 mm anterior to 4 mm posterior to bregma) were used to determine hippocampal damage as depicted in Supplementary Figure S1B.

Evaluation of lesion volume by magnetic resonance imaging

Lesion size after TBI was assessed longitudinally by T₂-weighted (T₂W) imaging using a 3 Tesla Nanoscan PET/MRI scanner (Mediso Medical Imaging Systems, Budapest, Hungary) on days 14, 60, 90, and 180 after TBI as previously described.²² On 19 coronal slices, both hemispheres were manually segmented (Supplementary Fig. S1C), and lesion volume was analyzed using an image analysis software (InterView™ FUSION; Mediso Medical Imaging Systems) and calculated as described above.

Immunohistochemistry

Sections were incubated overnight with the respective primary antibody in 1% bovine albumin, 0.1% gelatin, and 0.5% Triton X-100 in 0.01 M of phosphate-buffered saline before addition of the secondary antibody (1:200, 2 h, Alexa Fluor® 594; Jackson ImmunoResearch Labs Inc. West Grove, PA). The following primary antibodies were used: ionized calcium-binding adaptor molecule 1 (Iba-1; #019-19741, 1:200; Wako Chemicals U.S.A. Corporation, Richmond, VA); CD68 (#MAB1435, 1:200; Millipore, Bedford, MA); and neuronal nuclei (NeuN; #266004; Synaptic Systems, Goettingen, Germany).

To quantify Iba-1- and CD68-positive cells, maximum projection Z-stacks were obtained at bregma level with a 40 \times oil immersion objective using a confocal microscope (Zeiss LSM810; Carl Zeiss), as previously described.⁵⁷ Quantitative image analysis was performed by an investigator blinded to the genotype (ImageJ software; NIH, Bethesda, MD). Quantitative image analysis was performed by an investigator blinded to the genotype (ImageJ software; NIH). Three corresponding regions of interest (x, 354 μ m; y, 354 μ m; z, 25 μ m) in the ipsi- as well as the contralateral hemisphere were analyzed; after background correction, all Iba-1- or CD68-positive signals/pixels were subjected to automated threshold processing and subsequently counted.

Statistical analysis

Statistical analysis was performed using Sigma plot software (version 13.0; Systat, Erkrath, Germany). Sample-size calculations were performed with the following parameters: alpha-error = 0.05, beta-error = 0.2, standard deviation (SD) 15–20% (depending on the parameter investigated), and a biologically relevant difference of 30%. For comparing two groups, the Mann-Whitney U test was used, whereas the Kruskal-Wallis test, followed by Dunn's *post hoc* test, was used for multiple-group comparisons. For correlation analysis, the Pearson test was used. Survival rate was analyzed by the log-rank test. Differences between groups were considered significant at $p < 0.05$. All data are expressed as mean – SD.

Results

ASIC1a deficiency does not affect mortality and body weight after traumatic brain injury

Two animals in the WT group, 3 in the *ASIC1a*^{+/-} group, and 3 in the *ASIC1a*^{-/-} group died within 7 days after trauma. All other mice survived until at least 180 days after TBI. After 3 more WT and 2 more *ASIC1a*^{+/-} mice and 1 more *ASIC1a*^{-/-} mouse died *190 days after trauma, the study was terminated and all animals were euthanized. There was no significant difference between groups regarding acute or delayed mortality (Fig. 2A). Body weight of all mice decreased by *13% 1 day after TBI, then gradually recovered back to baseline. There was no significant difference between genotypes (Fig. 2B).

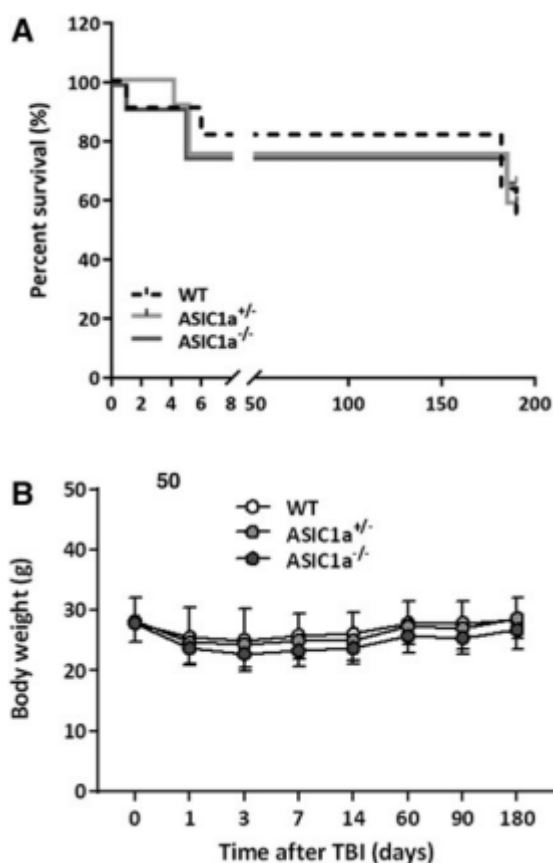


Figure 2: Survival rate (A) and changes in body weight (B) in WT littermates (n = 11) and heterozygous (n = 12) and homozygous (n = 12) *ASIC1a*-deficient mice up to 190 days after TBI. Mean – SD. SD, standard deviation; TBI, traumatic brain injury; WT, wild type.

ASIC1a knockout reduces brain edema formation 24 h after traumatic brain injury

In WT littermates, TBI induced a significant increase in brain water content 24 h after injury (+2.5 – 2.0%). In ASIC1a^{-/-} animals, this increase was significantly reduced by almost 75% (0.6 – 1.4%; $p < 0.01$), indicating a reduction of brain edema formation in these animals (Fig. 3).

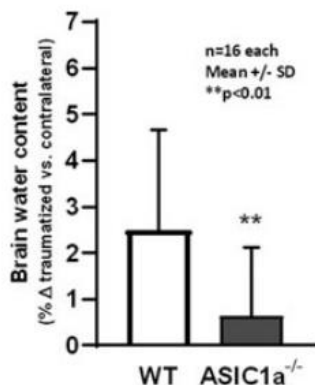


Figure 3: Change in brain water content, a measure for brain edema formation, in WT littermates and homozygous ASIC1a-deficient mice 24 h after TBI. Mean – SD, $n = 16$ per group. ** $p = 0.01$ versus WT. SD, standard deviation; TBI, traumatic brain injury; WT, wild type.

ASIC1a deficiency has no effect on motor function after traumatic brain injury

Three days before TBI, all animals crossed the beam in *10 sec and without missteps. One day after CCI, motor function significantly deteriorated in all investigated groups, as indicated by a prolonged crossing time (70–100 sec; $p < 0.01$ vs. baseline; Fig. 4A) and an increase in the number of missteps (Fig. 4B; $p < 0.01$). Both parameters partially recovered within 7 days, but did not return to pre-trauma values. There was no difference between groups at any time point.

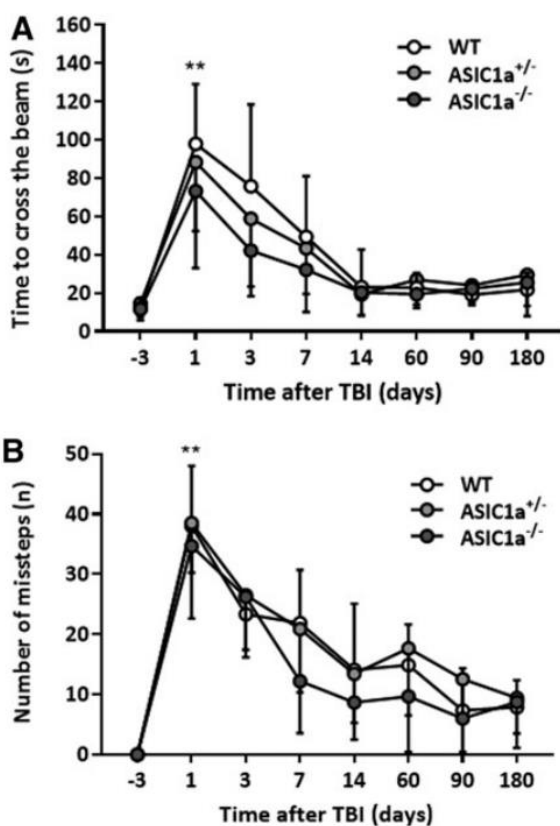


Figure 4: Motor function after TBI. Time needed to cross a beam (A) and the number of missteps (B) in WT littermates and heterozygous and homozygous ASIC1a-deficient mice up to 6 months after TBI. ** $p < 0.01$, all groups versus 3 days before TBI (3). Mean – SD, $n = 9$ per group. SD, standard deviation; TBI, traumatic brain injury; WT, wild type.

ASIC1a deficiency reduces depression-like behavior after traumatic brain injury long term

When hanging the head down by the tail, mice usually try to right themselves up for most of the observation time (i.e., 180 sec). In WT and heterozygous mice, TBI reduced the time animals

tried to right themselves up (mobility time) to *100 sec. Homozygous ASIC1a-deficient animals, however, showed a significantly higher mobility time of *140 sec at all time-points (Fig. 5; $p < 0.01$). These findings strongly suggest that ASIC1a deficiency improves depression-like behavior after TBI.

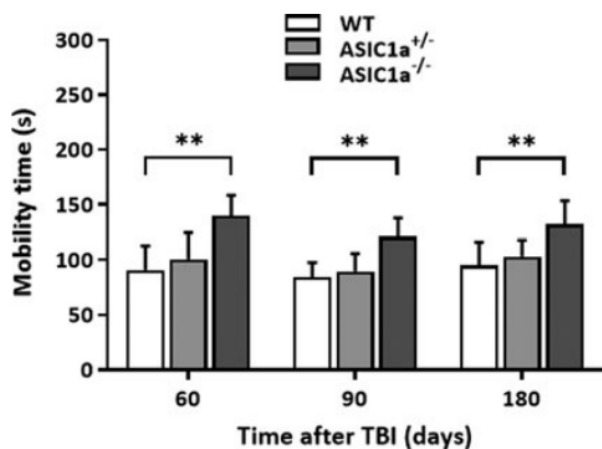


Figure 5: Depression-like behavior 1, 3, and 6 months after TBI assessed by the tail hanging test. Higher mobility time in homozygous ASIC1a-deficient mice indicates less depression-like behavior in these animals as compared to WT littermates ($*p < 0.01$). Mean – SD, $n = 9$ per group. SD, standard deviation; TBI, traumatic brain injury; WT, wild type.

ASIC1a deficiency improves long-term memory function after traumatic brain injury

After TBI, WT and ASIC1a^{+/-} mice had difficulties finding their home cage as evidenced by representative heatmap analysis (Fig. 6A). When quantifying memory function, latency to goal as well as the distance traveled improved over time in all groups (Fig. 6B,C); however, ASIC1a^{-/-} mice found their home cage twice as fast (Fig. 6B; $p < 0.05$) and covered half of the distance compared to their WT littermates at the end of the observation time (Fig. 6C; $p < 0.05$). These results suggest that ASIC1a deficiency preserved memory function after TBI.

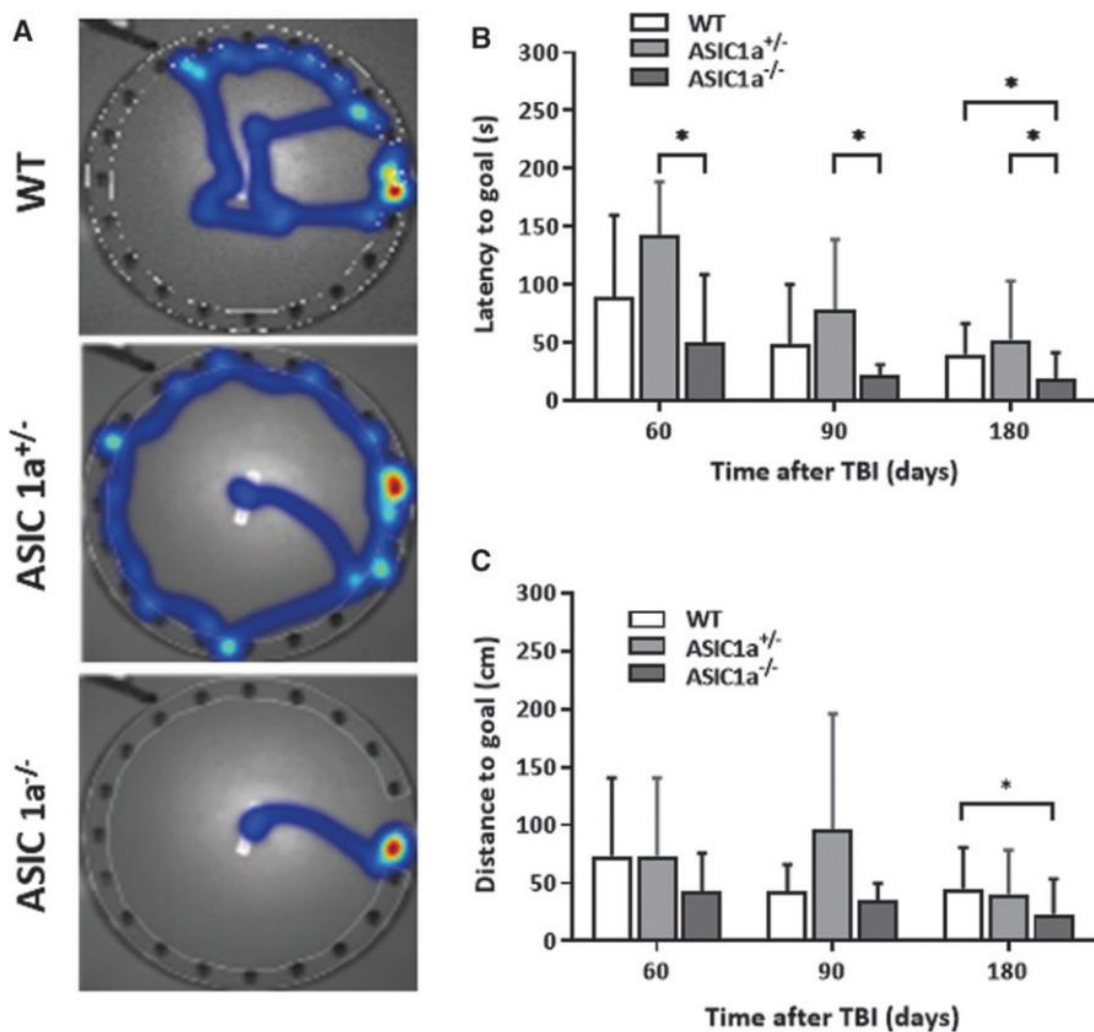


Figure 6: Memory function 1, 3, and 6 months after TBI assessed by the Barnes maze test. Representative heatmaps of all three investigated genotypes (A). Shorter latency times to find the goal (B) and shorter distance traveled to goal (C) indicate better memory function in homozygous ASIC1a-deficient mice as compared to heterozygous ASIC1a-deficient mice and WT littermates (* $p < 0.05$). Mean \pm SD, $n = 9$ per group. SD, standard deviation; TBI, traumatic brain injury; WT, wild type.

ASIC1a deficiency protects the brain against traumatic brain injury–induced neurodegeneration

In order to evaluate lesion volume in the same animals over time, we performed longitudinal T2W magnetic resonance imaging (MRI) up to 6 months after injury (Fig. 7A). In WT mice, lesion volume steadily increased from 14 until 180 days after TBI (Fig. 7B; open circles; $p < 0.01$ vs. 14 days after TBI). In hetero- and homozygous ASIC1a-deficient animals, however, this increase was not observed (Fig. 7B, closed circles). Despite similar lesion volumes 14 days after brain injury, there was no obvious longitudinal lesion progression in these animals. Sixty, 90, and 180 days after TBI, hetero- and homozygous ASIC1a-deficient animals had significantly smaller lesion volumes than their WT littermates (Fig. 7B). There was, however, no difference between homo- and heterozygous ASIC1a-deficient mice.

At the end of the observation time, lesion volume was also determined by histomorphometry (Fig. 7C). Also, this analysis revealed that WT mice had significantly larger lesion volumes (37.0 ± 5.1 mm³) than ASIC1a^{+/-} (26.9 ± 3.3 mm³; $p < 0.01$ vs. WT) and ASIC1a^{-/-} mice (25.8 ± 3.9 mm³; $p < 0.01$ vs. WT; Fig. 7D). Volumes obtained by histology strongly correlated with those measured

by MRI ($r = 0.8266$; $p < 0.0001$; Fig. 7E), indicating that MRI measurements are a reliable way to quantify post-traumatic brain damage.

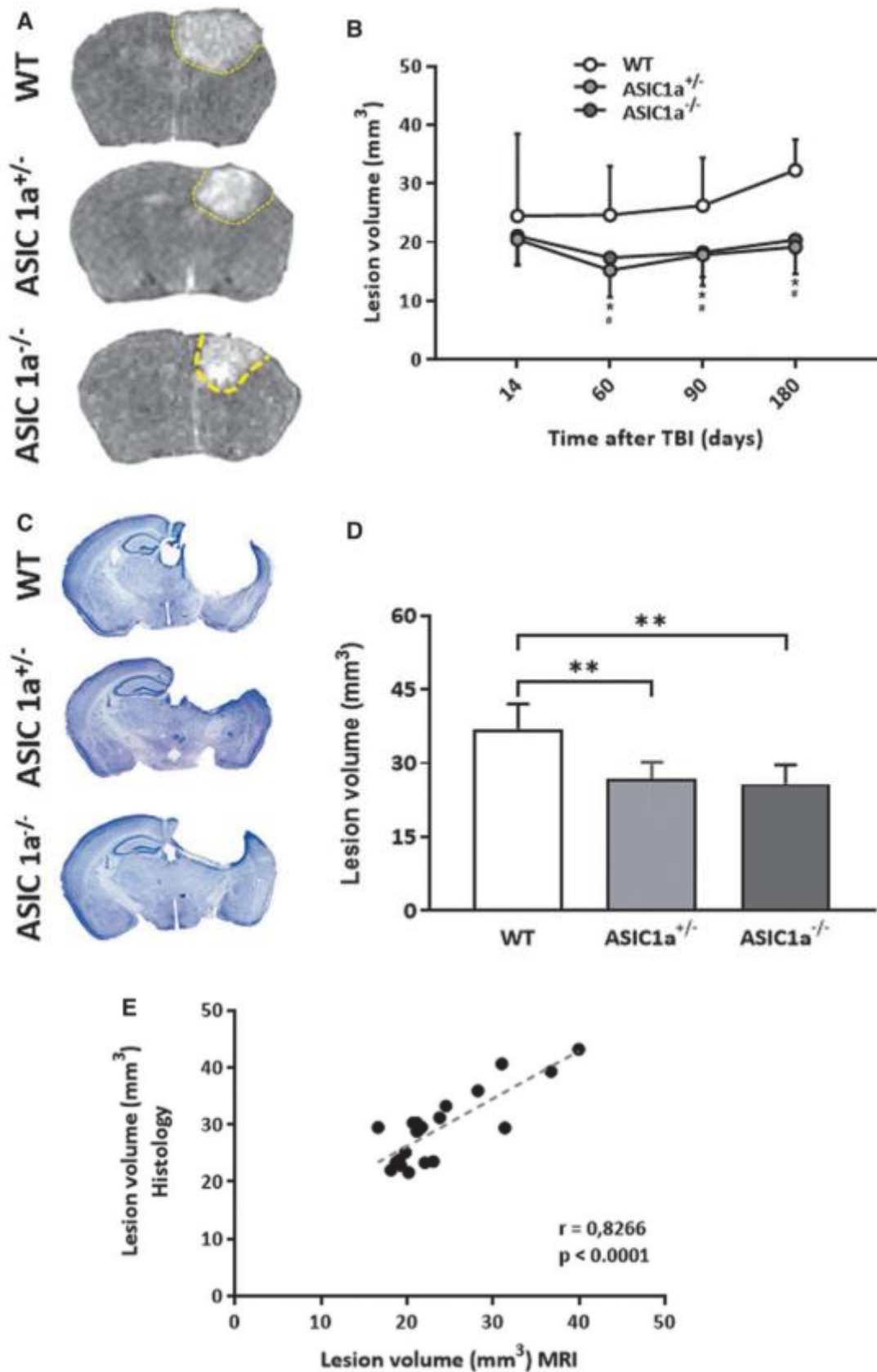


Figure 7: Cortical brain damage assessed by MRI (A,B) 2 weeks and 1, 3, and 6 months after injury post-TBI and at the end of the observation period by histology (C,D) in all investigated

genotypes. MRI indicates progressive brain damage occurring in WT littermate controls, whereas no such increase was observed in hetero- and homozygous ASIC1a-deficient mice (B; * $p < 0.01$ ASIC1a^{+/-} vs. wt; # $p < 0.01$ ASIC1a^{-/-} vs. wt; $n = 9$ per group). These findings were confirmed by histomorphometry of histological sections (D; ** $p < 0.001$; $n = 6-8$ per group). Lesion volumes quantified by histology and MRI showed a tight correlation ($r = 0.83$; $p < 0.0001$). Mean – SD. MRI, magnetic resonance imaging; SD, standard deviation; TBI, traumatic brain injury; WT, wild type.

TBI caused significant hippocampal damage in the traumatized hemisphere (Fig. 8A). WT animals lost >80% of their ipsilateral hippocampal volume 180 days after injury (26.3 – 4.0% of hippocampal volume pre- served vs. non-traumatized side). In homo- and heterozygous ASIC1a-deficient mice, hippocampal volume loss was significantly reduced from 80% to *55% (ASIC1a^{+/-}, 44.2 – 13.1%; ASIC1a^{-/-}, 45.4 – 4.8%; Fig. 8B).

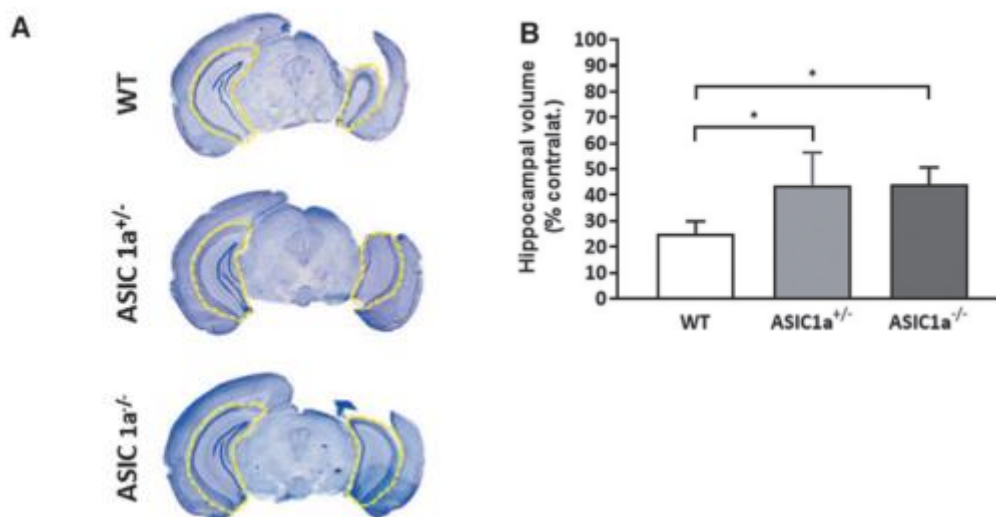


Figure 8: Hippocampal brain damage assessed by histology 6 months after TBI (A) in all investigated genotypes. In WT littermates, hippocampal volume was reduced by 75%, whereas significantly more hippocampal volume was preserved in heterozygous and homozygous ASIC1a-deficient mice (B; * $p < 0.05$; $n = 6-8$ per group). Mean – SD. SD, standard deviation; TBI, traumatic brain injury; WT, wild type.

ASIC1a deficiency results in less neuroinflammation after traumatic brain injury

In order to examine neuroinflammation, we assessed microgliosis by Iba-1 staining and microglial activation by CD68 staining near the rim of the contusion and in the same area of the contralateral hemisphere in WT and homozygous ASIC1a-deficient mice 6 months after TBI (Fig. 9A). Even at this very late time point after injury, the traumatic contusion was surrounded by a large number of Iba-1- (red fluorescence) and CD68-positive (green fluorescence) cells, suggesting massive microglia proliferation and activation (Fig. 9A; ipsi WT). No such changes were observed in the contralateral hemisphere (Fig. 9A; contra WT). In homozygous ASIC1a-deficient mice, much less Iba-1- and CD68-positive cells were observed and most cells were located in the immediate

proximity of the lesion boarder (Fig. 9A; ipsi ASIC1a^{-/-}). Again no activated microglia were observed in the contralateral hemisphere (Fig. 9A; contra ASIC1a^{-/-}).

When quantifying Iba-1 and CD68-fluorescence signals by integrated density analysis, we found the same amount of Iba-1 fluorescence in the contralateral hemisphere of both genotypes, suggesting that our approach was sensitive enough to detect quiescent microglia in healthy brain tissue (Fig. 9B, open and closed bars). After TBI, the Iba-1 signal increased by >9-fold in WT mice, but only 3.5-fold in homozygous ASIC1a-deficient mice (Fig. 9B, striped bars; $p < 0.01$ vs. contralateral and vs. WT). Regarding CD68, a marker for microglia activation, as expected, almost no CD68 signal was detected in healthy brain, that is, in the contralateral hemisphere (Fig. 9C, open and closed bars). After TBI, however, the CD68 signal in WT mice increased by >25-fold (Fig. 9C, striped open bar; $p < 0.001$). This massive activation of microglial cells was significantly reduced in homozygous ASIC1a-deficient mice ($p < 0.01$); in these animals, the CD68 signal increased only 3-fold (Fig. 9C, striped closed bar; $p < 0.001$), suggesting that ASIC1a may play a significant role for microglial activation and maintenance of neuroinflammation after TBI.

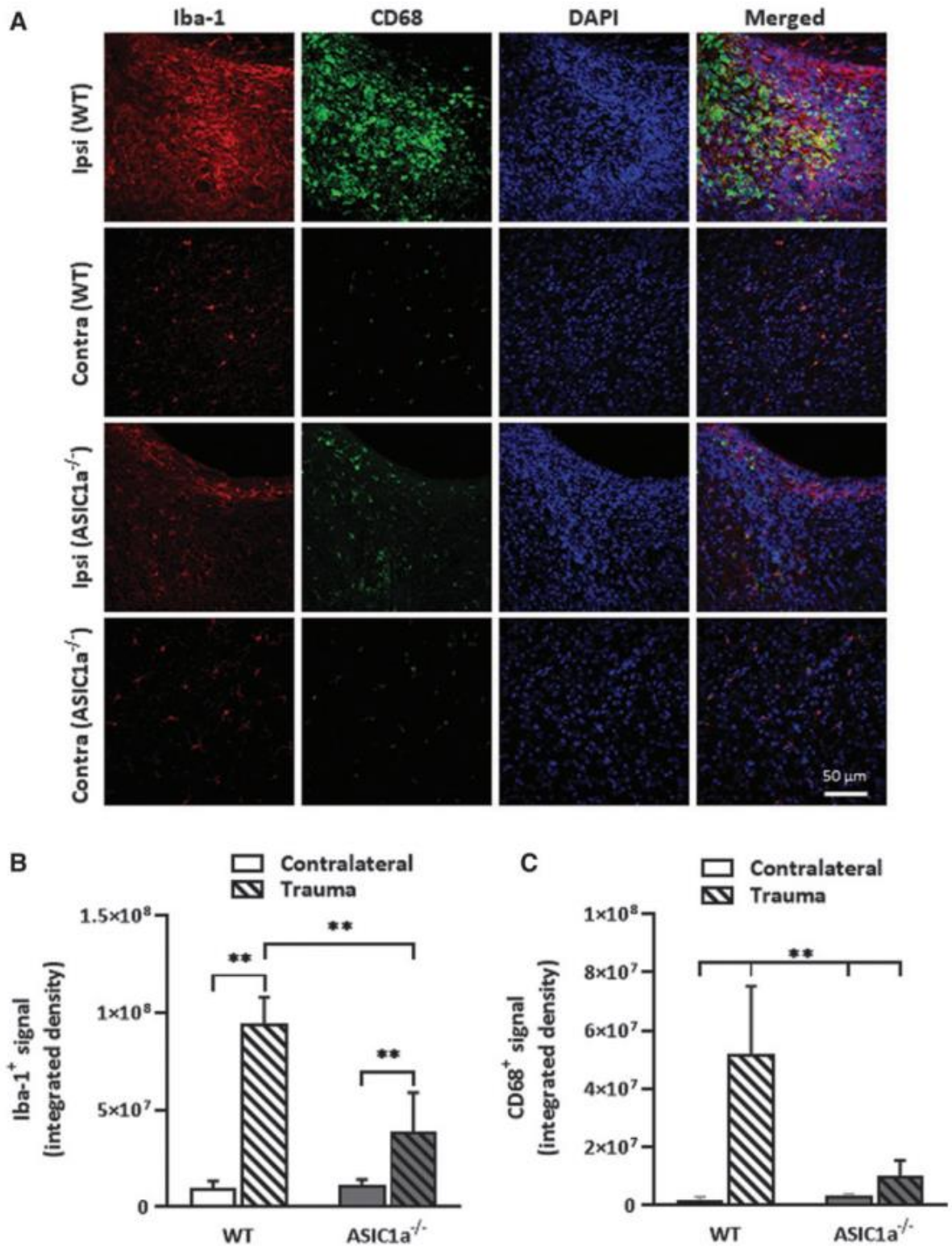


Figure 9: Microglia proliferation and activation 6 months after TBI. Whereas WT mice show massive microglia proliferation and activation in the traumatized hemisphere as evidenced by Iba-1 and CD68 staining, respectively, this microglial phenotype was significantly attenuated in ASIC1a^{-/-} mice (A–C; ** $p < 0.01$; $n = 6–8$ per group). Mean \pm SD. DAPI, 4',6-diamidino-2-phenylindole; Iba-1, ionized calcium-binding adaptor molecule 1; SD, standard deviation; TBI, traumatic brain injury; WT, wild type.

Discussion

Here, we investigated the effect of ASIC1a deficiency on long-term structural and functional outcome after experimental TBI. We observed a significant reduction of cortical and hippocampal brain damage accompanied by improvement of cognitive and behavioral deficits, as compared to littermate controls, up to 6 months after TBI. The improved outcome seems to be mainly caused by reduction of hippocampal damage, given that the extent of post-traumatic hippocampal atrophy has been shown to correlate to cognitive deficits and mood disorders.^{58–61}

Heterozygous knockout of ASIC1a led to a significant reduction of structural brain damage, comparable to that observed in homozygous knockout mice; however, behavioral testing yielded variable results, that is, there was a trend toward reduced depression-like behavior and toward worse performance in learning and memory function. However, these changes were not significantly different, as compared to WT animals, and may be caused by varying ASIC1a activity levels in heterozygous animals. Nevertheless, to our knowledge, this is the first report of a gene-dose effect in ASIC1a-mediated neuronal damage. The results in heterozygous animals may have implications for a future putative pharmacological treatment strategy with possibly incomplete ASIC1a inhibition.

Acidosis is considered a pivotal factor in the pathophysiology of secondary brain injury after cerebral insults.^{62–64} After TBI, a drop in extracellular pH occurs and seems to correlate with injury severity and adverse outcome.^{65–68} Acidosis is most commonly caused by post-traumatic cerebral ischemia, which is a major pathomechanism of secondary brain damage after TBI and can be detected very early on after TBI,^{25,69–72} but has also been described to occur and persist at later time points, for example, in association with delayed phenomena like post-traumatic vasospasm^{73,74} and cortical spreading depolarizations.^{75–77} Acidosis may, however, also develop without obvious ischemia, most probably attributable to metabolic derangement, dysfunctional autoregulatory mechanisms, or a mismatch between cerebral blood flow and energy demand after TBI.^{78,79} Although it is well established that acidosis induces and exacerbates neuronal injury,⁶⁴ for example, by protein denaturation,⁸⁰ induction of cell swelling,^{81–84} or impeding mitochondrial energy metabolism,⁸⁵ the exact damage pathways are not yet entirely clear.

ASIC1a are pH-dependent sodium and (to a lesser degree) calcium channels expressed on the post-synaptic membrane of central and peripheral neurons.⁸⁶ ASIC1a facilitate excitatory neurotransmission, thereby mediating synaptic plasticity and memory functions under physiological conditions.^{28,34,87} It is increasingly recognized that ASICs also may mediate acidosis-associated damage after cerebral insults by inducing glutamate-independent neuronal cell death.^{29,40,88} They also seem to be involved in necroptotic neuronal cell death,^{89,90} a caspase-independent form of cell death that is mediated by receptor-interacting protein 1 and 3.^{91,92} ASIC1a have been shown to play a role in the development of neuronal damage in the acute phase after TBI.⁴⁴

In the present study, this was corroborated by our finding that ASIC1a deficiency significantly decreased brain edema formation 24 h after TBI. This acute protection has previously been reported to partially improve memory function in the first days after fluid percussion TBI.⁴⁴ However, ASIC1a effects on structural or functional outcome in the chronic post-traumatic phase have not been previously investigated. Thus, it remained unclear whether ASIC1a-mediated protection was only short-lived or covered also clinically relevant time windows (i.e., 3 or 6 months). Here, we show that ASIC1a deficiency notably attenuates progression of lesion volume and hippocampal tissue loss for up to 6 months after trauma. Further, it ameliorated depressive behavior and cognitive dysfunction at 6 months post-TBI, while not affecting motor deficits.

Chronic changes after a single TBI are characterized by progressive global, hippocampal, and gray matter atrophy, as well as ventricular enlargement.^{21,22,93–96} These long-term progressive post-traumatic changes are thought to be caused by chronic neuroinflammation^{96,97} and to persist for years and even decades after a single TBI.^{94,98} Anti-inflammatory strategies have been shown to reduce chronic post-traumatic neuroinflammation, thereby improving neurocognitive deficits long term.^{24,99} Chronic inflammation promotes low tissue pH and may thus activate ASICs. Whether this is a pathway of importance when it comes to chronic post-traumatic changes, however, has previously not been investigated. ASIC1a have been shown to contribute to inflammasome activation,¹⁰⁰ cytosolic multi-protein complexes which play an important role for neuroinflammation after TBI.^{101–104} Further, in dorsal root ganglia, inflammatory cytokines increased ASIC1a activity.¹⁰⁵

Our data support the notion that acidosis-related ASIC1a activation is (at least) partially responsible for the chronic inflammatory reaction after TBI, given that ASIC1a deficiency resulted in reduced microglia activation in the present investigation. Our results therefore indicate that ASIC1a-mediated inflammatory pathways play an important role for chronic lesion progression after TBI. Acidosis-induced brain damage mediated by ASIC1a is a novel and previously not considered factor in the pathogenesis of chronic post-traumatic brain damage and may therefore be a suitable target to reduce long-term sequelae of TBI.

Conclusion

Acidosis-associated mechanisms seem to play an important role in the development of long-term consequences of TBI. ASIC1a deficiency led to an improvement of structural and functional outcome, most probably by attenuating post-traumatic inflammatory changes. Targeting ASIC1a channels may therefore be a pharmacological treatment strategy for chronic post-traumatic brain damage.

Acknowledgments

The authors thank Anna-Lena Müller and Janina Biller for technical assistance.

Authors' Contributions

Conception or design of the study: S.C., N.P., N.A.T., M.W., and F.R. Acquisition, analysis, or interpretation of the data: S.C., X.M., X.L., A.W., S.H., U.M., I.K., N.P., and N.A.T. Drafting the paper or revising it critically for important intellectual content: all authors.

All authors gave final approval of the current manuscript version to be published and agree to be accountable for all aspects of the work in ensuring that questions related to the accuracy or integrity of any part of the work are appropriately investigated and resolved.

Funding Information

This project was funded by the Munich Cluster of Systems Neurology (SyNergy; Project ID: EXC 2145 / ID 390857198) and the Friedrich-Baur-Foundation (grant no.: 61/18). Shiqi Cheng was supported by the China Scholarship Council (grant no.: 201706820029).

Author Disclosure Statement

No competing interests exist.

References

1. Hyder, A.A., Wunderlich, C.A., Puvanachandra, P., Gururaj, G., and Kobusingye, O.C. (2007). The impact of traumatic brain injuries: a global perspective. *NeuroRehabilitation* 22, 341–353.

2. Kassi, A.A.Y., Mahavadi, A.K., Clavijo, A., Caliz, D., Lee, S.W., Ahmed, A.I., Yokobori, S., Hu, Z., Spurlock, M.S., Wasserman, J.M., Rivera, K.N., Nodal, S., Powell, H.R., Di, L., Torres, R., Leung, L.Y., Rubiano, A.M., Bullock, R.M., and Gajavelli, S. (2018). Enduring neuroprotective effect of subacute neural stem cell transplantation after penetrating TBI. *Front. Neurol.* 9, 1097.
3. Tagliaferri, F., Compagnone, C., Korsic, M., Servadei, F., and Kraus, J. (2006). A systematic review of brain injury epidemiology in Europe. *Acta Neurochir. (Wien)* 148, 255–268; discussion, 268.
4. Trivedi, M.A., Ward, M.A., Hess, T.M., Gale, S.D., Dempsey, R.J., Rowley, H.A., and Johnson, S.C. (2007). Longitudinal changes in global brain volume between 79 and 409 days after traumatic brain injury: relationship with duration of coma. *J. Neurotrauma* 24, 766–771.
5. Bendlin, B.B., Ries, M.L., Lazar, M., Alexander, A.L., Dempsey, R.J., Rowley, H.A., Sherman, J.E., and Johnson, S.C. (2008). Longitudinal changes in patients with traumatic brain injury assessed with diffusion-tensor and volumetric imaging. *Neuroimage* 42, 503–514.
6. Sidaros, A., Engberg, A.W., Sidaros, K., Liptrot, M.G., Herning, M., Petersen, P., Paulson, O.B., Jernigan, T.L., and Rostrup, E. (2008). Diffusion tensor imaging during recovery from severe traumatic brain injury and relation to clinical outcome: a longitudinal study. *Brain* 131, 559–572.
7. Kumar, A., and Loane, D.J. (2012). Neuroinflammation after traumatic brain injury: opportunities for therapeutic intervention. *Brain Behav. Immun.* 26, 1191–1201.
8. Guo, Z., Cupples, L., Kurz, A., Auerbach, S., Volicer, L., Chui, H., Green, R., Sadovnick, A., Duara, R., and DeCarli, C. (2000). Head injury and the risk of AD in the MIRAGE study. *Neurology* 54, 1316–1323.
9. Wang, H.-K., Lin, S.-H., Sung, P.-S., Wu, M.-H., Hung, K.-W., Wang, L.-C., Huang, C.-Y., Lu, K., Chen, H.-J., and Tsai, K.-J. (2012). Population based study on patients with traumatic brain injury suggests increased risk of dementia. *J. Neurol. Neurosurg. Psychiatry* 83, 1080–1085.
10. Dikmen, S.S., Corrigan, J.D., Levin, H.S., Machamer, J., Stiers, W., and Weisskopf, M.G. (2009). Cognitive outcome following traumatic brain injury. *J. Head Trauma Rehabil.* 24, 430–438.
11. Himanen, L., Portin, R., Isoniemi, H., Helenius, H., Kurki, T., and Tenonuo, O. (2005). Cognitive functions in relation to MRI findings 30 years after traumatic brain injury. *Brain Inj.* 19, 93–100.
12. Chauhan, N.B. (2014). Chronic neurodegenerative consequences of traumatic brain injury. *Restor. Neurol. Neurosci.* 32, 337–365.
13. Johnson, V.E., Stewart, W., Arena, J.D. and Smith, D.H. (2017). Traumatic brain injury as a trigger of neurodegeneration. *Adv. Neurobiol.* 15, 383–400.
14. Bryant, R.A., O'Donnell, M.L., Creamer, M., McFarlane, A.C., Clark, C.R., and Silove, D. (2010). The psychiatric sequelae of traumatic injury. *Am. J. Psychiatry* 167, 312–320.
15. Kim, E., Lauterbach, E.C., Reeve, A., Arciniegas, D.B., Coburn, K.L., Mendez, M.F., Rumans, T.A., and Coffey, E.C.; ANPA Committee on Research. (2007). Neuropsychiatric complications of traumatic brain injury: a critical review of the literature (a report by the ANPA Committee on Research). *J. Neuropsychiatry Clin. Neurosci.* 19, 106–127.
16. Perry, D.C., Sturm, V.E., Peterson, M.J., Pieper, C.F., Bullock, T., Boeve, B.F., Miller, B.L., Guskiewicz, K.M., Berger, M.S., Kramer, J.H., and Welsh-Bohmer, K.A. (2016). Association of traumatic brain injury with subsequent neurological and psychiatric disease: a meta-analysis. *J. Neurosurg.* 124, 511–526.

17. Harrison-Felix, C., Pretz, C., Hammond, F.M., Cuthbert, J.P., Bell, J., Corrigan, J., Miller, A.C., and Haarbauer-Krupa, J. (2015). Life expectancy after inpatient rehabilitation for traumatic brain injury in the United States. *J. Neurotrauma* 32, 1893–1901.
18. Harrison-Felix, C.L., Whiteneck, G.G., Jha, A., DeVivo, M.J., Hammond, F.M., and Hart, D.M. (2009). Mortality over four decades after traumatic brain injury rehabilitation: a retrospective cohort study. *Arch. Phys. Med. Rehabil.* 90, 1506–1513.
19. Smith, C., Gentleman, S.M., Leclercq, P.D., Murray, L.S., Griffin, W.S., Graham, D.I., and Nicoll, J.A. (2013). The neuroinflammatory response in humans after traumatic brain injury. *Neuropathol. Appl. Neurobiol.* 39, 654–666.
20. Aungst, S.L., Kabadi, S.V., Thompson, S.M., Stoica, B.A., and Faden, A.I. (2014). Repeated mild traumatic brain injury causes chronic neuroinflammation, changes in hippocampal synaptic plasticity, and associated cognitive deficits. *J. Cereb. Blood Flow Metab.* 34, 1223–1232.
21. Loane, D.J., Kumar, A., Stoica, B.A., Cabatbat, R., and Faden, A.I. (2014). Progressive neurodegeneration after experimental brain trauma: association with chronic microglial activation. *J. Neuropathol. Exp. Neurol.* 73, 14–29.
22. Mao, X., Terpolilli, N.A., Wehn, A., Chen, S., Hellal, F., Liu, B., Seker, B., and Plesnila, N. (2020). Progressive histopathological damage occurring up to one year after experimental traumatic brain injury is associated with cognitive decline and depression-like behavior. *J. Neurotrauma* 37, 1331–1341.
23. Mouzon, B.C., Bachmeier, C., Ferro, A., Ojo, J.O., Crynen, G., Acker, C.M., Davies, P., Mullan, M., Stewart, W., and Crawford, F. (2014). Chronic neuropathological and neurobehavioral changes in a repetitive mild traumatic brain injury model. *Ann. Neurol.* 75, 241–254.
24. Campos-Pires, R., Hirnet, T., Valeo, F., Ong, B.E., Radyushkin, K., Aldhoun, J., Saville, J., Edge, C.J., Franks, N.P., Thal, S.C., and Dickinson, R. (2019). Xenon improves long-term cognitive function, reduces neuronal loss and chronic neuroinflammation, and improves survival after traumatic brain injury in mice. *Br. J. Anaesth.* 123, 60–73.
25. Bouma, G.J., Muizelaar, J.P., Choi, S.C., Newlon, P.G., and Young, H.F. (1991). Cerebral circulation and metabolism after severe traumatic brain injury: the elusive role of ischemia. *J. Neurosurg.* 75, 685–693.
26. Coles, J.P., Fryer, T.D., Smielewski, P., Chatfield, D.A., Steiner, L.A., Johnston, A.J., Downey, S.P., Williams, G.B., Aigbirhio, F., and Hutchinson, P.J. (2004). Incidence and mechanisms of cerebral ischemia in early clinical head injury. *J. Cereb. Blood Flow Metab.* 24, 202–211.
27. Diringier, M.N., Videen, T.O., Yundt, K., Zazulia, A.R., Aiyagari, V., Dacey, R.G., Grubb, R.L., and Powers, W.J. (2002). Regional cerebrovascular and metabolic effects of hyperventilation after severe traumatic brain injury. *J. Neurosurg.* 96, 103–108.
28. Wemmie, J.A., Askwith, C.C., Lamani, E., Cassell, M.D., Freeman, J.H., Jr., and Welsh, M.J. (2003). Acid-sensing ion channel 1 is localized in brain regions with high synaptic density and contributes to fear conditioning. *J. Neurosci.* 23, 5496–5502.
29. Li, M., Inoue, K., Branigan, D., Kratzer, E., Hansen, J.C., Chen, J.W., Simon, R.P., and Xiong, Z.G. (2010). Acid-sensing ion channels in acidosis-induced injury of human brain neurons. *J. Cereb. Blood Flow Metab.* 30, 1247–1260.
30. Li, M.H., Leng, T.D., Feng, X.C., Yang, T., Simon, R.P., and Xiong, Z.G. (2016). Modulation of acid-sensing ion channel 1a by intracellular pH and its role in ischemic stroke. *J. Biol. Chem.* 291, 18370–18383.
31. Xiong, Z.G., Chu, X.P., and Simon, R.P. (2006). Ca²⁺-permeable acid-sensing ion channels and ischemic brain injury. *J. Membr. Biol.* 209, 59–68.

-
32. Hanukoglu, I. (2017). ASIC and ENaC type sodium channels: conformational states and the structures of the ion selectivity filters. *FEBS J.* 284, 525–545.
 33. Duan, B., Wang, Y.-Z., Yang, T., Chu, X.-P., Yu, Y., Huang, Y., Cao, H., Hansen, J., Simon, R.P., and Zhu, M.X. (2011). Extracellular spermine exacerbates ischemic neuronal injury through sensitization of ASIC1a channels to extracellular acidosis. *J. Neurosci.* 31, 2101–2112.
 34. Wemmie, J.A., Chen, J., Askwith, C.C., Hruska-Hageman, A.M., Price, M.P., Nolan, B.C., Yoder, P.G., Lamani, E., Hoshi, T., and Freeman, J.H. Jr. (2002). The acid-activated ion channel ASIC contributes to synaptic plasticity, learning, and memory. *Neuron* 34, 463–477.
 35. Askwith, C.C., Wemmie, J.A., Price, M.P., Rokhlina, T., and Welsh, M.J. (2004). Acid-sensing ion channel 2 (ASIC2) modulates ASIC1 H⁺-activated currents in hippocampal neurons. *J. Biol. Chem.* 279, 18296–18305.
 36. Lingueglia, E., de Weille, J.R., Bassilana, F., Heurteaux, C., Sakai, H., Waldmann, R., and Lazdunski, M. (1997). A modulatory subunit of acid sensing ion channels in brain and dorsal root ganglion cells. *J. Biol. Chem.* 272, 29778–29783.
 37. Sherwood, T.W., Lee, K.G., Gormley, M.G., and Askwith, C.C. (2011). Heteromeric acid-sensing ion channels (ASICs) composed of ASIC2b and ASIC1a display novel channel properties and contribute to acidosis-induced neuronal death. *J. Neurosci.* 31, 9723–9734.
 38. Chu, X.-P., Papasian, C.J., Wang, J.Q., and Xiong, Z.-G. (2011). Modulation of acid-sensing ion channels: molecular mechanisms and therapeutic potential. *Int. J. Physiol. Pathophysiol. Pharmacol.* 3, 288–309.
 39. Chassagnon, I.R., McCarthy, C.A., Chin, Y.K., Pineda, S.S., Keramidas, A., Mobli, M., Pham, V., De Silva, T.M., Lynch, J.W., Widdop, R.E., Rash, L.D., and King, G.F. (2017). Potent neuroprotection after stroke afforded by a double-knot spider-venom peptide that inhibits acid-sensing ion channel 1a. *Proc. Natl. Acad. Sci. U. S. A.* 114, 3750–3755.
 40. Xiong, Z.G., Zhu, X.M., Chu, X.P., Minami, M., Hey, J., Wei, W.L., MacDonald, J.F., Wemmie, J.A., Price, M.P., Welsh, M.J., and Simon, R.P. (2004). Neuroprotection in ischemia: blocking calcium-permeable acid-sensing ion channels. *Cell* 118, 687–698.
 41. Pignataro, G., Cuomo, O., Esposito, E., Sirabella, R., Di Renzo, G., and Annunziato, L. (2011). ASIC1a contributes to neuroprotection elicited by ischemic preconditioning and postconditioning. *Int. J. Physiol. Pathophysiol. Pharmacol.* 3, 1.
 42. Friese, M.A., Craner, M.J., Etzensperger, R., Vergo, S., Wemmie, J.A., Welsh, M.J., Vincent, A., and Fugger, L. (2007). Acid-sensing ion channel-1 contributes to axonal degeneration in autoimmune inflammation of the central nervous system. *Nat. Med.* 13, 1483–1489.
 43. Wong, H.K., Bauer, P.O., Kurosawa, M., Goswami, A., Washizu, C., Machida, Y., Tosaki, A., Yamada, M., Knopfel, T., Nakamura, T., and Nukina, N. (2008). Blocking acid-sensing ion channel 1 alleviates Huntington's disease pathology via an ubiquitin-proteasome system-dependent mechanism. *Hum. Mol. Genet.* 17, 3223–3235.
 44. Yin, T., Lindley, T.E., Albert, G.W., Ahmed, R., Schmeiser, P.B., Grady, M.S., Howard, M.A., and Welsh, M.J. (2013). Loss of acid sensing ion channel-1a and bicarbonate administration attenuate the severity of traumatic brain injury. *PLoS One* 8, e72379.
 45. Page, A.J., Brierley, S.M., Martin, C.M., Martinez-Salgado, C., Wemmie, J.A., Brennan, T.J., Symonds, E., Omari, T., Lewin, G.R., Welsh, M.J., and Blackshaw, L.A. (2004). The ion channel ASIC1 contributes to visceral but not cutaneous mechanoreceptor function. *Gastroenterology* 127, 1739–1747.
 46. Trabold, R., Eros, C., Zweckberger, K., Relton, J., Beck, H., Nussberger, J., Muller-Esterl, W., Bader, M., Whalley, E., and Plesnila, N. (2010). The role of bradykinin B(1) and B(2)

- receptors for secondary brain damage after traumatic brain injury in mice. *J. Cereb. Blood Flow Metab.* 30, 130–139.
47. Zweckberger, K., Eros, C., Zimmermann, R., Kim, S.W., Engel, D., and Plesnila, N. (2006). Effect of early and delayed decompressive craniectomy on secondary brain damage after controlled cortical impact in mice. *J. Neurotrauma* 23, 1083–1093.
 48. Zweckberger, K., Stoffel, M., Baethmann, A., and Plesnila, N. (2003). Effect of decompression craniotomy on increase of contusion volume and functional outcome after controlled cortical impact in mice. *J. Neurotrauma* 20, 1307–1314.
 49. Krieg, S.M., Trabold, R., and Plesnila, N. (2017). Time-dependent effects of arginine-vasopressin V1 receptor inhibition on secondary brain damage after traumatic brain injury. *J. Neurotrauma* 34, 1329–1336.
 50. Terpolilli, N.A., Kim, S.W., Thal, S.C., Kuebler, W.M., and Plesnila, N. (2013). Inhaled nitric oxide reduces secondary brain damage after traumatic brain injury in mice. *J. Cereb. Blood Flow Metab.* 33, 311–318.
 51. Terpolilli, N.A., Kim, S.-W., Thal, S.C., Kuebler, W.M., and Plesnila, N. (2013). Inhaled nitric oxide reduces secondary brain damage after traumatic brain injury in mice. *J. Cereb. Blood Flow Metab.* 33, 311–318.
 52. Terpolilli, N.A., Zweckberger, K., Trabold, R., Schilling, L., Schinzel, R., Tegtmeyer, F., and Plesnila, N. (2009). The novel nitric oxide synthase inhibitor 4-amino-tetrahydro-L-biopterine prevents brain edema formation and intracranial hypertension following traumatic brain injury in mice. *J. Neurotrauma* 26, 1963–1975.
 53. Can, A., Dao, D.T., Terrillion, C.E., Piantadosi, S.C., Bhat, S., and Gould, T.D. (2012). The tail suspension test. *J. Vis. Exp.* doi: 10.3791/3769.
 54. Steru, L., Chermat, R., Thierry, B., and Simon, P. (1985). The tail suspension test: a new method for screening antidepressants in mice. *Psychopharmacology* 85, 367–370.
 55. Rosenfeld, C.S., and Ferguson, S.A. (2014). Barnes maze testing strategies with small and large rodent models. *J. Vis. Exp.* doi: 10.3791/51194.
 56. McLay, R.N., Freeman, S.M., and Zadina, J.E. (1998). Chronic corticosterone impairs memory performance in the Barnes maze. *Physiol. Behav.* 63, 933–937.
 57. Ghosh, M., Balbi, M., Hellal, F., Dichgans, M., Lindauer, U., and Plesnila, N. (2015). Pericytes are involved in the pathogenesis of cerebral autosomal dominant arteriopathy with subcortical infarcts and leukoencephalopathy. *Ann. Neurol.* 78, 887–900.
 58. Rosenzweig, E.S., and Barnes, C.A. (2003). Impact of aging on hippocampal function: plasticity, network dynamics, and cognition. *Prog. Neurobiol.* 69, 143–179.
 59. Hicks, R., Smith, D., Lowenstein, D., Saint Marie, R., and McIntosh, T. (1993). Mild experimental brain injury in the rat induces cognitive deficits associated with regional neuronal loss in the hippocampus. *J. Neurotrauma* 10, 405–414.
 60. Ariza, M., Serra-Grabulosa, J.M., Junque, C., Ramirez, B., Mataro, M., Poca, A., Bargallo, N., and Sahuquillo, J. (2006). Hippocampal head atrophy after traumatic brain injury. *Neuropsychologia* 44, 1956–1961.
 61. Jorge, R.E., Acion, L., Starkstein, S.E., and Magnotta, V. (2007). Hippocampal volume and mood disorders after traumatic brain injury. *Biol. Psychiatry* 62, 332–338.
 62. Rehnöron, S., Rose´n, I., and Siesjö , B.K. (1981). Brain lactic acidosis and ischemic cell damage: 1. Biochemistry and neurophysiology. *J. Cereb. Blood Flow Metab.* 1, 297–311.
 63. Siesjö, B.K. (1988). Acidosis and ischemic brain damage. *Neurochem. Pathol.* 9, 31–88.

-
64. Siesjo, B.K., Katsura, K. and Kristian, T. (1996). Acidosis-related damage. *Adv. Neurol.* 71, 209–233; discussion, 234–206.
65. Clausen, T., Khaldi, A., Zauner, A., Reinert, M., Doppenberg, E., Menzel, M., Soukup, J., Alves, O.L., and Bullock, M.R. (2005). Cerebral acid–base homeostasis after severe traumatic brain injury. *J. Neurosurg.* 103, 597–607.
66. Gupta, A.K., Zygun, D.A., Johnston, A.J., Steiner, L.A., Al-Rawi, P.G., Chatfield, D., Shepherd, E., Kirkpatrick, P.J., Hutchinson, P.J., and Menon, D.K. (2004). Extracellular brain pH and outcome following severe traumatic brain injury. *J. Neurotrauma* 21, 678–684.
67. Enevoldsen, E.M., Cold, G., Jensen, F.T., and Malmros, R. (1976). Dynamic changes in regional CBF, intraventricular pressure, CSF pH and lactate levels during the acute phase of head injury. *J. Neurosurg.* 44, 191–214.
68. DeSalles, A.A., Kontos, H.A., Becker, D.P., Yang, M.S., Ward, J.D., Moulton, R., Gruemer, H.D., Lutz, H., Maset, A.L., Jenkins, L., Marmarou, A., and Paul Muizelaar, P. (1986). Prognostic significance of ventricular CSF lactic acidosis in severe head injury. *J. Neurosurg.* 65, 615–624.
69. Krishnappa, I.K., Contant, C.F., and Robertson, C.S. (1999). Regional changes in cerebral extracellular glucose and lactate concentrations following severe cortical impact injury and secondary ischemia in rats. *J. Neurotrauma* 16, 213–224.
70. Engel, D.C., Mies, G., Terpolilli, N.A., Trabold, R., Loch, A., De Zeeuw, C.I., Weber, J.T., Maas, A.I., and Plesnila, N. (2008). Changes of cerebral blood flow during the secondary expansion of a cortical contusion assessed by ¹⁴C-iodoantipyrine autoradiography in mice using a non-invasive protocol. *J. Neurotrauma* 25, 739–753.
71. Bouma, G.J., and Muizelaar, J.P. (1992). Cerebral blood flow, cerebral blood volume, and cerebrovascular reactivity after severe head injury. *J. Neurotrauma* 9, Suppl. 1, S333–S348.
72. Graham, D.I., and Adams, J.H. (1971). Ischaemic brain damage in fatal head injuries. *Lancet* 1, 265–266
73. Desai, M., and Morris, N.A. (2018). Prolonged post-traumatic vasospasm resulting in delayed cerebral ischemia after mild traumatic brain injury. *Neurocrit. Care* 29, 512–518.
74. Al-Mufti, F., Amuluru, K., Changa, A., Lander, M., Patel, N., Wajswol, E., Al-Marsoumi, S., Alzubaidi, B., Singh, I.P., Nuoman, R., and Gandhi, C. (2017). Traumatic brain injury and intracranial hemorrhage-induced cerebral vasospasm: a systematic review. *Neurosurg. Focus* 43, E14.
75. Dreier, J.P. (2011). The role of spreading depression, spreading depolarization and spreading ischemia in neurological disease. *Nat. Med.* 17, 439–447.
76. Hinzman, J.M., Andaluz, N., Shutter, L.A., Okonkwo, D.O., Pahl, C., Strong, A.J., Dreier, J.P., and Hartings, J.A. (2014). Inverse neurovascular coupling to cortical spreading depolarizations in severe brain trauma. *Brain* 137, 2960–2972.
77. Menyhart, A., Zolei-Szenasi, D., Puskas, T., Makra, P., Orsolya, M.T., Szepes, B.E., Toth, R., Ivankovits-Kiss, O., Obrenovitch, T.P., Bari, F., and Farkas, E. (2017). Spreading depolarization remarkably exacerbates ischemia-induced tissue acidosis in the young and aged rat brain. *Sci. Rep.* 7, 1154.
78. Vespa, P., Bergsneider, M., Hattori, N., Wu, H.M., Huang, S.C., Martin, N.A., Glenn, T.C., McArthur, D.L., and Hovda, D.A. (2005). Metabolic crisis without brain ischemia is common after traumatic brain injury: a combined microdialysis and positron emission tomography study. *J. Cereb. Blood Flow Metab.* 25, 763–774.
79. Johnston, A.J., Steiner, L.A., Coles, J.P., Chatfield, D.A., Fryer, T.D., Smielewski, P., Hutchinson, P.J., O’Connell, M.T., Al-Rawi, P.G., Aigbirihio, F.I., Clark, J.C., Pickard, J.D.,

- Gupta, A.K., and Menon, D.K. (2005). Effect of cerebral perfusion pressure augmentation on regional oxygenation and metabolism after head injury. *Crit. Care Med.* 33, 189–195; discussion, 255–187.
80. Kalimo, H., Rehnörona, S., Soderfeldt, B., Olsson, Y., and Siesjö, B.K. (1981). Brain lactic acidosis and ischemic cell damage: 2. Histopathology. *J. Cereb. Blood Flow Metab.* 1, 313–327.
81. Plesnila, N., Haberstock, J., Peters, J., Kolbl, I., Baethmann, A., and Staub, F. (1999). Effect of lactacidosis on cell volume and intracellular pH of astrocytes. *J. Neurotrauma* 16, 831–841.
82. Ringel, F., Chang, R.C., Staub, F., Baethmann, A., and Plesnila, N. (2000). Contribution of anion transporters to the acidosis-induced swelling and intracellular acidification of glial cells. *J. Neurochem.* 75, 125–132.
83. Staub, F., Winkler, A., Haberstock, J., Plesnila, N., Peters, J., Chang, R.C., Kempfski, O., and Baethmann, A. (1996). Swelling, intracellular acidosis, and damage of glial cells. *Acta Neurochir. Suppl.* 66, 56–62.
84. Kimelberg, H.K., Barron, K.D., Bourke, R.S., Nelson, L.R., and Cragoe, E.J. (1990). Brain anti-cyotoxic edema agents. *Prog. Clin. Biol. Res.* 361, 363–385.
85. Hillered, L., Smith, M.L., and Siesjö, B.K. (1985). Lactic acidosis and recovery of mitochondrial function following forebrain ischemia in the rat. *J. Cereb. Blood Flow Metab.* 5, 259–266.
86. Osmakov, D., Andreev, Y.A., and Kozlov, S. (2014). Acid-sensing ion channels and their modulators. *Biochemistry (Moscow)* 79, 1528–1545.
87. Gonzalez-Inchauspe, C., Urbano, F.J., Di Guilmi, M.N., and Uchitel, O.D. (2017). Acid-sensing ion channels activated by evoked released protons modulate synaptic transmission at the mouse calyx of held synapse. *J. Neurosci.* 37, 2589–2599.
88. Yermolaieva, O., Leonard, A.S., Schnizler, M.K., Abboud, F.M., and Welsh, M.J. (2004). Extracellular acidosis increases neuronal cell calcium by activating acid-sensing ion channel 1a. *Proc. Natl. Acad. Sci. U. S. A.* 101, 6752–6757.
89. Wang, J.J., Liu, F., Yang, F., Wang, Y.Z., Qi, X., Li, Y., Hu, Q., Zhu, M.X., and Xu, T.L. (2020). Disruption of auto-inhibition underlies conformational signaling of ASIC1a to induce neuronal necroptosis. *Nat. Commun.* 11, 475.
90. Wang, Y.Z., Wang, J.J., Huang, Y., Liu, F., Zeng, W.Z., Li, Y., Xiong, Z.G., Zhu, M.X., and Xu, T.L. (2015). Tissue acidosis induces neuronal necroptosis via ASIC1a channel independent of its ionic conduction. *Elife* 4, e05682.
91. Declercq, W., Vanden Berghe, T., and Vandenabeele, P. (2009). RIP kinases at the crossroads of cell death and survival. *Cell* 138, 229–232.
92. Degterev, A., Hitomi, J., Gemscheid, M., Ch'en, I.L., Korkina, O., Teng, X., Abbott, D., Cuny, G.D., Yuan, C., Wagner, G., Hedrick, S.M., Gerber, S.A., Lugovskoy, A., and Yuan, J. (2008). Identification of RIP1 kinase as a specific cellular target of necrostatins. *Nat. Chem. Biol.* 4, 313–321.
93. Collins-Praino, L.E., Arulsamy, A., Katharesan, V., and Corrigan, F. (2018). The effect of an acute systemic inflammatory insult on the chronic effects of a single mild traumatic brain injury. *Behav. Brain Res.* 336, 22–31.
94. Johnson, V.E., Stewart, J.E., Begbie, F.D., Trojanowski, J.Q., Smith, D.H., and Stewart, W. (2013). Inflammation and white matter degeneration persist for years after a single traumatic brain injury. *Brain* 136, 28–42.

-
95. MacKenzie, J.D., Siddiqi, F., Babb, J.S., Bagley, L.J., Mannon, L.J., Sinson, G.P., and Grossman, R.I. (2002). Brain atrophy in mild or moderate traumatic brain injury: a longitudinal quantitative analysis. *AJNR Am. J. Neuroradiol.* 23, 1509–1515.
 96. Pischitta, F., Micotti, E., Hay, J.R., Marongiu, I., Sammali, E., Tolomeo, D., Vegliante, G., Stocchetti, N., Forloni, G., and De Simoni, M.-G. (2018). Single severe traumatic brain injury produces progressive pathology with ongoing contralateral white matter damage one year after injury. *Exp. Neurol.* 300, 167–178.
 97. Erturk, A., Mentz, S., Stout, E.E., Hedehus, M., Dominguez, S.L., Neumaier, L., Krammer, F., Llovera, G., Srinivasan, K., Hansen, D.V., Liesz, A., Searce-Levie, K.A., and Sheng, M. (2016). Interfering with the chronic immune response rescues chronic degeneration after traumatic brain injury. *J. Neurosci.* 36, 9962–9975.
 98. Ramlackhansingh, A.F., Brooks, D.J., Greenwood, R.J., Bose, S.K., Turkheimer, F.E., Kinunen, K.M., Gentleman, S., Heckemann, R.A., Gunanayagam, K., Gelosa, G., and Sharp, D.J. (2011). Inflammation after trauma: microglial activation and traumatic brain injury. *Ann. Neurol.* 70, 374–383.
 99. Byrnes, K.R., Loane, D.J., Stoica, B.A., Zhang, J., and Faden, A.I. (2012). Delayed mGluR5 activation limits neuroinflammation and neurodegeneration after traumatic brain injury. *J. Neuroinflammation* 9, 43.
 100. Wang, Y.C., Li, W.Z., Wu, Y., Yin, Y.Y., Dong, L.Y., Chen, Z.W., and Wu, W.N. (2015). Acid-sensing ion channel 1a contributes to the effect of extracellular acidosis on NLRP1 inflammasome activation in cortical neurons. *J. Neuroinflammation* 12, 246.
 101. de Rivero Vaccari, J.P., Brand, F. III, Adamczak, S., Lee, S.W., Perez-Barcena, J., Wang, M.Y., Bullock, M.R., Dietrich, W.D., and Keane, R.W. (2016). Exosome-mediated inflammasome signaling after central nervous system injury. *J. Neurochem.* 136, Suppl. 1, 39–48.
 102. de Rivero Vaccari, J.P., Dietrich, W.D., and Keane, R.W. (2014). Activation and regulation of cellular inflammasomes: gaps in our knowledge for central nervous system injury. *J. Cereb. Blood Flow Metab.* 34, 369–375.
 103. de Rivero Vaccari, J.P., Lotocki, G., Alonso, O.F., Bramlett, H.M., Dietrich, W.D., and Keane, R.W. (2009). Therapeutic neutralization of the NLRP1 inflammasome reduces the innate immune response and improves histopathology after traumatic brain injury. *J. Cereb. Blood Flow Metab.* 29, 1251–1261.
 104. Tomura, S., de Rivero Vaccari, J.P., Keane, R.W., Bramlett, H.M., and Dietrich, W.D. (2012). Effects of therapeutic hypothermia on inflammasome signaling after traumatic brain injury. *J. Cereb. Blood Flow Metab.* 32, 1939–1947.
 105. Mamet, J., Baron, A., Lazdunski, M., and Voilley, N. (2002). Proinflammatory mediators, stimulators of sensory neuron excitability via the expression of acid-sensing ion channels. *J. Neurosci.* 22, 10662–10670

8. References

1. Iaccarino, C., et al., *Epidemiology of severe traumatic brain injury*. J Neurosurg Sci, 2018. **62**(5): p. 535-541.
2. Brazinova, A., et al., *Epidemiology of Traumatic Brain Injury in Europe: A Living Systematic Review*. J Neurotrauma, 2018.
3. Maas, A.I.R., et al., *Traumatic brain injury: integrated approaches to improve prevention, clinical care, and research*. Lancet Neurol, 2017. **16**(12): p. 987-1048.
4. Selassie, A.W., et al., *Incidence of long-term disability following traumatic brain injury hospitalization, United States, 2003*. J Head Trauma Rehabil, 2008. **23**(2): p. 123-31.
5. Rabinowitz, A.R. and H.S. Levin, *Cognitive sequelae of traumatic brain injury*. Psychiatr Clin North Am, 2014. **37**(1): p. 1-11.
6. Abdul-Muneer, P.M., N. Chandra, and J. Haorah, *Interactions of oxidative stress and neurovascular inflammation in the pathogenesis of traumatic brain injury*. Mol Neurobiol, 2015. **51**(3): p. 966-79.
7. Injury, G.B.D.T.B. and C. Spinal Cord Injury, *Global, regional, and national burden of traumatic brain injury and spinal cord injury, 1990-2016: a systematic analysis for the Global Burden of Disease Study 2016*. Lancet Neurol, 2019. **18**(1): p. 56-87.
8. Koskinen, S. and H. Alaranta, *Traumatic brain injury in Finland 1991-2005: a nationwide register study of hospitalized and fatal TBI*. Brain Inj, 2008. **22**(3): p. 205-14.
9. Ramanathan, D.M., et al., *Epidemiological shifts in elderly traumatic brain injury: 18-year trends in Pennsylvania*. J Neurotrauma, 2012. **29**(7): p. 1371-8.
10. Gardner, R.C., et al., *Geriatric Traumatic Brain Injury: Epidemiology, Outcomes, Knowledge Gaps, and Future Directions*. J Neurotrauma, 2018.
11. Dewan, M.C., et al., *Estimating the global incidence of traumatic brain injury*. J Neurosurg, 2018: p. 1-18.
12. Tagliaferri, F., et al., *A systematic review of brain injury epidemiology in Europe*. Acta Neurochir (Wien), 2006. **148**(3): p. 255-68; discussion 268.
13. Flanagan, S.R., *Invited Commentary on "Centers for Disease Control and Prevention Report to Congress: Traumatic Brain Injury in the United States: Epidemiology and Rehabilitation"*. Arch Phys Med Rehabil, 2015. **96**(10): p. 1753-5.
14. Richardson, J.T.E., *Clinical and neuropsychological aspects of closed head injury*. 2000, Hove: Psychology Press. 2.
15. Andriessen, T.M., B. Jacobs, and P.E. Vos, *Clinical characteristics and pathophysiological mechanisms of focal and diffuse traumatic brain injury*. J Cell Mol Med, 2010. **14**(10): p. 2381-92.
16. Greenfield, J.G., et al., *Greenfield's neuropathology*. 2015, Boca Raton: CRC Press.
17. Roy, D., et al., *Loss of consciousness and altered mental state predicting depressive and post-concussive symptoms after mild traumatic brain injury*. Brain Inj, 2019. **33**(8): p. 1064-1069.
18. Teasdale, G. and B. Jennett, *Assessment of coma and impaired consciousness. A practical scale*. Lancet, 1974. **2**(7872): p. 81-4.

19. Saatman, K.E., et al., *Classification of traumatic brain injury for targeted therapies*. J Neurotrauma, 2008. **25**(7): p. 719-38.
20. Eken, C., et al., *Comparison of the Full Outline of Unresponsiveness Score Coma Scale and the Glasgow Coma Scale in an emergency setting population*. Eur J Emerg Med, 2009. **16**(1): p. 29-36.
21. Daneshvar, D.H., et al., *Long-term consequences: effects on normal development profile after concussion*. Phys Med Rehabil Clin N Am, 2011. **22**(4): p. 683-700, ix.
22. Rosenfeld, J.V., et al., *Early management of severe traumatic brain injury*. Lancet, 2012. **380**(9847): p. 1088-98.
23. McKee, A.C. and D.H. Daneshvar, *The neuropathology of traumatic brain injury*. Handb Clin Neurol, 2015. **127**: p. 45-66.
24. Carney, N., et al., *Guidelines for the Management of Severe Traumatic Brain Injury, Fourth Edition*. Neurosurgery, 2017. **80**(1): p. 6-15.
25. Muizelaar, J.P., et al., *Cerebral blood flow and metabolism in severely head-injured children. Part 1: Relationship with GCS score, outcome, ICP, and PVI*. J Neurosurg, 1989. **71**(1): p. 63-71.
26. Carrera, E., et al., *Spontaneous hyperventilation and brain tissue hypoxia in patients with severe brain injury*. J Neurol Neurosurg Psychiatry, 2010. **81**(7): p. 793-7.
27. Spaite, D.W., et al., *The Effect of Combined Out-of-Hospital Hypotension and Hypoxia on Mortality in Major Traumatic Brain Injury*. Ann Emerg Med, 2017. **69**(1): p. 62-72.
28. Feldman, Z., et al., *Effect of head elevation on intracranial pressure, cerebral perfusion pressure, and cerebral blood flow in head-injured patients*. J Neurosurg, 1992. **76**(2): p. 207-11.
29. R. Firsching, E.R., U.M. Mauer, O.W. Sakowitz, M. Messing-Jünger, K. Engelhard für DGAI, P. Schwenkreis für DGN, J. Linn für DGNR und K. Schwerdtfeger., *Leitlinie Schädelhirntrauma im Erwachsenenalter*. Arbeitsgemeinschaft der Wissenschaftlichen Medizinischen Fachgesellschaften (AWMF)- Ständige Kommission Leitlinien., 2015: p. 1-110.
30. Nancy Carney, A.M.T., Cindy O'Reilly, Jamie S. Ullman, Gregory W. J. Hawryluk, Michael J. Bell, Susan L. Bratton, Randall Chesnut, Odette A. Harris, Niranjana Kissoon, Andres M. Rubiano, Lori Shutter, Robert C. Tasker, MBBS, Monica S. Vavilala, Jack Wilberger, David W. Wright, Jamshid Ghajar, *Guidelines for the Management of Severe Traumatic Brain Injury* Brain Trauma Foundation (BTF), 2016(4th Edition): p. 1-244.
31. Andrews, R.J., J.R. Bringas, and R.P. Muto, *Effects of mannitol on cerebral blood flow, blood pressure, blood viscosity, hematocrit, sodium, and potassium*. Surg Neurol, 1993. **39**(3): p. 218-22.
32. Grubb, R.L., Jr., et al., *The effects of changes in PaCO₂ on cerebral blood volume, blood flow, and vascular mean transit time*. Stroke, 1974. **5**(5): p. 630-9.
33. Darby, J.M., et al., *Local "inverse steal" induced by hyperventilation in head injury*. Neurosurgery, 1988. **23**(1): p. 84-8.
34. Greenberg, M.S., *Handbook of neurosurgery*. 2020.

35. Bayir, H., et al., *Therapeutic hypothermia preserves antioxidant defenses after severe traumatic brain injury in infants and children*. Crit Care Med, 2009. **37**(2): p. 689-95.
36. Cooper, D.J., et al., *Decompressive craniectomy in diffuse traumatic brain injury*. N Engl J Med, 2011. **364**(16): p. 1493-502.
37. Cooper, D.J., et al., *Patient Outcomes at Twelve Months after Early Decompressive Craniectomy for Diffuse Traumatic Brain Injury in the Randomized DECRA Clinical Trial*. J Neurotrauma, 2020. **37**(5): p. 810-816.
38. Hutchinson, P.J., et al., *Trial of Decompressive Craniectomy for Traumatic Intracranial Hypertension*. N Engl J Med, 2016. **375**(12): p. 1119-30.
39. Hutchinson, P.J., et al., *Consensus statement from the International Consensus Meeting on the Role of Decompressive Craniectomy in the Management of Traumatic Brain Injury : Consensus statement*. Acta Neurochir (Wien), 2019. **161**(7): p. 1261-1274.
40. Narayan, R.K., et al., *Clinical trials in head injury*. J Neurotrauma, 2002. **19**(5): p. 503-57.
41. Stein, D.G., *Embracing failure: What the Phase III progesterone studies can teach about TBI clinical trials*. Brain Inj, 2015. **29**(11): p. 1259-72.
42. Lee, B. and A. Newberg, *Neuroimaging in traumatic brain imaging*. NeuroRx, 2005. **2**(2): p. 372-83.
43. Wintermark, M., et al., *Imaging evidence and recommendations for traumatic brain injury: conventional neuroimaging techniques*. J Am Coll Radiol, 2015. **12**(2): p. e1-14.
44. Yealy, D.M. and D.E. Hogan, *Imaging after head trauma. Who needs what?* Emerg Med Clin North Am, 1991. **9**(4): p. 707-17.
45. Kelly, A.B., et al., *Head trauma: comparison of MR and CT--experience in 100 patients*. AJNR Am J Neuroradiol, 1988. **9**(4): p. 699-708.
46. Servadei, F., et al., *CT prognostic factors in acute subdural haematomas: the value of the 'worst' CT scan*. Br J Neurosurg, 2000. **14**(2): p. 110-6.
47. Fainardi, E., et al., *Time course of CT evolution in traumatic subarachnoid haemorrhage: a study of 141 patients*. Acta Neurochir (Wien), 2004. **146**(3): p. 257-63; discussion 263.
48. Figg, R.E., T.S. Burry, and W.E. Vander Kolk, *Clinical efficacy of serial computed tomographic scanning in severe closed head injury patients*. J Trauma, 2003. **55**(6): p. 1061-4.
49. Bee, T.K., et al., *Necessity of repeat head CT and ICU monitoring in patients with minimal brain injury*. J Trauma, 2009. **66**(4): p. 1015-8.
50. DeQuesada, I.M., 2nd and F.H. Chokshi, *Neuroimaging of acute traumatic brain injury: emphasis on magnetic resonance imaging and prognostic factors*. Semin Roentgenol, 2014. **49**(1): p. 64-75.
51. Plantinga, B.R., et al., *Ultra-high field magnetic resonance imaging of the basal ganglia and related structures*. Front Hum Neurosci, 2014. **8**: p. 876.
52. Jassam, Y.N., et al., *Neuroimmunology of Traumatic Brain Injury: Time for a Paradigm Shift*. Neuron, 2017. **95**(6): p. 1246-1265.
53. Huisman, T.A. and A. Poretti, *Trauma*. Handb Clin Neurol, 2016. **136**: p. 1199-220.

54. Pavlova, V., et al., *Pioglitazone Therapy and Fractures: Systematic Review and Meta- Analysis*. *Endocr Metab Immune Disord Drug Targets*, 2018. **18**(5): p. 502-507.
55. Eisenberg, H.M., et al., *Initial CT findings in 753 patients with severe head injury. A report from the NIH Traumatic Coma Data Bank*. *J Neurosurg*, 1990. **73**(5): p. 688-98.
56. Hart, T., et al., *Concordance of patient and family report of neurobehavioral symptoms at 1 year after traumatic brain injury*. *Arch Phys Med Rehabil*, 2003. **84**(2): p. 204-13.
57. Losurdo, M., J. Davidsson, and M.K. Skold, *Diffuse Axonal Injury in the Rat Brain: Axonal Injury and Oligodendrocyte Activity Following Rotational Injury*. *Brain Sci*, 2020. **10**(4).
58. McAllister, T.W., *Neurobiological consequences of traumatic brain injury*. *Dialogues Clin Neurosci*, 2011. **13**(3): p. 287-300.
59. Armstrong, R.C., et al., *White matter involvement after TBI: Clues to axon and myelin repair capacity*. *Exp Neurol*, 2016. **275 Pt 3**: p. 328-333.
60. Mesfin, F.B., et al., *Diffuse Axonal Injury (DAI)*, in *StatPearls*. 2020: Treasure Island (FL).
61. Ray, S.K., C.E. Dixon, and N.L. Banik, *Molecular mechanisms in the pathogenesis of traumatic brain injury*. *Histol Histopathol*, 2002. **17**(4): p. 1137-52.
62. Yi, J.H. and A.S. Hazell, *Excitotoxic mechanisms and the role of astrocytic glutamate transporters in traumatic brain injury*. *Neurochem Int*, 2006. **48**(5): p. 394-403.
63. Tehse, J. and C. Taghibiglou, *The overlooked aspect of excitotoxicity: Glutamate-independent excitotoxicity in traumatic brain injuries*. *Eur J Neurosci*, 2019. **49**(9): p. 1157-1170.
64. Palmer, A.M., et al., *Therapeutic hypothermia is cytoprotective without attenuating the traumatic brain injury-induced elevations in interstitial concentrations of aspartate and glutamate*. *J Neurotrauma*, 1993. **10**(4): p. 363-72.
65. Palmer, A.M., et al., *Traumatic brain injury-induced excitotoxicity assessed in a controlled cortical impact model*. *J Neurochem*, 1993. **61**(6): p. 2015-24.
66. Bullock, R., et al., *Factors affecting excitatory amino acid release following severe human head injury*. *J Neurosurg*, 1998. **89**(4): p. 507-18.
67. Rothstein, J.D., et al., *Knockout of glutamate transporters reveals a major role for astroglial transport in excitotoxicity and clearance of glutamate*. *Neuron*, 1996. **16**(3): p. 675-86.
68. Rosenberg, P.A. and E. Aizenman, *Hundred-fold increase in neuronal vulnerability to glutamate toxicity in astrocyte-poor cultures of rat cerebral cortex*. *Neurosci Lett*, 1989. **103**(2): p. 162-8.
69. Kimelberg, H.K., et al., *Swelling-induced release of glutamate, aspartate, and taurine from astrocyte cultures*. *J Neurosci*, 1990. **10**(5): p. 1583-91.
70. Cheng, Y.R., B.Y. Jiang, and C.C. Chen, *Acid-sensing ion channels: dual function proteins for chemo-sensing and mechano-sensing*. *J Biomed Sci*, 2018. **25**(1): p. 46.
71. Werner, C. and K. Engelhard, *Pathophysiology of traumatic brain injury*. *Br J Anaesth*, 2007. **99**(1): p. 4-9.

72. Lucas, S.M., N.J. Rothwell, and R.M. Gibson, *The role of inflammation in CNS injury and disease*. Br J Pharmacol, 2006. **147 Suppl 1**: p. S232-40.
73. Potts, M.B., et al., *Traumatic injury to the immature brain: inflammation, oxidative injury, and iron-mediated damage as potential therapeutic targets*. NeuroRx, 2006. **3(2)**: p. 143-53.
74. Zhang, Z., et al., *Early infiltration of CD8+ macrophages/microglia to lesions of rat traumatic brain injury*. Neuroscience, 2006. **141(2)**: p. 637-644.
75. Balabanov, R., et al., *Endothelial cell activation following moderate traumatic brain injury*. Neurol Res, 2001. **23(2-3)**: p. 175-82.
76. Das, M., et al., *Lateral fluid percussion injury of the brain induces CCL20 inflammatory chemokine expression in rats*. J Neuroinflammation, 2011. **8**: p. 148.
77. Streit, W.J., *Microglia as neuroprotective, immunocompetent cells of the CNS*. Glia, 2002. **40(2)**: p. 133-9.
78. Guimaraes, J.S., et al., *Minocycline treatment reduces white matter damage after excitotoxic striatal injury*. Brain Res, 2010. **1329**: p. 182-93.
79. Fabricius, M., et al., *Cortical spreading depression and peri-infarct depolarization in acutely injured human cerebral cortex*. Brain, 2006. **129(Pt 3)**: p. 778-90.
80. Tower, J., *Programmed cell death in aging*. Ageing Res Rev, 2015. **23(Pt A)**: p. 90-100.
81. Fricker, M., et al., *Neuronal Cell Death*. Physiol Rev, 2018. **98(2)**: p. 813-880.
82. Nathoo, N., et al., *Influence of apoptosis on neurological outcome following traumatic cerebral contusion*. J Neurosurg, 2004. **101(2)**: p. 233-40.
83. Ladak, A.A., S.A. Enam, and M.T. Ibrahim, *A Review of the Molecular Mechanisms of Traumatic Brain Injury*. World Neurosurg, 2019. **131**: p. 126-132.
84. Eldadah, B.A. and A.I. Faden, *Caspase pathways, neuronal apoptosis, and CNS injury*. J Neurotrauma, 2000. **17(10)**: p. 811-29.
85. Liu, X.Z., et al., *Neuronal and glial apoptosis after traumatic spinal cord injury*. J Neurosci, 1997. **17(14)**: p. 5395-406.
86. Kenny, E.M., et al., *Ferroptosis Contributes to Neuronal Death and Functional Outcome After Traumatic Brain Injury*. Crit Care Med, 2019. **47(3)**: p. 410-418.
87. Vanden Berghe, T., et al., *Regulated necrosis: the expanding network of non-apoptotic cell death pathways*. Nat Rev Mol Cell Biol, 2014. **15(2)**: p. 135-47.
88. You, Z., et al., *Necrostatin-1 reduces histopathology and improves functional outcome after controlled cortical impact in mice*. J Cereb Blood Flow Metab, 2008. **28(9)**: p. 1564-73.
89. Xie, B.S., et al., *Inhibition of ferroptosis attenuates tissue damage and improves long-term outcomes after traumatic brain injury in mice*. CNS Neurosci Ther, 2019. **25(4)**: p. 465-475.
90. Li, J., et al., *Ferroptosis: past, present and future*. Cell Death Dis, 2020. **11(2)**: p. 88.
91. Dixon, S.J., et al., *Ferroptosis: an iron-dependent form of nonapoptotic cell death*. Cell, 2012. **149(5)**: p. 1060-72.

92. Lighthall, J.W., *Controlled cortical impact: a new experimental brain injury model*. J Neurotrauma, 1988. **5**(1): p. 1-15.
93. Marmarou, A., et al., *A new model of diffuse brain injury in rats. Part I: Pathophysiology and biomechanics*. J Neurosurg, 1994. **80**(2): p. 291-300.
94. Foda, M.A. and A. Marmarou, *A new model of diffuse brain injury in rats. Part II: Morphological characterization*. J Neurosurg, 1994. **80**(2): p. 301-13.
95. Dixon, C.E., et al., *A fluid percussion model of experimental brain injury in the rat*. J Neurosurg, 1987. **67**(1): p. 110-9.
96. Cernak, I., et al., *Involvement of the central nervous system in the general response to pulmonary blast injury*. J Trauma, 1996. **40**(3 Suppl): p. S100-4.
97. Dixon, C.E., et al., *A controlled cortical impact model of traumatic brain injury in the rat*. J Neurosci Methods, 1991. **39**(3): p. 253-62.
98. Hall, E.D., et al., *Spatial and temporal characteristics of neurodegeneration after controlled cortical impact in mice: more than a focal brain injury*. J Neurotrauma, 2005. **22**(2): p. 252-65.
99. Gennarelli, T.A., *Animate models of human head injury*. J Neurotrauma, 1994. **11**(4): p. 357-68.
100. Hodge, R.D., et al., *Conserved cell types with divergent features in human versus mouse cortex*. Nature, 2019. **573**(7772): p. 61-68.
101. Zhao, S., et al., *Delayed and progressive damages to juvenile mice after moderate traumatic brain injury*. Sci Rep, 2018. **8**(1): p. 7339.
102. Niesman, I.R., et al., *Traumatic brain injury enhances neuroinflammation and lesion volume in caveolin deficient mice*. J Neuroinflammation, 2014. **11**: p. 39.
103. Gao, X. and J. Chen, *Mild traumatic brain injury results in extensive neuronal degeneration in the cerebral cortex*. J Neuropathol Exp Neurol, 2011. **70**(3): p. 183-91.
104. Nissl, F.J.N.C., *Ueber eine neue Untersuchungsmethode des Centralorgans zur Feststellung der Localisation der Nervenzellen*. 1894. **13**: p. 507-508.
105. Scott, J.E. and I.H. Willett, *Binding of cationic dyes to nucleic acids and their biological polyanions*. Nature, 1966. **209**(5027): p. 985-7.
106. Baier, J., et al., *Influence of MRI Examinations on Animal Welfare and Study Results*. Invest Radiol, 2020. **55**(8): p. 507-514.
107. Hohlbaum, K., et al., *Severity classification of repeated isoflurane anesthesia in C57BL/6JRj mice-Assessing the degree of distress*. PLoS One, 2017. **12**(6): p. e0179588.
108. Wehn, A.C., et al., *RIPK1 or RIPK3 deletion prevents progressive neuronal cell death and improves memory function after traumatic brain injury*. Acta Neuropathol Commun, 2021. **9**(1): p. 138.
109. Grauwmeijer, E., M.H. Heijenbrok-Kal, and G.M. Ribbers, *Health-related quality of life 3 years after moderate to severe traumatic brain injury: a prospective cohort study*. Arch Phys Med Rehabil, 2014. **95**(7): p. 1268-76.
110. Hawthorne, G., R.L. Gruen, and A.H. Kaye, *Traumatic brain injury and long-term quality of life: findings from an Australian study*. J Neurotrauma, 2009. **26**(10): p. 1623-33.
111. Sousa, N., O.F. Almeida, and C.T. Wotjak, *A hitchhiker's guide to behavioral analysis in laboratory rodents*. Genes Brain Behav, 2006. **5 Suppl 2**: p. 5-24.

112. Wahlsten, D., *Standardizing tests of mouse behavior: reasons, recommendations, and reality*. *Physiol Behav*, 2001. **73**(5): p. 695-704.
113. Chesler, E.J., et al., *Influences of laboratory environment on behavior*. *Nat Neurosci*, 2002. **5**(11): p. 1101-2.
114. Iaccarino, M.A., S. Bhatnagar, and R. Zafonte, *Rehabilitation after traumatic brain injury*. *Handb Clin Neurol*, 2015. **127**: p. 411-22.
115. Mao, X., et al., *Progressive histopathological damage occurring up to one year after experimental traumatic brain injury is associated with cognitive decline and depression-like behavior*. *J Neurotrauma*, 2019.

Acknowledgements

First and foremost, I would like to express my gratitude to my supervisors Prof. Nikolaus Plesnila and PD Dr. Nicole Terpolilli for giving me the opportunity to do this work and who guided me throughout this project. I wish to extend my special thanks to Dr. Igor Khalin for the valuable scientific discussions.

Many thanks also to Dr. Xiang Mao and Dr. Susanne Schwarzmaier for teaching me during my first months in the lab, to Dr. Farida Hellal for the valuable scientific discussions, as well as to Uta Mamrak and Hedwig Pietsch for their continuous help and support in the lab. Thanks also to my lab mates and friends, Dr. Susana Valero-Freitag, Rebecca Siemel, Bernhard Groschup, Dr. Joshua Shrouder, Dr. Severin Filser, Dr. Shiqi Cheng, Dr. Burcu Seker, Dr. Sodai Yoshimura, Stergios Tsitos, Chiara Braun, Ardela Cara, Carina Exner, Eva Krestel, Xianjiang Lin, Kosisochukwu Umeasalugo for their continuous support and encouragement, in- and outside the lab. Also many thanks to my closest friends, Tobias Meisinger, Tanja Schwarzmeier and Alexandra Gritz for bearing with me and supporting me continuously during this period.

Finally yet importantly, I wish to give thanks to my parents for their unconditional love and support they have given and continue to give me.